UNIVERSITY OF NOTTINGHAM

# Development of a sustainable primary human airway cell culture model for respiratory research

MPhil Thesis

**Amanda Lewis**

## Abstract

The airway epithelium has an important protective role and is known to be abnormal in asthmatic individuals. However, epithelial cell research is restricted by the limited lifespan of primary human epithelial cells *in vitro* and therefore the cells isolated via bronchoscopy are exhausted after only a few experiments. This project aimed to extend cell lifespan by over-expressing Bmi1 in a controlled and temporal manner using an inducible Cumate Switch system.

Bmi1 has previously been shown to extend cell lifespan whilst maintaining plasticity. In this study, lentiviruses have been generated to deliver and over-express Bmi1 to primary human bronchial epithelial cells (HBECs) which contain the Cumate Switch System to control gene expression. Infected cells show evidence of fluorescent reporter proteins indicating successful gene delivery and expression. The effects of Bmi1 over-expression have been assessed through Electric Cell Substrate Impedance Sensing (ECIS) and also through differential gene expression (RNA-seq) using the data from a study published in Gene Expression Omnibus. Preliminary data show that barrier function differs in modified cells, but transcriptomic analysis does not identify differential expression of barrier function genes in correlation with elevated Bmi1. A large number of genes are identified as being differentially expressed (1024 by CuffDiff and 380 by Rank Prod), although this number is reduced when using multiple analyses, and amongst those genes consistently up-regulated with Bmi1 expression are genes involved in cell growth and migration.

The rationale behind this project is that Bmi1 over-expression can be returned to endogenous levels by removing gene induction. Initial data suggested that Bmi1 expression can be turned on and at least turned down in this system, but further work is needed.

Bmi1 has the potential to extend cell lifespan, providing the primary cells with a proliferative advantage to allow further expansion in culture than currently possible. This study has provided initial support that a Bmi1 switch system may be viable, but also demonstrated that Bmi1 induction may alter barrier properties and significantly influence the expression of many genes. The development of a Bmi1 switch system has the potential to significantly expand our ability to utilise primary cells from patients and provide an extended platform to study airway epithelial cell biology.

## Acknowledgements

With thanks to my supervisor Dr. Ian Sayers for his guidance and direction throughout the project.

Everyone in the Division of Respiratory Medicine at the University of Nottingham, particularly Dr. Michael Portelli and Dr. Sangita Bhaker for their help, as well as Dr. Vincent Pang of Tumour and Vascular Biology for his assistance and use of ECIS equipment.

Special thanks to Tim Lewis for his endless support and patience through difficult times and my parents to whom I owe so much.

## Contents

# Abbreviations

**ALI** Air-liquid interface

**BEBM** Bronchial epithelial basal medium

**BEGM** Bronchial epithelial cell growth medium

**Bmi1** B lymphoma Mo-MLV insertion region 1 homolog

**bp** Base pairs

**CymR** Cumate Repressor Virus

**DMEM** Dulbecco's Modified Eagle Medium

**ECIS** Electric Cell Substrate Impedance Sensing

**ECL** Enhanced Chemiluminescence

**EV** Empty Vector

**FACS** Fluorescence-activated cell sorting

**FBS** Fetal bovine serum

**FC** Fold change

**FDR** False discovery rate

**FPKM** Fragments per kilobase of transcript per million mapped reads

**GEO** Gene Expression Omnibus

**GFP** Green Fluorescent Protein

**HBEC** Human Bronchial Epithelial Cell

**hTERT** Telomerase reverse transcriptase

**LTR** Long Terminal Repeat

**MOI** Multiplicity of infection

**PBS** Phosphate Buffered saline

**pCDH** pCDH-CMV-MCS-EF1-copGFP constitutive expression plasmid

**PCR** Polymerase Chain Reaction

**pfp** Percentage of false predictions

**qPCR** Quantitative polymerase chain reaction

**rcf** Relative Centrifugal Force

**rpm** Revolutions per minute

**RFP** Red Fluorescent Protein

**SparQ** inducible expression plasmid

**TEER** Trans-epithelial Electrical Resistance

**TLR** Toll-like receptor

**WPRE** Woodchuck Hepatitis Virus Posttranscriptional Regulatory Element

# 1. Introduction

In this MPhil thesis, I set out to develop an approach to extend the lifespan of primary human bronchial epithelial cells *in vitro* whilst maintaining cell plasticity. The ultimate purpose of this cell model is as a platform for the study of respiratory disease. To achieve this, I developed a system which can over-express Bmi1, a protein that can prevent cell cycle arrest. This system incorporates an inducible mechanism allowing controlled gene expression. Analyses were performed to determine the effects of Bmi1 over-expression and evaluate the potential of this methodology for producing a sustainable airway cell line. This chapter highlights the important role of airway epithelial cells and the need for a representative model *in vitro*.

## 1.1. The airway epithelium: a dynamic barrier against environmental insult

The epithelial cells which line the airway form part of the innate immune system and play a protective role; effectively separating the internal environment from a myriad of potential external insults and preserving the homeostasis of the airways (Ganesan *et al.,* 2013). The mature epithelium is a pseudo-stratified layer comprised of several cell types including secretory cells, ciliated cells and basal cells, although the types and frequency of these cell types vary depending on their location along the respiratory tract, with basal cells becoming less common towards the alveoli and small airways (reviewed in Camelo *et al.,* 2014).

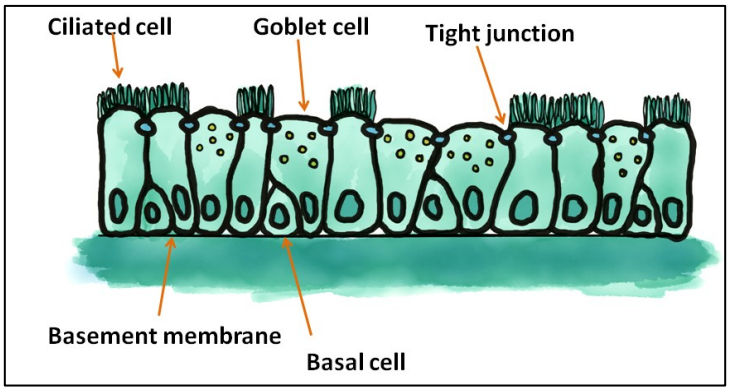


**Figure 1.1 The airway epithelium is a pseudo-stratified layer primarily comprised of ciliated cells, goblet cells and basal cells on top of a basement membrane.** Based on Grainge & Davies (2013).

Between the cells of the upper respiratory tract are tight junctions and other adhesive components that serve to uphold the integrity of the barrier and preserve the intercellular seal (Holgate, 2011). This occurs through the interaction of various tight junction proteins and their corresponding receptors, such as the zonula-occludens proteins (ZO-1, ZO-2 and ZO-3) and

occludin, which is frequently used as an immunohistochemical marker of tight junctions (Kojima *et al.,* 2013). The tight junctions also regulate the permeability of the cells, controlling intercellular passage of ions and small molecules and preventing unwanted transport between the external lumen and internal environment (Godfrey, 1997). Furthermore, tight junctions play a role in regulating the polarity of the cells in the epithelial layer through various protein interactions (Shin *et al.,* 2006), ensuring that they function appropriately, which is crucial due to the apical location of cilia and mucosal secretion in the epithelium.

Enhancing the protective barrier, the goblet cells and seromucous glands rapidly secrete mucus to trap any airborne pathogens or harmful particles. These trapped particles are then swept away by ciliated cells which push the mucus up and away from the lungs in what is known as mucociliary clearance (Rogers, 2002). Mucin proteins are encoded by MUC genes, primarily MUC5AC and MUC5B in the airways (reviewed in Rose & Voynow, 2006). Along with mucus, the cells of the epithelium secrete a range of proteins, defensive peptides and anti-microbial factors that contribute to the protective function by forming a chemical barrier, which not only prevents the surface from drying out but can selectively protect against bacterial attack and detoxify inhaled particles (Swindle *et al.,* 2009). Membrane tethered mucins and glycolipids are also thought to be present near the surface to provide an aqueous environment in which the cilia can successfully beat (Randell & Boucher, 2006).

In addition to these innate immunological devices, the epithelium also serves as a means of communication between the external environment and the cells of the adaptive immune system. It is capable of secreting a variety of signalling molecules such as growth factors, cytokines, chemokines and pro-inflammatory factors (Knight & Holgate, 2003) and in order to detect and respond to incoming threats, the epithelial cells possess Toll-like Receptors (TLRs) (Ritter *et al*., 2005). There are many varieties of TLR and each type acts to recognise specific pathogen-associated molecular patterns (PAMPs) which are key to initiating immune responses; for example, TLR-2 is found on the cell surface and involved in binding bacterial lipoproteins and others such as TLR-3 and 7 are found in the cytoplasmic compartment of the cell where they act to identify viral nucleic acids which may have infected the cells (Li *et al.,* 2012b). The epithelial cells then communicate this threat to the appropriate immune cells, such as T cells, via cytokine production and pathogen presentation in order to initiate an immune response (Akira *et al.,* 2001). Furthermore, the epithelium also plays a role in actively suppressing immune responses, via secretion of IL-10 (Swindle *et al.,* 2009).

Overall, the airway epithelium is much more than a physical barrier and plays a key role in ensuring the health of the airways and triggering of host defence mechanisms through various signalling pathways and secretion of protective factors. Consequently, epithelial dysfunction can be severely detrimental and is thought to contribute to several respiratory diseases, including asthma, which will be the main interest in this project.

## 1.2 Respiratory disease burden and the need for physiologically relevant models

Asthma is a respiratory disorder estimated to affect approximately 235 million people worldwide (World Health Organisation, 2017) and which puts an ever increasing strain on medical resources (Barnett *et al*., 2011). The European Respiratory Society (2017) defines asthma as:

**"A chronic inflammatory disease of the airways that causes recurring episodes of wheezing, breathlessness, chest tightness and coughing".**

It is primarily characterised by a combination of both inflammatory and structural changes to the airways, resulting in features such as bronchial hyper-responsiveness and airflow limitation, but also abnormalities at a cellular level which are deemed equally significant in terms of disease progression (Fixman *et al.,* 2007). These changes in the airway cells can provide further insight into asthma and may highlight therapeutic opportunities which can be taken advantage of.

### 1.2.1 Defective epithelial barrier function in asthmatic individuals

There are many observable and functional changes in asthmatic airway epithelium compared to healthy epithelium. However, there is ongoing debate as to whether this epithelial remodelling is causative of asthma or occurs as a subsequent result of asthma pathogenesis - an inevitable stage in the disease progression (Fahy, 2001).

A particularly deleterious characteristic of asthmatic epithelium is that the barrier function becomes compromised, which may in turn worsen and increase the frequency of exacerbations by allowing access of environmental insults to the smooth muscle below (Folkerts & Nijkamp, 1998). The integrity of the protective barrier hinges on the permeability of the epithelium and the formation of appropriate intercellular junctions and cell-cell interactions, such as tight junctions, adherens junctions and desmosomes (reviewed in Xiao *et al*., 2013). In cell culture, the trans-epithelial electrical resistance (TEER) can be measured to give an indication of how successful a monolayer is formed by the epithelial cells; a low TEER

can denote an incomplete 'leaky' cell layer and can suggest poor tight junction formation and lower electrochemical gradients (Anderson & Van Itallie, 2009). Asthmatic epithelial airway cells form aberrant barriers both *in vitro* and *in vivo*, often with absent or discontinuous tight junction proteins and a reduced TEER *in vitro* (regardless of the severity of the asthma) suggesting a decline in function in comparison to non-asthmatic cells (Xiao *et al*., 2011).

Tight junctions are the apical most junctional complexes (Kojima *et al*., 2013) and therefore the most exposed to environmental attack. However, other junctional complexes are also affected in asthma. For example, E-cadherin is a major component of adherens junctions and forms connections with the cytoskeletal components of the cells to facilitate cell-cell adhesion and provide structural support for tight junction formation (Nawijn *et al.,* 2011). In the asthmatic epithelium, E-cadherin expression is altered and found to be expressed at lower levels at sites of epithelial damage, which consequently increases EGFR signalling and levels of TARC, a Th-2 attracting chemokine (Heijink *et al*., 2007). E-cadherin not only plays an important physical role but moderates the immune response through repression of NF-κB signalling, allowing immune tolerance (Nawijn *et al.,* 2011).

Shedding of the epithelium has long been associated with asthma pathogenesis (Yukawa *et al.,* 1990) and could have a huge impact on its structure and function. Shebani *et al.* (2005) show that there is decreased attachment and surface area contact of columnar cells to the basal lamina in asthmatics and that attachment occurs indirectly via desmosome connections between columnar and basal cells, signifying abnormal desmosome function. However, Ordoñez *et al.* (2000) suggest that desquamation of the epithelium is actually an artefact of bronchial tissue sampling rather than a pathological feature of asthma and does not correlate with other disease characteristics. Furthermore, Dorscheid and colleagues (2001) suggest that the treatment of asthma may encourage cell death in order to decrease airway inflammation.

Breakdown of the epithelial barrier has the overall effect of allowing entry of environmental insults which otherwise would not be able to pass through and therefore weakens the resilience of the airways and increases the likelihood of exacerbations.

### 1.2.2 Excessive mucus results in airflow limitation

As well as abnormal barrier formation, the functional properties of the airway epithelial cells are also modified in asthma. Goblet cell hyperplasia (increased proliferation) occurs as a result of airway remodelling (Vermeer

*et al*., 2003) and is thought to be triggered by the T-helper 2 type (Th2) response (Park *et al*., 2007). Th2 cells release cytokines IL-4, IL-5, IL-9 and IL-13 which are involved in asthma pathogenesis and trigger inflammatory responses (Barnes, 2001b). Hyperplasia does also occur in non-asthmatic individuals to enhance protection in response to continual insult, which could suggest an exaggerated defensive response in asthma (Rogers, 1994).

Mast cells also play a significant role in the immune response. They are highly responsive, capable of rapidly releasing various mediators which favour an inflammatory and defensive environment. Asthmatic individuals are known to have higher levels of mast cells and mast-cells derived mediators, stimulating the recruitment of a wide range of other immune cells and ultimately inducing the asthmatic phenotype (reviewed in Hart, 2001).

Mast cells are also known to produce IL-4, IL-5 and IL-13, along with histamine and IL-6, which promote migration of circulating inflammatory cells from the blood into adjacent tissues (reviewed in Amin, 2012). Histamine is thought to regulate goblet cell hyperplasia, increasing the number of mucosal cells in both large and small airways; although the mechanism by which this happens is poorly understood (Yamauchi *et al*., 2008).

More recently, Group 2 innate lymphoid cells have been identified as potential contributors to asthma pathogenesis, as they have been found to produce Th2 cytokines in high quantities, particularly IL-5 and IL-13 which increase mucus production (reviewed in Doherty & Broide, 2015). The Group 2 innate lymphoid cells are prompted to do so by epithelial-derived IL-25 and IL-33 (Kabata *et al.* 2015).

In addition to hyperplasia, goblet cell metaplasia can take place, which is an increase in number at the expense of other cell types (rather than through increased proliferation); ciliated and Clara cells are trans-differentiated into goblet cells (reviewed in Hayashi, 2012) and subsequently the number of cilia becomes insufficient to effectively sweep away mucus. This is again thought to be triggered via a Th2 signalling pathway, increasing expression of IL-13 which cooperates with epidermal growth factor receptor (EGFR) to prevent epithelial cell apoptosis and induce MUC5AC gene expression, resulting in a goblet cell phenotype (Curran & Cohn, 2010). The goblet cells themselves also produce excessive mucus (hypersecretion) through increased expression of mucin genes (Curran & Cohn, 2010).

The overall result of these changes is that the airways become obstructed by mucus, causing difficulties in breathing. The stagnant mucus can present a breeding ground for bacteria (Perez-Vilar *et al.,* 2007) and excessive mucus has been linked to mortality in asthmatic individuals, being particularly problematic in the small, non-cartilaginous airways, where mucus cannot readily be displaced via coughing (Rogers, 2002).

### 1.2.3 The asthmatic epithelium displays an abnormal wound response

As well as being more susceptible to environmental challenges, the asthmatic epithelium also behaves differently to healthy, non-asthmatic epithelium when damaged. In response to mechanical wounding or environmental insult (exposure to particulate matter or infection with RSV) *in vitro*, asthmatic epithelial cells show an increased release of certain cytokines including IL-6 and GM-CSF compared to non-asthmatic controls, but not in the absence of insults, suggesting that the cells respond differently when faced with stress (Hackett *et al.,* 2011). The abnormal repair response is thought to be a result of diminished proliferation in basal and Clara cells (which are involved in bronchial repair and regeneration (Akram *et al.,* 2013)) and leads to a 'chronic wound scenario' (Holgate, 2011).

Furthermore, *in vitro,* asthmatic cells display a slower cell migration and repair response when compared to healthy non-asthmatic epithelial cells (Stevens *et al.,* 2008). Repair in asthmatic epithelium often results in structural changes which are ultimately detrimental to lung function (Rennard, 1996).

### 1.2.4 Existing drug therapies for the management of asthma

There is no cure for asthma, instead medications which are currently employed function to improve quality of life and to prevent and reduce the severity of exacerbations (Weiss, 2012). Inhaled treatments are favoured as they are delivered directly to the required site of action.

Corticosteroids are currently broadly utilised as an effective non-specific anti-inflammatory treatment for the symptoms of asthma and reduce the expression of various pro-inflammatory factors (Knight & Holgate, 2003). They function by binding to and activating certain glucocorticoid receptors causing them to be translocated from the cytoplasm into the nucleus (Eickelberg *et al.,* 1999), where they bind DNA and alter gene expression (Barnes, 2001a).

Beta-adrenergic agonists are another commonly used treatment which act as bronchodilators (Thanawala *et al.*, 2013) to immediately relax the smooth muscle in the airway during asthma attacks. However, high exposure is thought to actually worsen asthma symptoms (Cazzola *et al*., 2011) and there are concerns over the relationship of beta-adrenergic agonists and asthma-related deaths (Chowdhury *et al*., 2010). In fact, it has been shown that beta-adrenergic agonists are required for the development of an asthmatic model in mice (Thanawala *et al.*, 2013).

As part of asthma pathophysiology, cysteinyl leukotrienes are released by inflammatory cells and lead to airway constriction and inflammation (Noonan *et al.,* 1998). Therefore, leukotriene receptor antagonists, such as montelukast, have been used to improve the symptoms of asthma (Paggiaro & Bacci, 2011).

Additionally, IgE is an antibody which is elevated in allergic asthma and often binds to innocuous substances triggering immune responses (reviewed in Chang, 2000). Therefore, anti-IgE monoclonal antibodies, such as omalizumab, are used to bind IgE so that it can no longer interact with immune cells, thus providing an alternative for patients intolerant to corticosteroids (Busse *et al*., 2001). However, Bradding *et al.* (2006) state that anti-IgE treatment does not have a significant effect on bronchial hyper-responsiveness, highlighting that treatments require tailoring to the symptoms of the patient.

### 1.2.5 Drug responsiveness in epithelial cells

As airway epithelial cells are generally the first point of contact with inhaled asthma therapies, it is necessary to understand how the cells respond when directly exposed to these treatments.

Corticosteroids such as dexamethasone, beclomethasone, budesonide and triamcinolone have been shown to cause apoptosis in a dose-dependent manner in primary airway epithelial cells *in vitro*, suggesting that although there may be some relief by reducing inflammation, this may be achieved in a deleterious fashion (Dorscheid *et al,* 2001). However, this publication has been contested by Carayol *et al*. (2002) who considered Dorscheid's (2001) results to show only a small increase in apoptosis when exposed to relatively high concentrations of corticosteroids (not previously used in clinical observations).

Tse *et al.* (2003) building upon Dorcheid's (2001) work showed that beta-adrenergic agonists (which are commonly combined with corticosteroids to treat asthma) could prevent the 'corticosteroid-induced apoptosis' in

primary airway epithelial cells *in vitro*. However, they noted that the percentage of apoptotic cells due to corticosteroid treatment was relatively low (5-15%) and may not be clinically relevant *in vivo*, but suggest that continual and consistent apoptosis may lead to eventual damage in the airways and prove detrimental. The effect of corticosteroid treatment on epithelial apoptosis remains uncertain and currently the benefits of such treatment and combination with other treatments appear to outweigh any negative consequences.

Wadsworth *et al*. (2006) show that the corticosteroid, dexamethasone, increases survival in repeatedly wounded bronchial epithelial cells *in vitro*, whereas β2 adrenoceptor agonists did not. Additionally, pre-treatment of primary bronchial epithelial cells with the corticosteroid, budesonide, has been shown to restore barrier function following oxidant-induced and mechanical damage, whilst pre-treatment with the oxidant, $H_2O_2$, decreases responsiveness to budesonide treatment Heijink *et al*., (2014). Furthermore, although these results suggest the success of budesonide, Heijink and colleagues (2014) also reveal that the protective effects of the corticosteroid are reduced in asthmatic cells, possibly dampening its success as a treatment for asthma. They proposed that this is potentially due to higher oxidant levels in asthmatic individuals which could have the effect of phosphorylating the glucocorticoid receptor, and suggest that corticosteroids may be more effective if combined with a treatment to lower levels of oxidative stress.

### 1.2.6 Resistance to treatment

Severe (or refractory) asthma is often defined as non-responsive to glucocorticoid treatment and is becoming an increasing problem in the management of asthma, due to the lack of efficient alternative options available (Bradding, 2008). Understanding the mechanisms for non-responsiveness is therefore of great importance and there is a need for new and effective treatments for asthma. There are many different manifestations of asthma which also calls for prescription of tailored medicine to tackle the variations in asthma phenotype (Paggiaro & Bacci, 2011).

## 1.3 Uses and limitations of airway epithelial cells in respiratory research

In order to better understand the airway epithelium and increase the likelihood of developing successful therapies for disease, human airway epithelial cells need to be studied *in vitro*.

Primary human airway epithelial cells are the current gold standard and isolated from patients via invasive procedures such as bronchoscopy, brushings or biopsy for research purposes. When these cells are cultured in submerged media *in vitro* they tend not to be differentiated but comprised primarily of basal cells (Park *et al.,* 2015). However, when these cells are cultured at Air-Liquid Interface (ALI), where the apical surface of the cells is exposed to air (as shown in Fig. 1.2), they are capable of differentiating into the appropriate epithelial cell types (Wu *et al*., 1986).

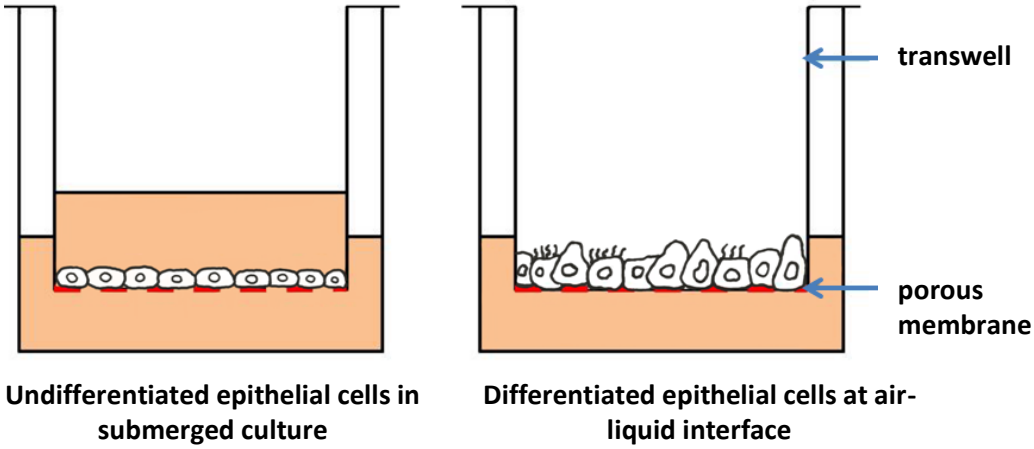


**Figure 1.2 Schematic diagram of airway epithelial cells cultured submerged and at air-liquid interface in transwells with porous membranes.** Exposing the apical surface of the cell layer to air represents the *in vivo* environment and drives differentiation from basal cells into goblet and ciliated cells (based on Stem Cell, 2016).

ALI involves culturing the cells on a semi-permeable membrane in a transwell. Culture media is added to both apical and basal compartments and the cells are grown until a confluent monolayer is produced. Following this an air-lift is performed, where media is removed from the apical compartment and the cells are apically exposed to air, mimicking the endogenous environment. This is sufficient to drive cells to differentiate into mucus-secreting and ciliated cell types.

Primary air way epithelial cells cultured at ALI have been shown to express a similar genome-wide expression profile to tracheal and bronchial epithelial cells *in vivo* (Pezzulo *et al.*, 2011). Additionally, Dvorak *et al*. (2011) also concluded that the transcriptome of human large airway epithelial cells grown at ALI were representative of cells isolated via brushing and

bronchoscopy, but there were slight differences which they state may need to be taken into account depending on the research conducted.

Unfortunately, there are a number of limitations when working with primary cells *in vitro*, including their high variability, expensiveness and restricted lifespan when cultured (Stewart *et al.*, 2012). Primary airway epithelial cells also lose their characteristics and dedifferentiate over time when cultured *in vitro* (Wu *et al.*, 1986). This rules out larger scale and long term studies.

### 1.3.1 Existing cell models

Cell lines provide a useful alternative to primary cells which are cheaper and more reproducible (Kaur & Dufour, 2012). Cell lines are usually cells which are modified to immortalise them or are obtained from carcinomas where cells are already mutated to allow continuous cell culture. However, cell lines are not without limitations; ideally they should represent the primary cells as best they can.

There are a range of existing cell models which are used for respiratory research. For example, Calu3 cells, which were originally obtained from a bronchial adenocarcinoma, BEAS-2B cells which are epithelial cells transformed by the adenovirus-12 SV40 hybrid virus (reviewed in Forbes, 2000) and 16HBE14o cells which are bronchial epithelial cells transformed by the SV40 large T-antigen to immortalise them (Cozens *et al.*, 1994).

A study by Stewart *et al.* (2012) compares BEAS-2B cells and Calu3 cells to primary airway epithelial cells. They found that BEAS-2B cells failed to produce a high TEER at ALI and did not show differentiation into mature epithelial cells, whereas Calu3 cells produced a high TEER and were comparable to primary cells in their expression of epithelial cell markers (Stewart *et al*., 2012). Furthermore, BEAS-2B cells are not able to form tight junctions as well as other airway cell lines (reviewed in Forbes, 2000), so are thus unsuitable for studying barrier function. On the other hand, both 16HBE14o and Calu3 cell lines show evidence of intercellular junction proteins (Wan *et al.*, 2000). Heijink *et al.* (2010) conclude that whilst 16HBe14o cells would be suitable for investigating barrier function, BEAS-2B cells may be more appropriate for studies involving cell-matrix interactions. This demonstrates that the type of airway cell line used depends on the type of research and aspect of the airway epithelium being studied.

Although Calu3 are able to form resistive barriers, they differ from endogenous cells in that they do not form a pseudostratified monolayer and show some abnormalities due to the cancerous nature of the cells (reviewed in Prytherch & BéruBé, 2013). Shan *et al.* (2011) state that Calu3 cells are

lacking in normal chromosomes 1, 13, 15 and 17 and so are missing genes in host defence. Furthermore, they are originally isolated from a submucosal gland rather than surface epithelium; this indicates they would likely have been apically exposed to liquid *in vivo* rather than air (Grainger *et al*., 2006).

In addition, Hughes *et al.* (2007) discuss the problems of cross-contamination and over-passaging of cell lines, warning of the need for vigorous authentication tests to avoid mis-identification. Overall, although current cell lines provide a useful option for research, they are not without limitations.

Whilst primary cells provide the closest representation to the *in vivo* situation, they are short-lived *in vitro*, meaning a relatively small window of time to complete research. This also limits expansion of the cells, so only a relatively small number of cells are available for study. Therefore, this project sets out to genetically modify primary airway epithelial cells in order to overcome these issues.

## 1.4 Measures to increase cell lifespan *in vitro* to develop a sustainable airway epithelial cell model

### 1.4.1 Cells have a restricted life span

Cells are prevented from excessive cell division by telomere shortening at each round of replication, putting a limit on the number of times a cell can divide, known as the Hayflick limit (Kuilman *et al.,* 2010). Cells which reach this limit undergo replicative senescence and are no longer able to proliferate (Park *et al*., 2004). Senescence involves a number of inherent changes such as altered gene expression, increased protein secretion and signalling factor release, altering the cell microenvironment (Coppé *et al.,* 2010) and making the cells unreliable representations of non-senescent cells.

### 1.4.2 Delaying cellular senescence is desirable for long-term cell culture

Primary cells cultured *in vitro* can currently only be maintained for a brief period of time before they undergo replicative senescence and irreversible senescence-associated changes (Kuilman *et al.,* 2010). Therefore, culture of primary airway cells is limited, restricting long term research of asthmatic epithelial cells and highlighting the benefit of techniques which can be employed to delay replicative senescence and overcome the Hayflick limit.

### 1.4.3 Over-expression of Bmi1 as a potential technique to overcome cellular senescence

Various genes are potential candidates for extending cell lifespan and delaying senescence. Of particular interest to this project is the Bmi1 gene. Bmi1 is a member of the Polycomb gene family involved in chromatin remodelling, and its over-expression in various cancers and stem cells (Park *et al.,* 2004) has stirred interest in its use as a mechanism to prolong cellular lifespan.

A significant target of BMI1 is the INK4a/Arf locus, which encodes the p16 and p19 (also known as p14 in humans) cyclin-dependant kinase inhibitors (Jacobs *et al.,* 1999) as shown in Figure 1.3. p16 is known to cause cell cycle arrest at the G1/S phase checkpoint of the cell cycle, by preventing phosphorylation of Retinoblastoma proteins - necessary for cell cycle progression (Serrano, 1997) and p19 binds to and inhibits MDM2 which results in the stabilisation of p53, again resulting in cell cycle arrest (Stott *et al.,* 1998). Bmi1 acts by epigenetically suppressing the expression of p16 and p19, which consequently leads to a delay in both cellular senescence and apoptosis and promotes cell cycle progression (Park *et al.,* 2004). However, Bmi1 has the potential to act as an oncogene independent of the INK4a/Arf locus (Xu *et al*., 2009), suggesting alternative mechanisms of regulating proliferation. Kim *et al.* (2010) suggest that Bmi1 can also function via inhibition of the TGF-beta signalling pathway.

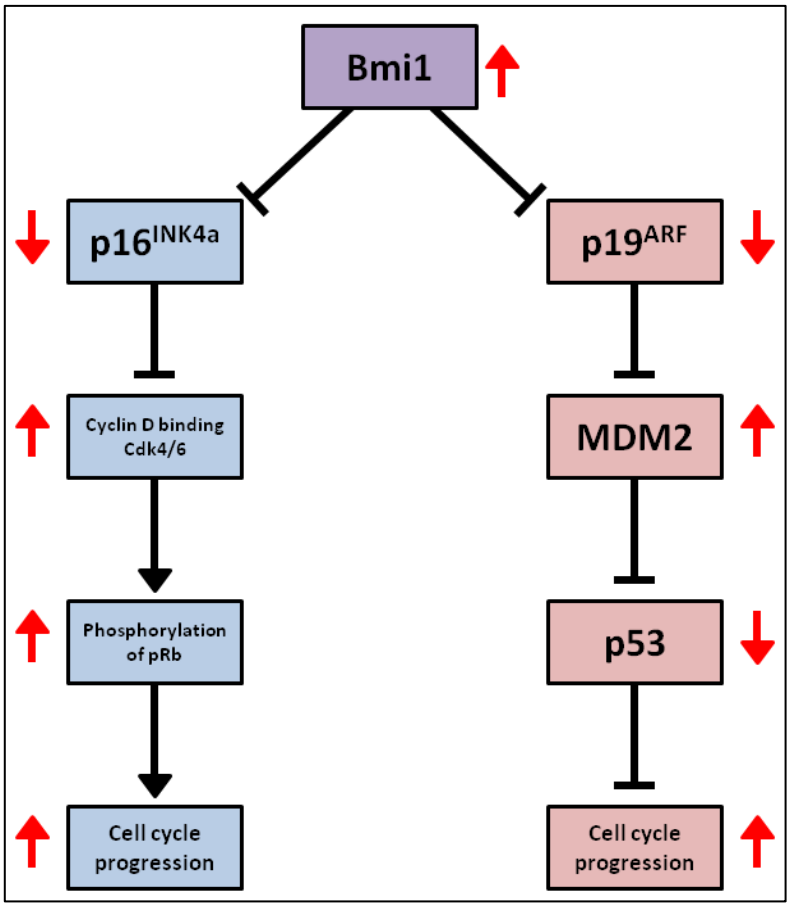


**Figure 1.3 The pathways Bmi1 affect to increase cell cycle progression.** Bmi1 targets the $p16^{INK4a}$ locus and the p19 alternative reading frame. The red arrows indicate the effect over-expression of Bmi1 has at each stage (based on Park *et al*., (2004)).

Bmi1 is involved in highly proliferative processes; it is necessary for self-renewal of neural stem cells (Molofsky *et al*., 2003) and has been shown to contribute to the proliferative ability of haematopoietic stem cells (Lessard & Sauvageau, 2003). On the other hand, a loss of Bmi1 expression in the epithelium of small bile ducts results in increased cellular senescence (Sasaki *et al.,* 2006) showing its endogenous importance in epithelial cells. Decreased Bmi1 expression also causes a reduction in proliferation of lung adenocarcinoma cells (Zheng *et al*., 2014) and leads to necroptosis (cell death) in ovarian cancer cells (Dey *et al*., 2016). Fulcher *et al.* (2009) show that *in vitro* Bmi1 expression is at its highest in passage 1 human bronchial epithelial cells, but that with repeated passages expression decreases and $p16^{INK4a}$ protein levels increase before senescence occurs, suggesting that Bmi1 may be necessary to prevent senescence in culture.

Bmi1 has been used in numerous cell types to generate cell lines. For example, Bmi1 was elevated in a number of nasopharyngeal carcinomas, so was used to immortalise nasopharyngeal epithelial cells to create a model

for research (Song *et al.,* 2006). It has also been shown to immortalise fibroblasts (Jacobs *et al.*, 1999) and to increase the longevity of oral keratinocytes (Kim *et al.*, 2010). Furthermore, Dimri *et al.* (2002) showed that Bmi1 was overexpressed in breast cancer cell lines and had the potential to immortalise mammary epithelial cells (MECs) without altering the DNA damage checkpoint. Bmi1, therefore, is well-renowned as a gene which functions to extend cell lifespan and can be manipulated to delay the senescence of cells in culture.

### 1.4.4 Alternative genes which can extend cell lifespan

Although Bmi1 is a plausible option, there are a number of alternative ways in which extended cellular lifespan can be achieved. One such method involves the introduction of viral genes such as E6 or E7 from human papillomavirus or H-Ras from SV40 which act to inactivate p53 or pRb (tumour suppressors) to overcome cell cycle checkpoints (reviewed by Maqsood *et al.,* 2013). However, cell telomeres (chromosome ends) continue to shorten leading the cells to enter a 'crisis' state where they cease proliferating (Ouellette *et al*., 2000).

Human telomerase reverse transcriptase (hTERT) functions to maintain and preserve telomeres so that they do not become shorter through successive rounds of replication (Armbruster *et* al., 2004). Lundberg et al. (2000) state that cells which are obtained from older organisms have already completed a certain number of replications, so tend to have shorter telomeres and reduced longevity *in vitro*, which could be a factor to consider when using human donors of varying ages. hTERT has been studied for its potential role in delaying senescence, however telomere shortening is believed to not be the sole foundation of senescence as there are inconsistencies in telomere length and onset of senescence (Lundberg *et al.* 2000).

This project will focus on the use of Bmi1 to extend cell lifespan in primary human epithelial cells. Bmi1 is a gene which is endogenously expressed in airway cells (Protein Atlas, n.d.) and has been successfully used within our research group previously.

### 1.4.5 Previous use of Bmi1 to extend lifespan in primary airway epithelial cells within the research group

Torr *et al.* (2016) produced lentiviruses conferring constitutive Bmi1 over-expression to primary HBECs. These cell cultures were monitored for a period of up to 12 months and were able to retain airway epithelial characteristics at a much later passage than endogenous HBECs (see Fig. 1.4).

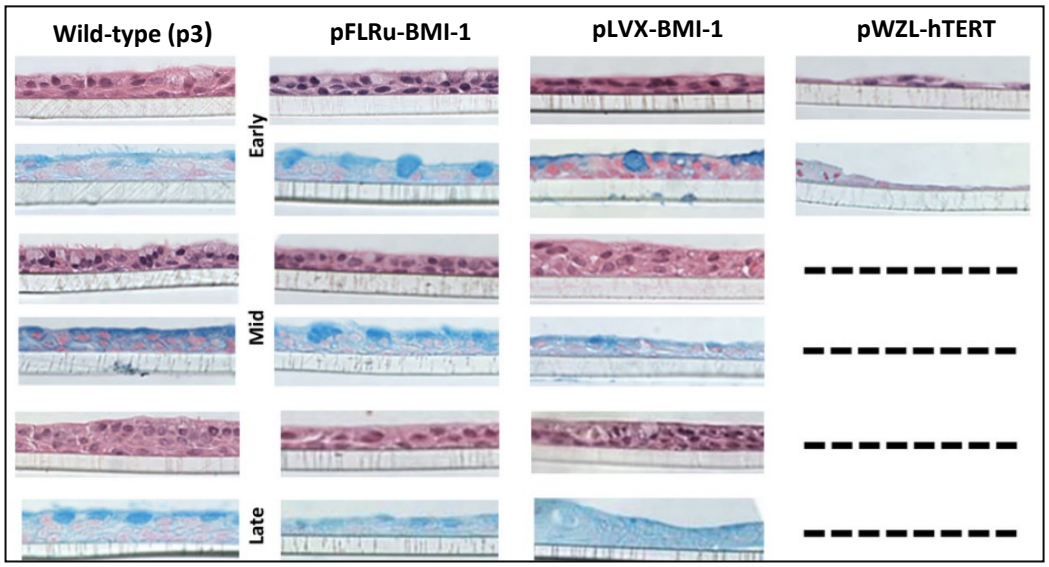


**Figure 1.4 Previously modified HBECs with constitutive Bmi1 over-expression retain the ability to form a pseudo-stratified layer at ALI and share similar morphology with matched WT cells at passage 3.** Early (p6), mid (p8-10) and late passage (p11-15) +Bmi1 HBECs shown. HBECs +hTERT failed to form successful monolayers at ALI (from Torr *et al*., 2016).

Over-expression of Bmi1 protein was accompanied by decreased protein expression of p16 and increased viability, but importantly modified HBECs were still able to differentiate at ALI and form a measurable TEER. Preliminary experiments were also conducted using over-expression of hTERT (an alternative candidate for extending cell lifespan) in HBECs but were not encouraging, with cells failing to grow at ALI (Fig. 1.4). The cells also possessed abnormal karyotypes unlike with Bmi1 alone and so the success of hTERT may be specific to the cell type used or the method of delivery. Therefore, research was directed away from hTERT to focus solely on Bmi1. This project is an extension of this research with the novel aspect of precision gene control.

### 1.4.6 Lentiviral genetic manipulation in mammalian cell culture

There are a range of methods which can be used to deliver genes to mammalian cells, however, this project makes use of lentiviral gene delivery.

Lentiviruses are a subtype of the retrovirus family, of which HIV is a member, and the viral infection mechanism has been adapted to deliver gene sequences into a desired mammalian cell, whilst avoiding an immune response (reviewed in Cockrell & Kafri, 2007). Lentiviruses allow delivery of a gene of interest into a wide variety of mammalian cells, with the advantage that the gene is permanently integrated into the host genome, therefore being maintained in future cell progeny. Secondly, they have the ability to infect non-dividing cells (reviewed in Connolly, 2002) which allows genetic modification of terminally differentiated cell types and thirdly, they result in a very high infection efficiency which is necessary for primary cell lines that can be difficult to transfect.

### 1.4.7 Unwanted side-effects of delaying cellular senescence may interfere with further research thus controlled expression is necessary

The most commonly studied function of Bmi1 is its inhibition of p16 and p14. However, Bmi1 does not function in a linear fashion alone, but global mapping analysis indicates that Bmi1 targets, to some extent, approximately 1536 genes (Meng *et al.,* 2010). Therefore, the effects of over-expressing Bmi1 need to be taken into consideration and thorough characterisation of the genetically engineered cells needs to be undertaken.

In order to minimise side-effects and prevent interference, it may be necessary to return Bmi1 expression to normal levels after the cells have been cultured for a sufficient amount of time. There are various options available to temporally control Bmi1 over-expression.

One such method is the cre-lox P system. This method relies on Cre-recombinase, an enzyme which facilitates DNA recombination at specific LoxP target sites which flank a gene of interest; the recombination event can be manipulated to either introduce or delete a gene sequence (reviewed in Sauer, 2006).

García-Escudero *et al.* (2010) aimed to incorporate cre-lox P technology, to reversibly deliver and over-express Bmi1 and various other genes in human

olfactory ensheathing glia such as Tag, shp53 and TERT, and then to cleave them out after a desired amount of time to see if the cells were capable of returning to normal. Their results showed that of the various genes examined, only a combination of Bmi1 and TERT was successful in delaying expression of senescence markers and avoiding any karyotypic alterations, whereas others could overcome proliferation constraints, but still expressed indications of senescence. There has also been some concern over the toxicity of Cre, which may need to be taken into consideration with appropriate controls (Schmidt-Supprian & Rajewsky, 2007). García-Escudero *et al.* (2010) found that in some instances the cre-recombinase or the cre-recombinase lentivector was detrimental to the cells and in the case of cells transduced with a Tag/TERT combination, the de-immortalisation process was highly toxic. On the other hand, BMI1/TERT expressing cells could successfully survive the process, suggesting that the success of this technique relies on the particular combination of genes expressed.

An alternative mechanism for switching expression on/off is to incorporate the use of an inducible gene expression system based on transcriptional regulation, where cells can be induced to over-express a gene such as Bmi1 and then induction can be discontinued when not required.

The Cumate Switch system (System Biosciences) will be used in this project and is explained in greater detail in Chapter 2.

As a brief overview, this system relies on two lentivectors, one containing your gene of interest (which will be integrated into the host genome) and another which encodes a CymR repressor protein which binds the operon upstream of your gene of interest and prevents transcription by steric blocking. The switch can then be controlled via addition of a molecule called cumate (see Fig. 1.5). Cumate binds to the repressor molecule and causes it to release the operon - allowing transcription to occur.

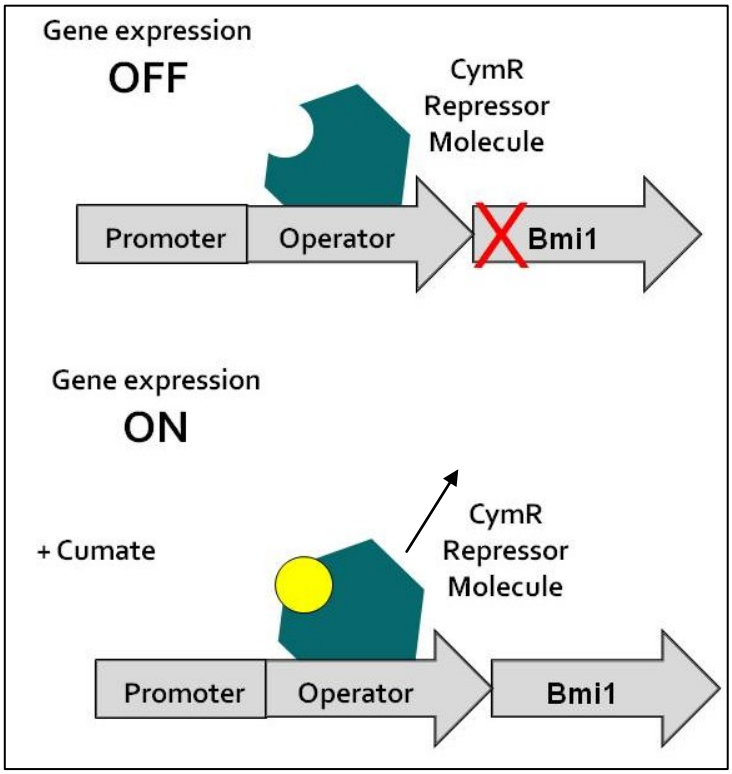


**Figure 1.5 Illustration of the Cumate Switch system to be used in this project.** The CymR virus encodes a repressor protein which binds to the operator upstream of the gene of interest (Bmi1 in this case). Repression is relieved by the addition of cumate which binds the repressor molecule and causes it to release the operator (Image adapted from System Biosciences, 2017).

Another option for inducible gene expression are tetracycline based systems which work in a similar fashion. These involve a Tet-controlled transactivator (tTA) and in the Tet-on system, the tTA is required to bind to a region upstream of the gene of interest to induce expression, but can only do so in the presence of tetracycline or a derivative (reviewed in Suzuki and Suzuki, 2011). This is a popular method also delivered via lentiviral vectors. However, a limitation of this system is that control of expression is 'leaky' (Wall *et al.,* 2016).

### 1.4.8 Utilisation of the Cumate Switch to control Bmi1 over-expression

For this project, the Cumate Switch system was chosen to deliver and over-express Bmi1 to primary human bronchial epithelial cells for its tight control of gene expression, ease of induction and reversible induction (System Biosciences, 2017). This is important as the aim of the project is not to immortalise the cells, but to temporarily give them a proliferative advantage which would be beneficial for cell, before returning level of Bmi1 to endogenous levels (without leakiness of expression) by removal of cumate.

The cells with Bmi1 over-expression can be maintained for additional passages, but over-expression can be reversed so that the epithelial cells can be studied without the interference of excess Bmi1. There may still be a baseline level of expression, so experiments must be carried out to determine the sensitivity of such a technique.

## 1.5 Rationale for the project

There is a need to develop new and efficient treatments for asthma, particularly for severe unresponsive individuals who may have a genetic predisposition to corticosteroid resistance. Much evidence shows that the asthmatic epithelium is considerably different from non-asthmatic epithelium and therefore highlights the importance of studying the airway epithelial cells in greater detail to further our understanding of asthma development, intercellular signalling and potential therapeutic opportunity.

Research into asthmatic epithelial cells is limited due to the difficulties in obtaining and culturing human primary airway cells. The current methods used to obtain bronchial epithelial cells are often invasive and potentially harmful, for example nasal brushings and biopsies, the risks of which can be life-threatening to patients. Furthermore, primary cells tend to be costly, variable and have a limited lifespan (Stewart *et al*., 2012) Therefore, there is the need for a reliable and reproducible cell line with which to further study the phenotypic changes of asthmatic epithelial cells and better understand progression and symptoms of the disease.

This project involves inducible over-expression of Bmi1 in order to temporarily extend the lifespan of primary human bronchial epithelial cells (HBECs). This will allow cell expansion of primary cells, for increased passages, to generate higher numbers of cells and then removal of induction to return Bmi1 expression to endogenous levels.

## 1.6 Overall aims of the MPhil

The aim of my project is to develop a method with which to delay replicative senescence, allowing the long-term study of human primary bronchial epithelial cells *in vitro*. This can be broken down into several stages:

- To generate an inducible Bmi1 switch system which will allow conditional gene control in primary human bronchial epithelial cells.
- To investigate the effects of elevated Bmi1 expression on airway epithelial cell barrier function.
- To investigate the global effects of Bmi1 over-expression in a human epithelial cell line using transcriptomic analyses.

This work initially began as a PhD, but due to health problems, I was not able to complete all of the work that I set out to do and subsequently decided to transfer to an MPhil. The original intentions have been outlined in this thesis to show the over-arching aims and relevance to respiratory research.

# 2. Development of second generation Bmi-1 expression vectors that allow inducible expression

## 2.1 Introduction

This chapter outlines the steps taken towards producing genetically modified +Bmi1 HBECs. The advantages of lentiviral gene delivery and an inducible system to deliver Bmi1 to HBECs were highlighted in Chapter 1.

Previously within the lab group (Torr *et al*., 2016), lentiviruses have been produced allowing constitutive over-expression of Bmi1. However, in order to minimise unwanted side-effects of Bmi1 over-expression, an inducible system was deemed more appropriate.

During this project, both inducible and constitutive systems have been produced for comparison. The constitutive plasmid used in this project differs from those previously used mainly in that it possesses a fluorescent reporter gene, allowing for ease in detection of positively infected cells.

### 2.1.1 Lentiviral Plasmids for delivery of Bmi1

The lentiviral plasmids chosen for this project are pCDH-CMV-MCS-EF1-copGFP (System Bioscience, catalogue number CD511B-1) which will constitutively express Bmi1 and SparQ$^{TM}$ (System Bioscience, catalogue number QM531A-2) which will inducibly express Bmi1 when cells are co-infected with a repressor virus, CymR (System Bioscience, catalogue number QM200PA-2) and exposed to cumate which prevents the repressor system. The plasmid maps for the vectors can be seen in Figure 2.1 and 2.2.

The pCDH-CMV-MCS-EF1-copGFP lentivector will be referred to as pCDH in the remaining text, SparQ$^{TM}$ as SparQ and CymR Repressor vector as CymR.

The lentiviruses generated in this project are second generation; the lentiviral genes required for a functional virus are separated onto 3 plasmids. For safety reasons, the virus produced will be replication incompetent.

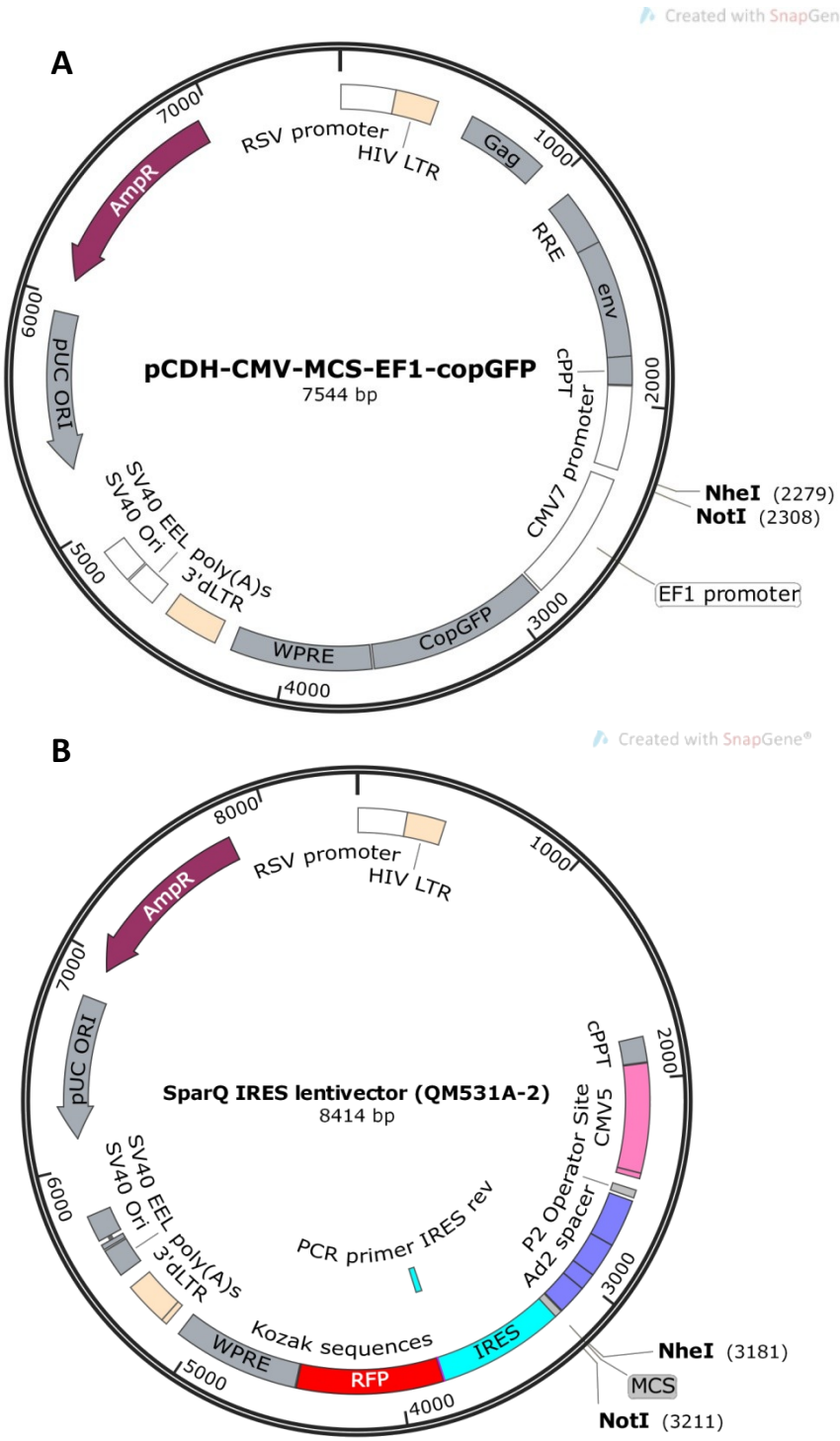


**Figure 2.1 Lentiviral vector plasmids utilised in this project and the restriction sites selected for inserting Bmi1. A) Constitutive expression vector pCDH-CMV-MCS-EF1-copGFP and B) inducible expression vector SparQ™.** The constitutive vector includes a CMV promoter and GFP reporter expression, whereas the inducible plasmid possesses a modified CMV promoter with Ad2 spacer including repressor binding site. An RFP reporter gene is also downstream from an internal ribosome entry site (IRES). Sequences were obtained from System Biosciences and plasmid maps constructed with SnapGene software (from GSL Biotech; available at snapgene.com).

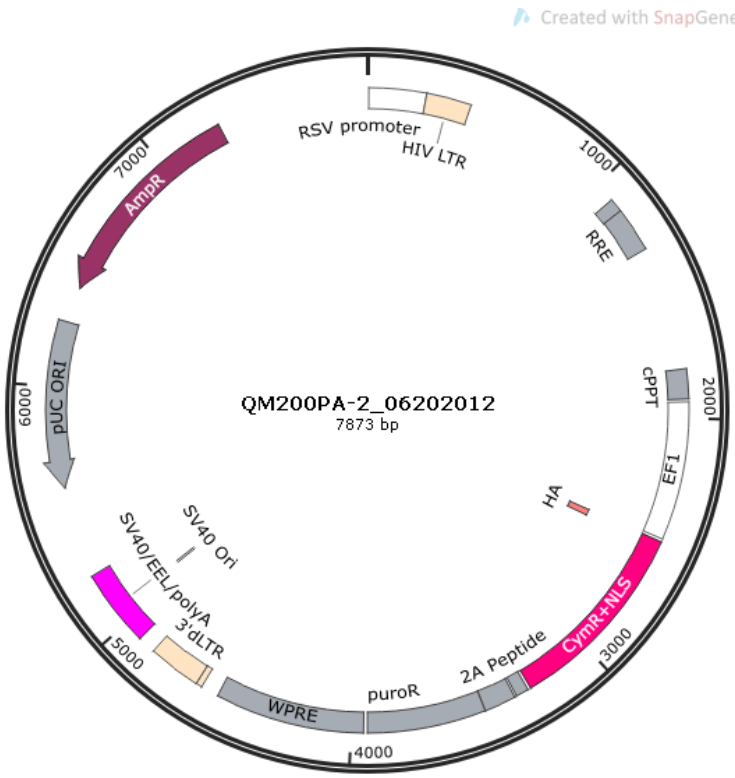


**Figure 2.2 The CymR Repressor Vector used to repress inducible expression.** The plasmid encodes a repressor protein which binds to the repressor binding site present on the SparQ inducible plasmid (upstream of the gene of interest) and causing expression of the gene of interest to be repressed. The CymR plasmid possesses a puromycin resistance gene which will be used to select CymR positively infected cells (plasmid map provided by System Biosciences using SnapGene)

The CymR virus produces a repressor protein which is able to bind to a region upstream of the operator (which will be integrated into the host genome). This blocks expression of the gene of interest from this modified CMV promoter. However, with the addition of a small molecule called cumate (which binds to the repressor) there is a conformational change in the repressor, causing it to release the DNA and allow expression (System Biosciences, 2017). Therefore, expression of the gene of interest can be controlled temporally by the addition and removal of cumate from the cell culture media.

The gene control used in the inducible system is derived from the *p-cmt* and *p-cym* operon of *Pseudomonas putida* and produced to be used in mammalian cell systems (Mullick *et al.*, 2006). Mullick *et al.* (2006) show that gene expression can be controlled in a dose dependent manner using this system. Cumate, also known as 4-isopropylbenzoate, is a small plant metabolite and non-toxic according to System Biosciences (2017). However, the potential effects on HBECs are unknown at this time.

### 2.1.2 Overview of methodology for this project

Fig. 2.3 shows how genetically modified HBECs have been produced using the constitutive and inducible lentiviral plasmids; from molecular biology through to lentiviral infections. The inducible system requires extra stages due to the dual infection with the SparQ-Bmi1 virus and CymR virus. At the end of this process, it would be ideal to possess a large stock of genetically modified HBECs with both the inducible and constitutive systems, preferably using cells from multiple donors to account for donor variation.

Fig. 2.4 highlights the characterisation techniques which will be used following production of genetically modified HBECs. These details will be expanded upon in Chapters 3 and 4.

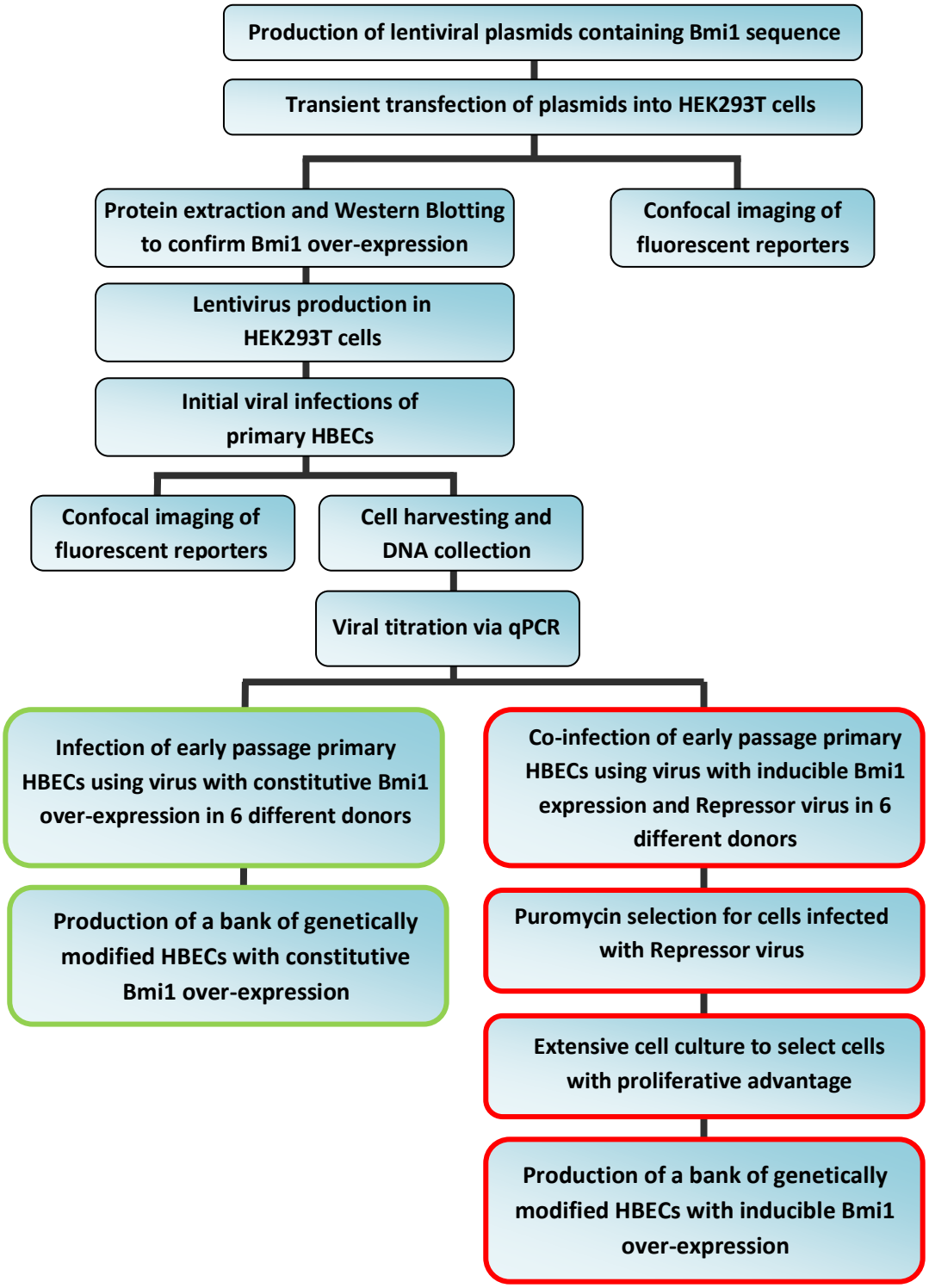


**Figure 2.3 Planned methodology for generation of a bank of genetically modified human bronchial epithelial cell lines.** An overview of the processes required in this project to generate Bmi1 over-expressing HBECs using constitutive and inducible lentiviral plasmids. The green and red boxes indicate the difference in methodologies for the constitutive (pCDH) and inducible (SparQ) cell lines respectively.

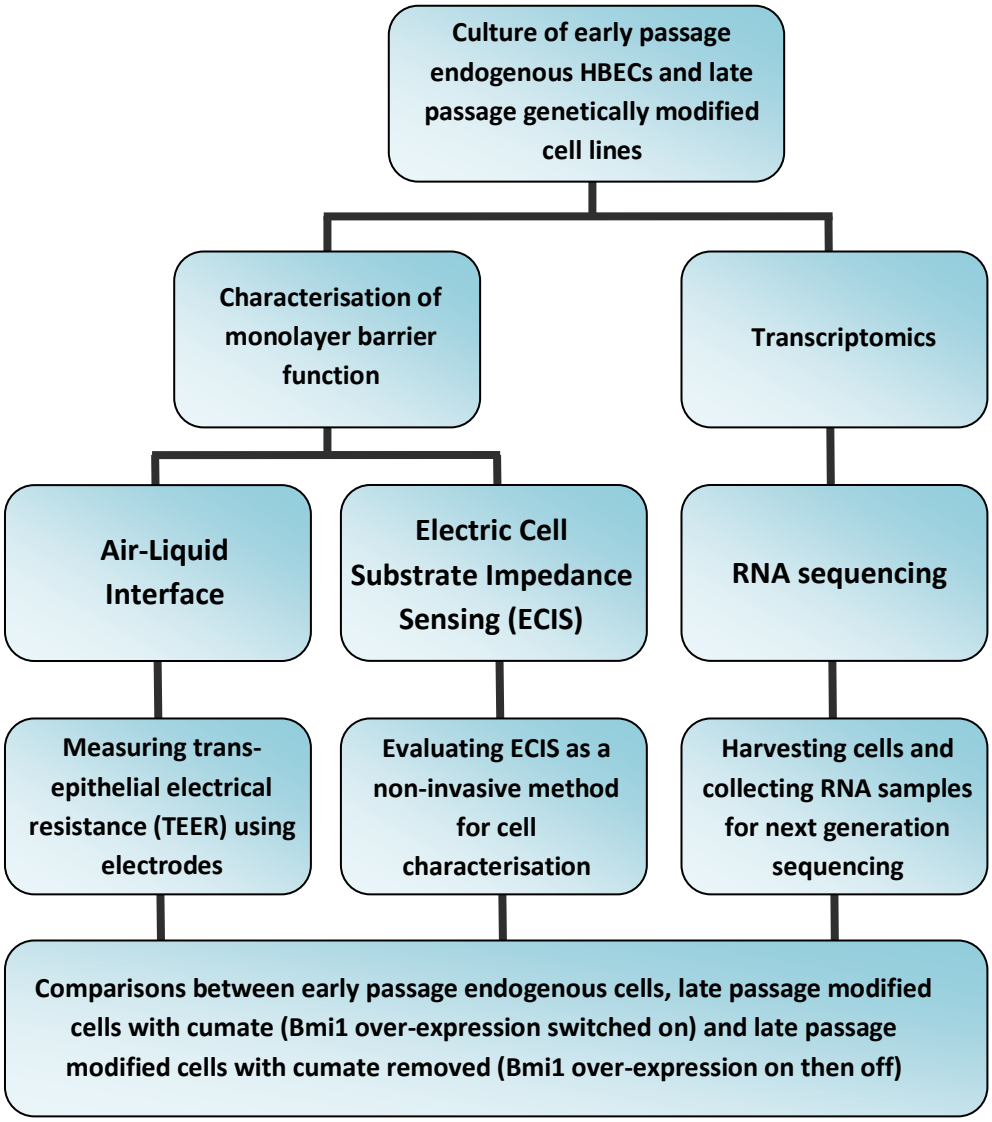


**Figure 2.4 Planned methodology for characterisation of genetically modified cell lines (Chapters 3 and 4).** Once genetically modified cell lines have been produced, they need to be characterised and compared to endogenous early passage HBECs. Air Liquid Interface and ECIS will be used to compare epithelial barrier function, whereas RNA sequencing will provide a more in depth view of how Bmi1 over-expression is modifying gene expression. Addition of cumate controls inducible expression of Bmi1 in modified cells. Therefore, it will also be important to observe differences in genetically modified cells with over-expression being repressed.

### 2.1.3 Strategies for lentiviral titration

Once the viruses have been produced, the next challenge will be to calculate the titre of each virus. The viral titre, or concentration, is required to ensure that a consistent dose of virus is used to infect cells and to determine the multiplicity of infection (MOI) or the 'expected number of gene transfer events per cell' (Andreadis *et al*., 2000). The SparQ cumate system protocol (System Biosciences, n.d.) recommends a 1:1 MOI ratio of CymR to SparQ-Bmi1 for dual infection.

There are a number of viral titration options available which have been reviewed in Geraerts *et al.* (2006) and a few are summarised below for the purpose of this project.

A commonly used titration technique involves using an Enzyme-linked immunosorbent assay (ELISA) to detect viral protein, in particular the p24 protein found on the nucleocapsid (outer shell) of the virus. The design of the assay is relatively expensive and has a major disadvantage in that the method does not distinguish between functional and non-functional vector particles (Geraerts *et al.,* 2006) - for example, viruses which have not assembled correctly but still possess the p24 antigen.

FACS (Fluorescence-activated cell sorting) can be used to separate cells with fluorescence via flow cytometry and is probably one of the simplest methods available. However, with regards to this project, not all of the viruses produced will have a fluorescent marker gene (the repressor virus incorporates puromycin selection instead of fluorescent expression) and it would be preferable to use the same titration method for each virus for consistency.

Finally, DNA analysis can be performed by lysing and extracting DNA from the virus-infected cells. The extracted DNA can then be probed via qPCR (see Section 2.2.5) for genes present on the lentiviral backbone. For example, commonly used target genes include WPRE (Woodchuck Hepatitis Virus Posttranscriptional Regulatory Element) and the LTR (long terminal repeat) region which flanks the gene of interest and aids genome integration (Geraerts *et al.* 2006). When the virus infects a cell, these genes are also incorporated into the cell genome along with the gene of interest. Therefore, the number of these copies relative to a 'single copy gene-specific reference gene', such as albumin, can be used to determine the initial viral titration (Barczak *et al.,* 2015), see Section 2.2.5. However, Geraerts *et al.* (2006) highlight that 'not all integrated vectors contribute to active gene expression' and that expression levels may vary.

Although there are some drawbacks to the latter method, it was deemed the most appropriate for this project. The LTR sequence will be present in all viruses used in this project allowing the same method to be utilised across all of the viruses produced. qPCR will provide evidence of viral infection and genome integration.

After the viruses have been titrated, the recommended dose can be used to infect HBECs and to determine the optimal infection conditions. Large stocks

of genetically modified HBECs can then be produced and stored in liquid nitrogen for future analysis (as shown in Fig. 2.4).

### 2.1.4 Aims of the chapter

- To generate lentiviruses conferring both inducible and constitutive Bmi1 over-expression
- To use these lentiviruses to successfully infect primary HBECs
- To titrate these viruses to determine an optimal infection dose for HBECs
- To generate a bank of genetically modified HBECs which over-express Bmi1 for further characterisation and ultimately for use in academic research and potential commercialisation.

## 2.2 Materials and methods

## 2.2.1 Molecular Biology

#### 2.2.1.1 Cloning strategy

Figure 2.5 shows a simplified overview of the cloning strategy used in this chapter. The human Bmi1 mRNA sequence is 978bp long (protein accession code: P35226 (UniProt, 2017)) and has 10 splice variants, only 4 of which produce viable proteins and 3 of which have a truncated coding region at the 3' end (Ensembl, 2017). The full length human Bmi1 cDNA was used in this project - previously used by Torr *et al.,* (2016) and originally obtained from Geneservice™ Mammalian Gene Collection.

#### 2.2.1.2 Polymerase Chain Reaction (PCR)

PCR was used to amplify the Bmi1 sequence from a previously constructed PFLRu lentiviral plasmid (Torr *et al.*, 2016). PCR exploits the DNA polymerase enzyme and involves cycling of various temperatures to denature and anneal the template DNA. DNA polymerase requires double stranded DNA to initiate DNA replication and therefore primers are needed to flank the sequence of interest. Complementary bases are then added to the 3' end of the primer as the polymerase moves along the template strand. The template and newly synthesised strand separate at the next heating stage to act as subsequent templates for the next cycle of synthesis, resulting in an exponential chain reaction (reviewed in McPherson & Moller, 2006).

Two sets of primers were designed to amplify Bmi1 and to incorporate restriction sites NotI (3’ end) and NheI (5’ end) along with a Kozak sequence upstream of Bmi1 (recommended by System Biosciences (2012) for improved translation efficiency) shown in Table 2.1. Set 1 was used by Torr *et al.* (2016) and incorporates a base pair change (shown in red in Table 2.1). This will result in a silent mutation at position 966 of the Bmi1 sequence (GCA to GCT, both encoding alanine) and was not amended in order to match the sequence used in the earlier publication from the research group (Torr *et al*., 2016).

| | | |
|---|---|---|
| Set 1 | Forward Bmi1 Primer | ACT(G^CTAGC)**GCCTCC**ATGCATCGAACAACGAGA |
| | Reverse Bmi1 Primer | ACTC(CG^CCGGCG)TCAACCAGAAGAAGTAGC |
| Set 2 | Forward Bmi1 Primer | ACT(G^CTAGC)**GCCACC**ATGCATCGAACAACGAGA |
| | Reverse Bmi1 Primer | ACGT(GCCGGCCGC)TCAACCAAGAAGTTGC |

**Table 2.1 Primer sequences used to amplify Bmi1.** The incorporated restriction sites are shown in parentheses; G^CTAGC for NheI and CG^CCGGCG for NotI. The red letter indicates a nucleotide in the primer which will result in a synonymous base pair change at position 966 following PCR to match the sequence used by Torr *et al.* (2016). The Kozak sequence which will be upstream of Bmi1 is shown in bold.

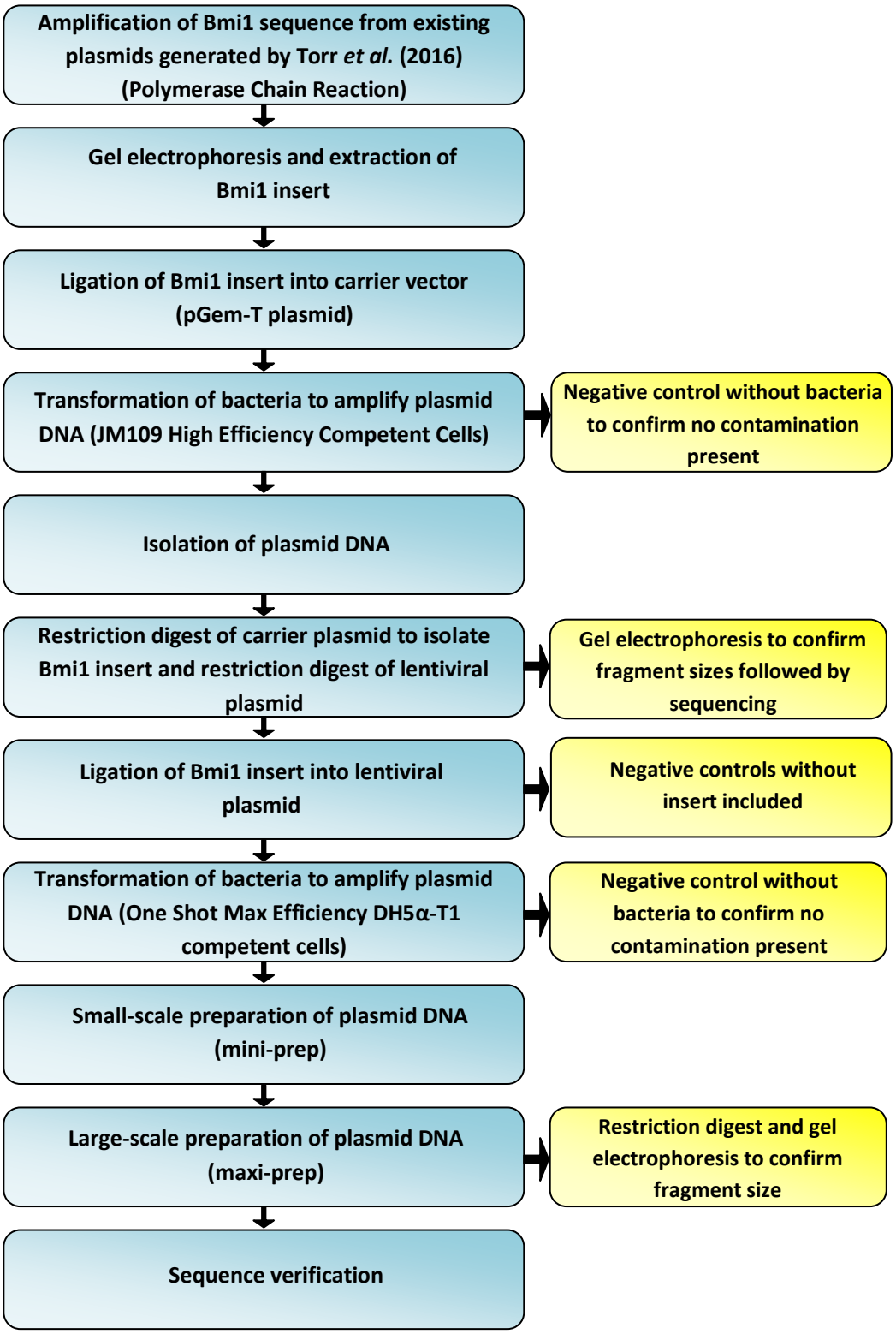


**Figure 2.5 Overview of molecular biology cloning strategy used to generate lentiviral plasmids containing the Bmi1 sequence.** These methods will be utilised at the start of the project in order to produce the lentiviral DNA plasmids which will later be packaged into Bmi1 lentiviruses. Boxes in red show the quality control checks performed at each stage.

The template used for amplification was a previously constructed PFLRu-Bmi1 lentivirus plasmid (by Torr *et al*., 2016) conferring constitutive Bmi1 expression.

The Bmi1 sequence was amplified via PCR using the Platinum® Taq Polymerase Kit (Invitrogen). The Taq Polymerase used to synthesise the DNA in this kit is derived from Pyrococcus species which possess 3->5 exonuclease activity; this provides a higher fidelity proof-reading mechanism for increased fidelity (Thermofisher Scientific, n.d. -c). Reagents and cycling times are shown below in Table 2.2 and 2.3:

| | |
|---|---|
| Water | 36.75µl |
| Biotaq Buffer (10x) | 5µl |
| 50mM Mg2+ | 2µl |
| 5mM dNTPs | 2µl |
| Platinum Taq Polymerase (5U/µl) | 0.25µl |
| 10µM Forward Primer | 1µl |
| 10µM Reverse Primer | 1µl |
| Template containing Bmi1 | 2µl |

**Table 2.2 Volumes of reagent used to amplify the Bmi1 sequence.** The Bmi1 sequence was amplified from a previously constructed PFLRu-Bmi1 lentiviral plasmid (by Torr *et al*., 2016) by PCR utilising the Platinum® Taq Polymerase Kit (Invitrogen).

| Temperature | Time |
|---|---|
| 94°C | 5 minutes |
| 94°C | 30 seconds |
| 60°C | 60 seconds x35 |
| 72°C | cycles |
| | 60 seconds |
| 72°C | 10 minutes |
| 10°C | Hold |

**Table 2.3 PCR thermal cycling conditions used for amplification of the Bmi1 sequence.** The template used for amplification is a previously constructed PFLRu-Bmi1 lentiviral plasmid (by Torr *et al.,* 2016).

#### 2.2.1.3 Gel electrophoresis

The product was analysed by gel electrophoresis using a 1% agarose gel and addition of 6x Orange G loading dye (1 in 6 dilution). This technique relies on preparing a porous agarose gel (see Appendix for protocol). An electric current is applied to the gel and the fragments of negatively charged DNA are driven through the gel, with larger fragments taking longer to travel through the pores, thus separating the fragments by size (reviewed in Smith, 1996). The gel is then imaged under an ultraviolet light. For gel extraction, a UV light box was used (8 Watt, 312nm UV bulbs, SLS catalogue no. ULT4042)

to visualise the bands. To capture images of gels, GeneGenius Gel Documentation (Syngene) software was used.

#### 2.2.1.4 Gel extraction

After DNA had been separated by size using gel electrophoresis, the correct molecular weight sized band of DNA was excised with a scalpel from the gel and purified using QIAGEN's QIAquick Gel Extraction Kit as per the manufacturer's instructions and eluted in 30µl of water. This gel extraction procedure relies on a silica membrane to bind DNA and purification steps to remove a range of contaminants including primers, ethidium bromide and agarose (QIAGEN, 2017).

#### 2.2.1.5 Ligation

Platinum® Taq polymerase which was used for PCR has increased specificity and adds a 3' A overhang to the PCR products (Thermo Fisher Scientific, 2015). Therefore, the product could be ligated directly into a ®-T vector (containing a 3' T overhang), a carrier vector for amplification (see Fig. 2.6). The ligation procedure involves joining together the insert (Bmi1) and the pGEM-T vector, via the action of the DNA Ligase enzyme. Ligation was performed as recommended by the pGEM-T Easy Vector System I Kit (Promega), with a control containing water instead of insert:

a. PCR product/Control Insert + sterile water
b. 5µl 2x Rapid Ligation Buffer
c. 1µl pGEM-T vector (50ng)
d. 1µl T4 DNA ligase (1–3u/µl)
e. Total volume 10µl

The reactions were mixed Reactions were left for 1 hour at 25˚C.

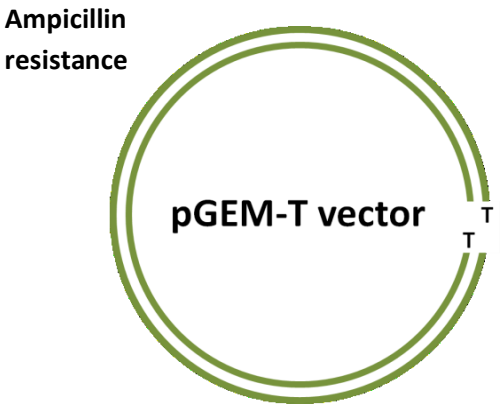


**Figure 2.6 Illustration of the pGEM-T vector with 3' T overhang.** Taq Polymerase leaves a 3'-overhang on PCR products, therefore the pGEM-T vector possesses a complementary 3'-overhang which eases ligation with the PCR product (Bmi1).

#### 2.2.1.6 Transformation

Transformation allows exogenous plasmid DNA to be introduced into bacteria, which can then be amplified by the bacteria. 2µl of ligation mix prepared in Section 2.2.2.5 was added to 50µl of JM109 High Efficiency Competent Cells (Promega). JM109 High Efficiency Competent Cells 'minimize recombination and improve the quality of plasmid DNA' during transformation (Promega, 2017). The cells were left on ice for 20 minutes, heat shocked at 42˚C for 45 seconds and returned to ice for 2 minutes - disrupting the cell membrane to allow for DNA delivery. 950µl of room temperature SOC medium was added to each reaction and incubated for 1.5 hours at 37˚C (shaking at 150rpm). 100µl of each transformation mix was pipetted onto (100µM ampicillin) agar plates and incubated overnight at 37˚C. Colonies were selected (negative plates contained no colonies) and added to 5ml of LB broth (+100µM ampicillin). The vials were left to shake at 200rpm and 37˚C overnight (see Appendix for agar plate and LB broth method).

#### 2.2.1.7 Small scale preparation of plasmid DNA (Mini-Prep)

Plasmid DNA was isolated from plasmid-transformed competent cells and purified by Mini-Prep. 1.4ml of the bacterial broth was taken into a tube and centrifuged at 10,000g for 5 minutes. DNA was isolated from the pellet and purified using the Wizard Plus SV Minipreps DNA purification system kit (Promega) following the kit protocol (Promega, 2010). The kit contains solutions to lyse the bacteria and columns to collect the DNA. DNA was eluted from the columns in 100µl of nuclease free water.

#### 2.2.1.8 Restriction digest of recombinant DNA to confirm presence of insert

Restriction endonucleases are utilised to cut DNA at specific target sequences. Having incorporated the relevant target sequences for NotI and NheI into the primers used for PCR, the Bmi1 sequence was now flanked by these two restriction sites. A restriction digest was performed on the pGEM-T-Bmi1 plasmid to see if the insert was present (if successfully ligated, then an NheI restriction site should be at the 5’ end of the Bmi1 sequence and NotI at the 3’ end), producing an insert of approximately 978bp. Reactions were set up as follows (per tube):

a. 5µl CutSmart Restriction Buffer
b. 0.5µl Nhe I-HF (10u/µl)
c. 0.5µl Not I-HF (10u/µl)
d. DNA (pGEM-T Bmi1)
e. 42µl water
f. Total volume 50µl

Reactions were left at 37˚C for 1 hour and analysed by gel electrophoresis (as outlined in Section 2.2.2.3) at 60V along with diluted uncut pGEM-T-Bmi1 plasmid for comparison.

#### 2.2.1.9 Sanger sequencing of ligated plasmids

Sanger sequencing relies on the action of DNA polymerase. DNA polymerase uses a template strand of DNA to create a new strand which is complementary to the original. It adds new nucleotides to the 3'-hydroxyl group of the previous nucleotide on the newly synthesised strand. dideoxynucleotides (ddNTPs) lack a 3'-hydroxyl group, necessary for addition of the next nucleotide. Therefore, when a ddNTP is present and incorporated into the strand, it causes extension to be terminated. By fluorescently labelling these ddNTPs and using them to create various fragment lengths, it is possible to determine the order of the sequence (Sanger *et al*., 1977).

Big Dye termination mix (Applied Biosystems) was utilised which consists of the relevant ddNTPs and enzymes required for sequencing.

pGEM-T-Bmi1 plasmid samples containing a correctly sized insert were prepared for sequencing. Reactions were set up containing:

a. 0.5µl Big Dye termination mix (Applied Biosystems)
b. 3.5µl BetterBase
c. 1µM M13 primer
d. 4µl water
e. pGEM-T-Bmi1 ligated plasmid

Reactions were placed in a thermal cycler with these conditions:

| Temperature | Time |
|---|---|
| 96$^{o}$C | 30 seconds |
| 50$^{o}$C | 15 seconds x25 |
| 60$^{o}$C | cycles |
| | 4 minutes |
| 28$^{o}$C | 60 seconds |
| 10$^{o}$C | Hold |

**Table 2.4 Cycling conditions used to prepare DNA for sequencing in a thermal cycler.** After ligating the Bmi1 sequence into the pGEM-T vector, the plasmid needed sequencing to confirm Bmi1 had been inserted correctly.

#### 2.2.1.10 Purification of sequencing reactions

The reaction was then precipitated as follows:

1. 2µl of 3M sodium acetate (pH 5.2) and 2µl of 125mM EDTA (pH 8) was added to the reaction and incubated for 15 minutes at 28˚C

2. 50µl of 100% ethanol was added and mixed. The tubes were centrifuged for 30 minutes at 13,000rcf.
3. The supernatant was discarded and 250µl of 70% ethanol was added. This was centrifuged for 5 minutes at 13,000rcf. Supernatant was discarded and the pellet left to air dry.
4. Samples were taken to the University of Nottingham DNA Sequencing Facility where a 3130xl ABI PRISM Genetic Analyzer (Life Technologies) was used for analysis. The output was analysed using NCBI BLAST (Altschul *et al.,* 1997) and EMBL-EBI ClustalW (Larkin *et al*., 2007).

#### 2.2.1.11 Sub-cloning of the Bmi1 expression cassette from pGEM-T into pCDH and SparQ vectors

Plasmid DNA containing Bmi1 and the lentiviral vectors to be used in this project - constitutive vector (pCDH) and inducible vector (SparQ) were restriction digested as follows:

a. 10µl CutSmart Restriction Buffer
b. 1µl Nhe I-HF (10u/µl)
c. 1µl Not I-HF (10u/µl)
d. DNA (1 tube of pGEM-T-Bmi1 and 1 of vector)
e. 84µl sterile water
f. Total volume 100µl

Reactions were left at 37$^{o}$C for 1 hour and analysed by gel electrophoresis. The insert (Bmi1) from the pGEM-T vector and the cut lentiviral vector were excised. A gel extraction was performed as before to purify the fragments using QIAGEN gel extraction kit (for microcentrifuge) and eluted in 30µl of water.

Ligation reactions between the lentivector and Bmi1 fragments were set up as follows:

a) 1µl T4 DNA ligase (500 units, Promega catalogue no. M179A)
b) 1µl ligase buffer
c) Ratio of vector:insert (from gel extraction)
d) Made up to 10µl with water

The following ratios were used (vector:insert): 1µl:6µl, 1µl:3µl, 1µl:1µl, 3µl:1µl, 6µl:1µl and left at 22˚C for 3 hours. Controls were also set up containing water instead of insert.

#### 2.2.1.12 Bacterial transformation of lentiviral plasmids

Reactions were transformed into One Shot Max Efficiency DH5α-T1 competent cells kit following the kit protocol. The One Shot kit is beneficial in that it provides resistance to bacteriophages (T1 and T5) and cleaner products downstream (Thermofisher Scientific, n.d. -b).

1. 5µl of ligation mix was added to 25µl of competent cells. A negative (water only) and positive control (pUC plasmid included in kit) were also performed.
2. The cells were left for 30 minutes on ice, before heat-shocking at 42˚C and being returned to ice for 2 minutes.
3. 125µl of SOC media (Fisher, VX15544034) was added to each reaction. The reactions were incubated at 37˚C for 1 hour shaken at 225rpm in Sanyo Gallenkamp Heated Orbital Incubator (Model: IOX402.XX1.C).

The mix was spread onto agar plates (+ampicillin) and incubated at 37˚C overnight. Colonies were selected and cultured in LB broth overnight. DNA was purified from the bacterial broth and restriction digested as before.

It was later decided to modify both inserts to contain the unique bp modification (contained in the SparQ vector.

#### 2.2.1.13 Large-scale preparation of plasmid DNA (Maxi-prep)

A maxiprep was utilised to obtain a higher DNA yield. Once lentiviral plasmids were achieved containing the Bmi1 insert, individual colonies were cultured in LB broth and added to fresh LB broth the following day at a higher volume of 100-250ml.

Plasmids were purified using QIAGEN maxiprep kit following the kit protocol. The resultant DNA pellet was re-suspended in 500-600µl of purified water, quantified via nanodrop (using Nanodrop 2000c UV/IV Spectrophotometer, Thermo Scientific) and sequence verified as before.

## 2.2.2 Genetic manipulation of cells

### 2.2.2.1 Cell culture

All mammalian cells were incubated at 37$^{o}$C, 5% $CO_2$. Media was changed every 2-3days. Cells were detached from flasks using Trypsin-EDTA (0.05% trypsin, 0.02% EDTA. Sigma T2934).

HEK293T cells

HEK293T cells were grown in Dulbecco's Modified Eagle's Medium with 10% Fetal Calf Serum (FCS, Sigma, C8056) and 1% Penicillin-Streptomycin (10,000 units penicillin and 10mg streptomycin/ml Sigma, P0781) unless stated otherwise (during lentiviral packaging, FCS is reduced to 2%). The HEK293T cells were derived from those used by Torr *et al*. (2016) and were used at passages 19, 22 and 31 for transient transfection and passage 21 for lentiviral production.

HBECs

HBECs were supplied by Clonetics (Lonza). The donor used was a 43 year old non-smoking Caucasian male, HIV and Hepatitis B negative. HBECs were cultured in Bronchial Epithelial Growth Media (BEGM, Lonza, CC-3170) which consists of Bronchial Epithelial Basal Media supplemented with the SingleQuot Kit (as described in Slater *et al.*, 2016), minus Gentamicin and Amphotericin-B. Trypsin inhibitor (Invitrogen, 17075-029) was used with HBECs. HBECs were at Passage 4 for lentiviral infections.

Cryopreservation

HBECs were frozen in 1ml of media, 10% DMSO at 250,000 cells and stored in liquid nitrogen for long term storage.

### 2.2.2.2 Transient Transfection in HEK293T cells

Transient transfection allows temporary introduction of exogenous DNA into actively dividing mammalian cells. As the DNA is not incorporated into the genome, it is gradually lost from the cell during cell division. Transient transfection provides a quick method to determine whether the plasmids are functioning before packaging them into lentiviruses.

HEK293T cells were cultured in T75 flasks and upon reaching confluency were seeded into 6 well plates at a density of 200,000 cells per well. At approximately 50-80% confluency, the cells were transfected using TransIT-LT1 (Mirus Bio, catalogue number MIR2300) at a ratio of 3µl TransIT:1µg DNA as per the product manual with the SparQ-Bmi1 and pCDH-Bmi1 plasmids. Plasmids containing inserts were corrected to adjust for the

difference in molar ratio. The transfection mix was added drop-wise to the cells.

### 2.2.2.3 Lentiviral production in HEK293T cells

The protocol for lentiviral production is based on that used by Torr *et al.* (2016).

The plasmids involved in lentiviral production possess genes from the Feline Immunodeficiency Virus (System Biosciences, n.d.). For safety reasons, in second generation systems the genes required to produce a functional virus are separated onto 3 distinct plasmids: a lentiviral transfer plasmid containing the gene of interest and long terminal repeats, an envelope plasmid containing the ENV gene and a packaging plasmid containing the genes GAG, POL, REV and TAT (Addgene, n.d.) as shown in Fig. 2.7.

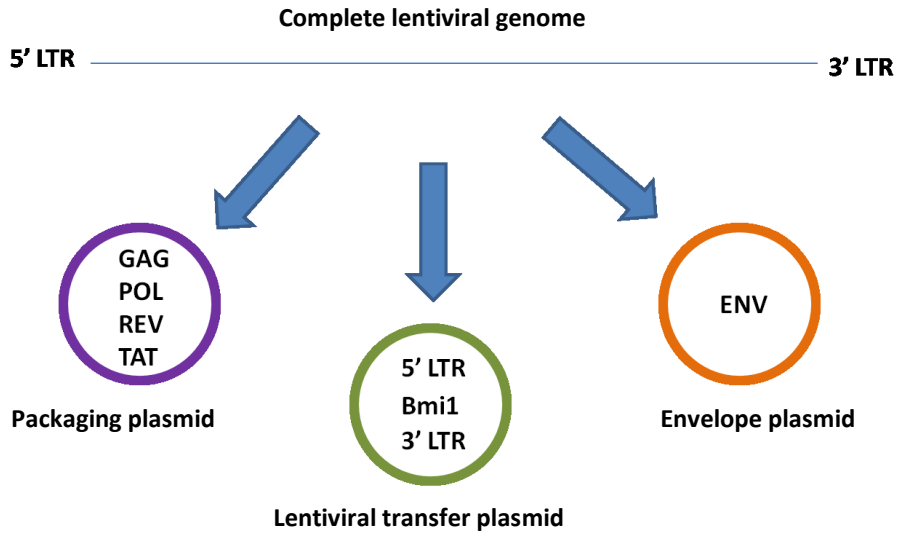


**Figure 2.7 Schematic illustrating how the lentivirus genome is separated onto three distinct plasmids (based on Addgene, n.d.).** The packaging and envelope plasmids consist of the genes required to assemble a functional lentivirus and the lentiviral transfer plasmid contains the gene of interest (Bmi1) along with Long Terminal Repeats required for integration into the host genome.

### 2.2.2.4 Packaging of lentiviruses

Functional lentiviruses were produced in HEK293T cells. This involved co-transfecting the lentiviral plasmid along with the packaging (pCMV delta R8.91) and envelope plasmid (pCMV-VSV-G) as outlined in Torr *et al.* (2016).

HEK293T cells were seeded into 10cm dishes at a density of 2 million cells per dish. One dish was used per virus. Before transfection, the media on the cells was changed for fresh media with 2% FCS, 1% Pen/Strep.

As detailed in Table 2.5, 10µg of total DNA was required for each dish; 5µg of the lentiviral packaging and envelope vectors at an 8:1 ratio (4.4µg packaging, 0.6µg envelope) and 5µg of the lentiviral vector (with or without gene of interest) as used by Torr *et al.* (2016).

| Type of plasmid | Name of plasmid | ng of DNA needed per tube |
|---|---|---|
| Envelope Plasmid | pCMV-VSV-G | 600 |
| Packaging Plasmid | pCMV delta R8.91 | 4400 |
| Lentiviral Transfer Plasmid | pCDH-copGFP empty plasmid (constitutive) | 5000 |
| Lentiviral Transfer Plasmid | pCDH-copGFP-Bmi1 (constitutive) | 5000 |
| Lentiviral Transfer Plasmid | pCDH-CuO-MCS-IRES-RFP (SparQ) empty plasmid (inducible) | 5000 |
| Lentiviral Transfer Plasmid | pCDH-CuO-MCS-IRES-RFP (SparQ)-Bmi1 (inducible) | 5000 |
| Lentiviral Transfer Plasmid | pCDH-EF1-CymR-T2A-Puro | 5000 |

**Table 2.5 Quantities of plasmids required for lentiviral packaging reactions.** For each lentiviral packaging reaction, a specific ratio (8:1) of packaging (pCMV delta R8.91): envelope (pCMV-VSV-G) plasmid was required along with 5000ng of one of the Lentiviral Transfer Plasmids. Five different lentiviruses were packaged, using the: constitutive plasmid +/- Bmi1, inducible plasmid +/- Bmi1 and the repressor plasmid (CymR).

A transfection mix was set up as follows for each virus:

- 800µl Optimem (Fisher, Catalogue no. 10149832)
- 10µg DNA (lentiviral transfer plasmid + envelope plasmid + packaging plasmid)
- 18µl of TransIT-LT1

This was incubated at room temperature for 30 minutes and added drop-wise to the cells. After 48 hours, the supernatant was collected and the cells were provided with fresh media. The media was also collected the following day and the two samples pooled together. Supernatant samples containing live virus were filtered through a 0.45µm filter to remove cell debris. The filtrate was centrifuged at 20,000rpm for 3.5 hours at 4$^{o}$C. The supernatant was discarded and the pellet containing the virus re-suspended in 1ml of BEGM. The virus was aliquoted and stored at -80$^{o}$C until required.

#### 2.2.2.5 Preliminary infection of HBEC culture

Infections were performed in 6 well plates in passage 4 HBECs. All repeats were performed in cells from the same donor.

HBECs were seeded at a density of 100,000 cells per well. On the day of infection, media was removed and replaced with 800µl BEGM (+2µg/ml of polybrene). Viruses were thawed and a range of volume were added drop-wise to the cells. The doses included 1µl, 2.5µl, 5µl and 7.5µl of virus based on previous experiments within the lab group using this infection protocol with HBECs.

The infected cells were rocked from side to side at intervals of approximately every 30 minutes for the next 2 hours to increase contact between the virus and the cells. After 6.5 hours, media was replaced without polybrene. Media was changed every 2-3 days until 10 days post infection, when the cells were deemed to be virus-free and no longer infectious.

### 2.2.3 Imaging

A Zeiss Axio-Observer D1 microscope was used with Volocity software to capture fluorescent images. Lasers are used to excite the reporter proteins which emit fluorescence at a particular wavelength that can be detected. To detect GFP in pCDH-Bmi1 infected/transfected cells, an excitation wavelength of 491nm was used. For detection of RFP in SparQ-Bmi1 infected/transfected cells, an excitation wavelength of 568nm was used.

HEK293T cells were imaged 24 hours post-transfection. Cell lysates were collected for future analysis of protein expression.

Lentiviral infected HBECs were imaged ten days post-infection to capture fluorescence. Phase-contrast images were taken to capture 3D structure using a Nikon Diaphot 300 Inverted Microscope with SPOT RT3 2MP CCD Slider Digital Camera attached and SPOT software.

#### 2.2.3.1 Fluorescent image analysis

Fluorescent images were analysed using ImageJ. There were 2-5 images taken of each well. The mean grey scale function was used to quantitatively measure the fluorescence of the cells using images of equal area. The mean grey scale function converts RGB images into greyscale and calculates the mean value, allowing direct comparisons to be made between the brightness of different images. The raw data was plotted onto a graph across a range of infection doses using GraphPad Prism.

## 2.2.4 Protein analyses

### 2.2.4.1 Western Blotting to confirm Bmi1 over-expression

Western Blotting involves separating proteins by molecular weight on a gel and transferring the protein bands onto a PVDF membrane. The membrane is probed by primary antibodies which specifically bind the protein of interest and unbound antibody is later removed. There are various methods which then allow visualisation of the target protein, such as fluorescent secondary antibodies, but in this case enzyme-labelled secondary antibodies are used which bind to the target primary antibodies and produce chemiluminescence when subsequently exposed to the appropriate substrate (Thermofisher Scientific, n.d -d).

In order to prepare the samples, the cell lysates of transfected cells were washed with 2ml cold PBS and collected by addition of 100µl SDS loading dye and use of a cell scraper. They were stored at -80$^{o}$C. Initial blots appeared overloaded, so samples were first diluted 1 in 5 and a smaller volume loaded into wells. Gels were made (see Appendix for details of gels and solutions). Before loading, protein samples were heated to 95$^{o}$C for 5 minutes and centrifuged at 13,000rpm for 3 minutes.

The gel was transferred onto a PVDF membrane (Millipore) in transfer buffer and blocked overnight with 5% milk in TBST. After washing with TBST, the membrane was treated with primary antibody overnight as shown in Table 2.6. Two gels were run in duplicate and treated separately, one with anti-Bmi1 and the other with anti-beta actin antibody.

The membrane was washed three times and treated with secondary antibody for one hour in darkness.

### 2.2.4.2 Enhanced Chemiluminescence (ECL)

The membrane was re-washed and treated with ECL$^{TM}$ reagents (GE Healthcare, catalogue number RPN203E). ECL is a technique used to visualise the proteins. The secondary antibody is horseradish peroxidase (HRP)-conjugated and when in the presence of hydrogen peroxide, HRP oxidises luminol (a chemiluminescent substrate) causing an emission of light relative to the amount of antibody-bound protein present (reviewed in Kurien & Scofield, 2005). This emission can then be detected with photographic film and developed.

| | Name | Dilution in 5% milk in TBST | Catalogue number |
|---|---|---|---|
| **Primary Antibody** | Mouse anti Bmi1 clone F6 IgG | 1 in 2000 | 05-637 (Millipore) |
| **Secondary Antibody** | Anti- Mouse HRP-conjugated antibody | 1 in 1000 | HAF018 (R&D) |
| **Primary Antibody** | Anti-beta actin | 1 in 2000 | ab8227 (Abcam) |
| **Secondary Antibody** | Anti- Rabbit HRP-conjugated antibody | 1 in 1000 | HAF008 (R&D) |

**Table 2.6 Antibodies and dilutions used for Western Blotting of HEK293T cell lysates.** To confirm that Bmi1 protein was being produced in transfected HEK293T cells, a mouse anti-Bmi1 antibody was used to probe cell lysates and a rabbit anti-beta actin antibody as a reference. Anti- mouse and anti-rabbit secondary antibodies were then used respectively to detect the primary antibodies.

#### 2.2.4.3 Quantification of protein expression level using densitometry

The blot was scanned to obtain a digital copy. The image was converted to black and white in Microsoft Office Picture Manager by changing the hue and saturation settings to -100. Image J was utilised to perform densitometry.

The colours were inverted to make the bands white on a black background. This technique relies on measuring the greyscale of each band. In greyscale, the pixel values range from 0-255, where zero is pure black and 255 is pure white. Therefore, in this case, the higher the pixel value, the more protein present.

The background of the Western Blot image was subtracted to provide a constant background and contrast was enhanced using the default settings of ImageJ. A box was drawn around the largest protein band and mean grey scale calculated. The same sized box was used to measure each band to ensure the same sized area was analysed. The values for the Bmi1 bands were divided by the values for beta actin in the corresponding lanes for normalisation.

## 2.2.5 Quantifying lentiviral titre using qPCR

### 2.2.5.1 Isolation of DNA to determine lentivirus titres

DNA was collected from HBEC cultures 10 days post-infection. HBECs were detached with trypsin and centrifuged for 5 minutes at 500rcf. The supernatants were discarded and the pellet stored at -80$^{o}$C overnight. DNA was extracted using QIAamp DNA mini and Blood Mini kit (QIAGEN) as per the instruction manual. Taqman quantitative PCR (qPCR) was utilised to measure the amount of product synthesised.

### 2.2.5.2 TAQMAN qPCR to quantify copies of viral LTR sequence

TAQMAN qPCR is based on the research of Holland *et al*. (1991). In the context of this study, the qPCR assay relies on a probe consisting of a FAM fluorophore and a TAMRA quencher. In close proximity, the quencher quenches the fluorescence released by the fluorophore. As the DNA polymerase moves along the template strand, it causes the probe to be displaced which results in the fluorophore being separated from the TAMRA. This in turn allows the fluorophore to fluoresce, the intensity of which can subsequently be detected and recorded.

To calculate viral titre, primers and probes were used (LTR primer and probe sequence obtained from Geraerts *et al.,* 2006) to perform qPCR using a gene on the lentiviral backbone (5'LTR). The sequences were analysed using BLAST (Altschul *et al.,* 1997) and NetPrimer (Premier Biosoft International) (Table 2.7) and can be visualised mapped against the lentiviral backbone in Fig 2.8.

| Gene used | Primer Sequence (5'->3') | BLAST results |
|---|---|---|
| LTR | F) TGTGTGCCCGTCTGTTGTGT | Only recognised in HIV isolates |
| LTR | R) GAGTCCTGCGTCGAGAGAGC | Only recognised in HIV isolates/cloning vectors |
| Probe | FAM-CAGTGGCGCCCGAACAGGGA-TAMRA | Only recognised in HIV isolates/cloning vectors |

**Table 2.7 LTR primer and probe sequences used for lentiviral titration via qPCR.** The lentiviruses used in this project all possess the LTR sequence, a region common in the backbone of many lentiviral vectors. Therefore DNA isolated from infected cells will be probed using this target region. These primer and probe sequences were initially used successfully for lentiviral titration and designed by Geraerts *et al.* (2009).

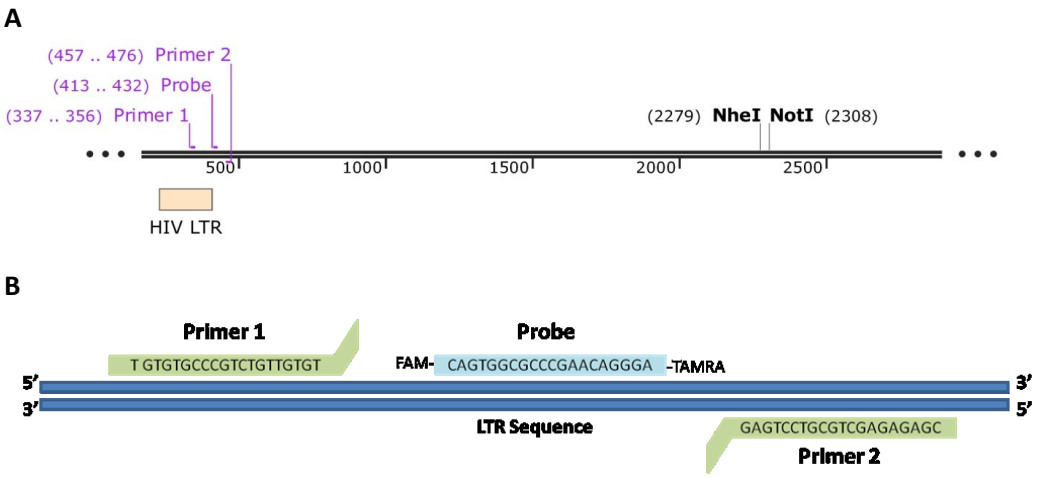


**Figure 2.8 LTR primers and probe used by Geraerts *et al*. (2006) for lentiviral titration.** Schematic of A) the lentiviral backbone and B) how the primers and probes will bind to the LTR sequence (not to scale). Lentiviral sequence provided by System Biosciences and visualised using SnapGene Viewer.

The qPCR reaction was set up as follows:

| | Volume (µl) |
|---|---|
| **Taqman Mastermix (Thermo Fisher Scientific)** | 10 |
| **DNA (10ng/µl stock)** | 2 |
| **10µM LTR F primer** | 0.6 |
| **10µM LTR R primer** | 0.6 |
| **5µM LTR probe** | 0.4 |
| **Water** | 6.4 |

**Table 2.8 qPCR reaction components and volumes.**

A range of dilutions were performed on the plasmid DNA (SparQ-Bmi1) to obtain a standard curve from known DNA concentrations, from which the viral copy number could be calculated. Control wells were also set up consisting of water instead of DNA and each condition was repeated three times per plate. Data was analysed using MxPro qPCR software (Agilent).

The following equations could then be utilised to calculate the viral titre:

**"Lentiviral copy number per cell = (copy number WPRE/copy number Albumin) x 2**

**Titre (TU/ml) = (Primary number of cells count in day 1 x lentiviral copy number per cell of the sample/volume of used lentivirus (ml)"**

which were taken from Barcazk *et al.* (2015), where albumin is used as a single copy reference gene and WPRE is a lentiviral backbone gene.

## 2.3 Results

### 2.3.1 Production of lentiviral plasmids containing the Bmi1 sequence

I first set out to generate a new series of Bmi1 expression vectors. The purpose of these vectors was to deliver the Bmi1 sequence to HBECs by assembling into lentiviruses and permanently introducing the sequence into the cell genome.

To begin with, the pGEM-T vector was used as a means to amplify the Bmi1 sequence. The Bmi1 insert was then transferred into both the constitutive pCDH vector and the inducible SparQ vector which would provide the means to produce lentiviruses containing the Bmi1 sequence. The ligated plasmids were cut and observed to possess inserts of approximately the expected size (Fig. 2.9). The insert size was a little higher than expected, but the plasmids were confirmed to contain the correct insert after being sequence verified.

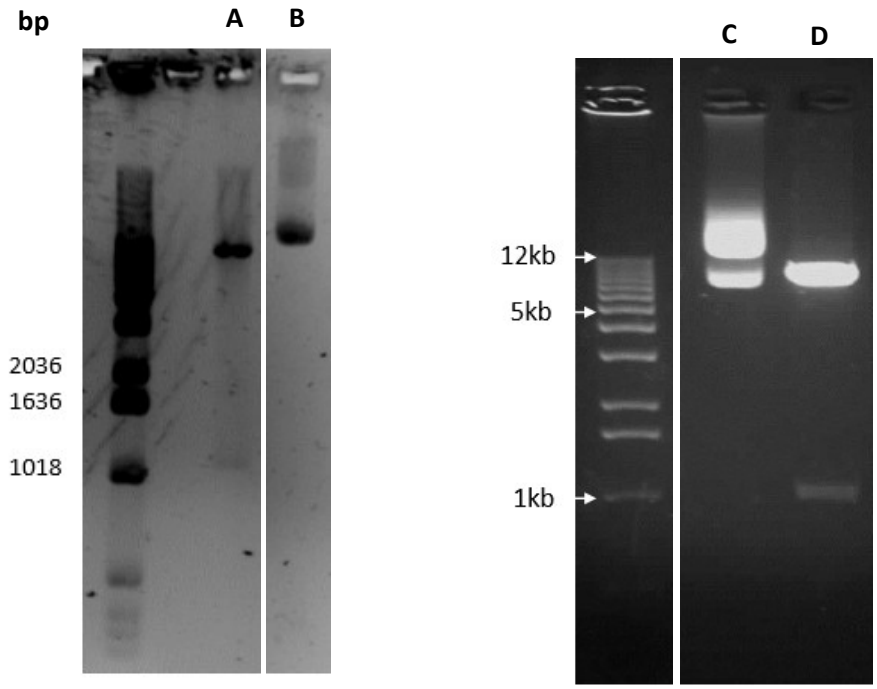


**Figure 2.9 Restriction digested pCDH-Bmi1 SparQ-Bmi1 plasmids both showing an insert of approximately 1kb, the expected size of the Bmi1 insert.** A) Restriction digested pCDH-Bmi1 plasmid, B) Uncut pCDH-Bmi1 plasmid, C) Uncut SparQ-Bmi1 plasmid and D) Restriction digested SparQ-Bmi1 plasmid. The Bmi1 insert is flanked by NotI and NheI restriction sites. When the pCDH-Bmi1 and SparQ-Bmi1 plasmids are cut with these enzymes, an insert of 998bp is expected, which can be seen in lanes A and D. The empty pCDH plasmid is 7544bp and the SparQ plasmid alone is 8414bp.

### 2.3.2 Transfected HEK293T cells successfully over-express RFP and GFP and can be identified using fluorescent microscopy

Having confirmed that the newly synthesised plasmids contained an insert and sequence verifying this insert as Bmi1, the next stage was to ensure that the plasmids were functioning correctly and able to express the genes present. In order to do this, the plasmids were transiently transfected into HEK293T cells. HEK293T cells are mammalian cells which are frequently used for transient transfections due to their ease of culture and gene delivery. They were deemed an appropriate cell type to use for initial transient transfections as they would be utilised for lentiviral production at a later stage of the project.

Each of the plasmids possesses a reporter gene, (GFP in pCDH-Bmi1 and RFP in SparQ-Bmi1) which provides a simple means of detecting whether transfection is successful or not via fluorescent confocal microscopy.

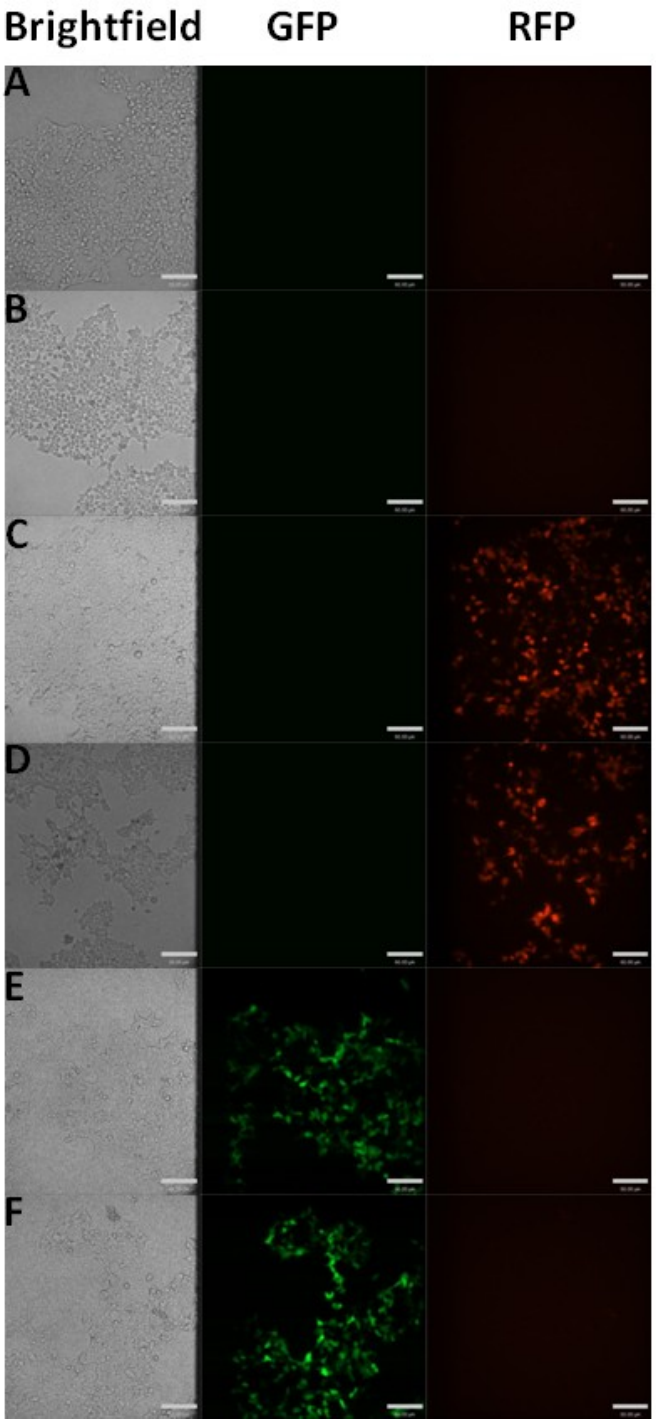


**Figure 2.10 RFP and GFP were observed in transiently transfected HEK293T cells showing successful delivery and function of lentiviral plasmids compared to negative controls.** A) Untransfected cells and B) TransIT-LT1 only vehicle control. HEK293T cells were transfected with C) SparQ EV, D) SparQ-Bmi1, E) pCDH EV and F) pCDH-Bmi1 plasmids. Fluorescent and Brightfield imaging of HEK293T cells 24 hours post-transfection. Representative of 3 independent replicates at passage 20, p20 and p30. Each replicate consisted of at least two replicate wells per condition. Images taken using 100x objective, Gain 1, Exposure 345ms, 491nm wavelength used for detection of RFP and excitation wavelength of 568nm, 40ms exposure and Gain 3 used for GFP. Seeded at 200,000 cells per well in a 6 well plate and transfected at a ratio of 7.5µl TransIT:2.5µg DNA (corrected to account for insert). Scale bar shows 60µm.

As shown in Fig. 2.10, both RFP and GFP could be detected 24 hours post-transfection, meaning the cells were successfully transfected; the plasmids were delivered to the cells and they were able to produce the fluorescent proteins. On the other hand, no fluorescence was detected in untransfected and vehicle-only controls. Furthermore, the confluency of all of the cells appeared similar in Brightfield images.

### 2.3.3 Bmi1 protein over-expression is observed in transfected cell lysates

To then determine whether Bmi1 protein was being over-expressed using these newly generated vectors compared to controls, the cell lysates from the transfected and untransfected HEK293T cells were visualised in Fig. 2.11 by Western Blot.

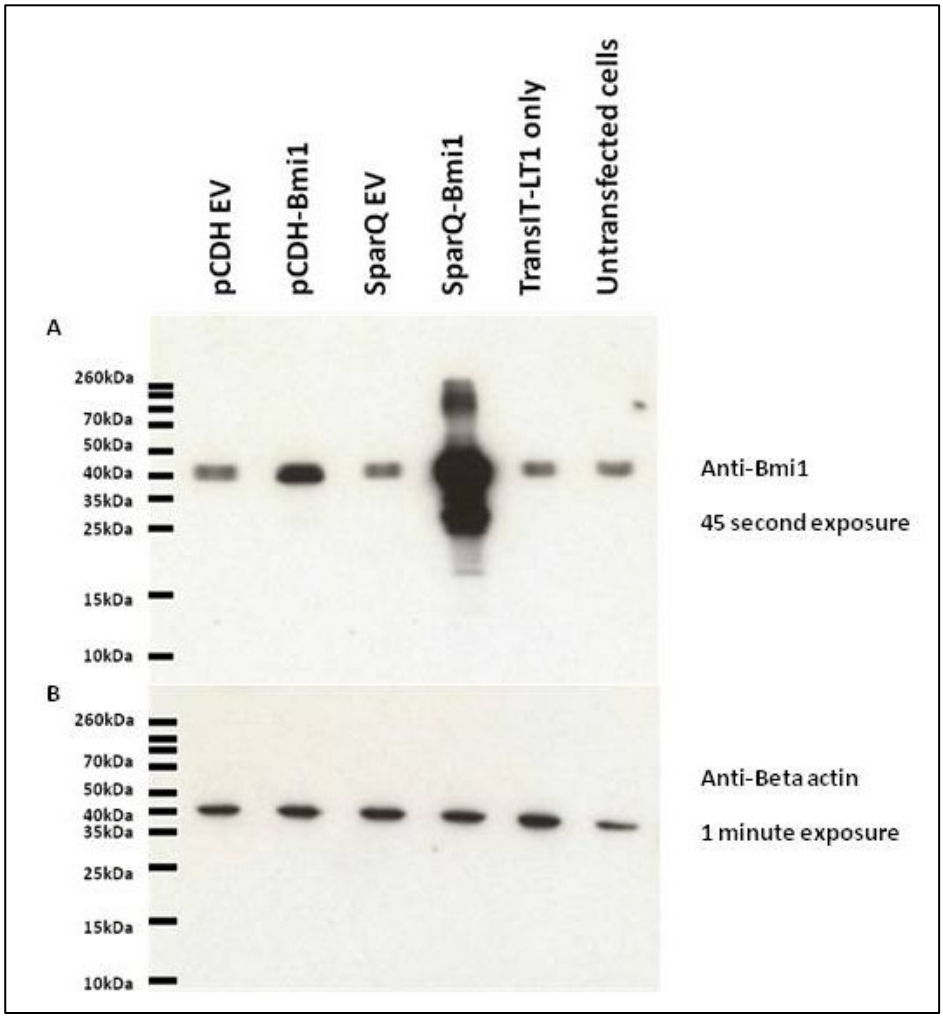


**Figure 2.11 A) Bmi1 protein levels are elevated in HEK293T cell transiently transfected with vectors containing the Bmi1 expression cassette, B) relatively equal baseline levels of beta-actin reference protein.** Increased Bmi1 was observed in 2 independent repeats with protein samples acquired from 2 independent transient transfections in HEK293T cells. Equal volumes of protein were loaded per well. Separate gels were used for Bmi1 and beta-actin due to problems during the stripping stage. The expected protein size of Bmi1 is 36.9kDa and beta-actin is 41.7kDa (UniProt, 2016).

Increased protein signals of the expected size can be observed in samples from +Bmi1 transfected cells. The unusual banding observed in Figure 2.11A is thought to be due to the excess of protein and made stripping the membrane particularly difficult. To overcome this, beta actin had to be analysed on a separate gel run in parallel. Each well contained the same volume of total protein sample in order for comparisons to be made.

The beta actin bands indicate relatively equal amounts of protein. Whereas, the Bmi1 bands in Figure 2.11A show that although all cell samples contain a baseline level of Bmi1, the level is much increased in those transfected with plasmids containing Bmi1.

To quantitatively compare the bands of the Western Blot, densitometry was performed to analyse the differences between the mean grey scale of each band (effectively how dark the band is).

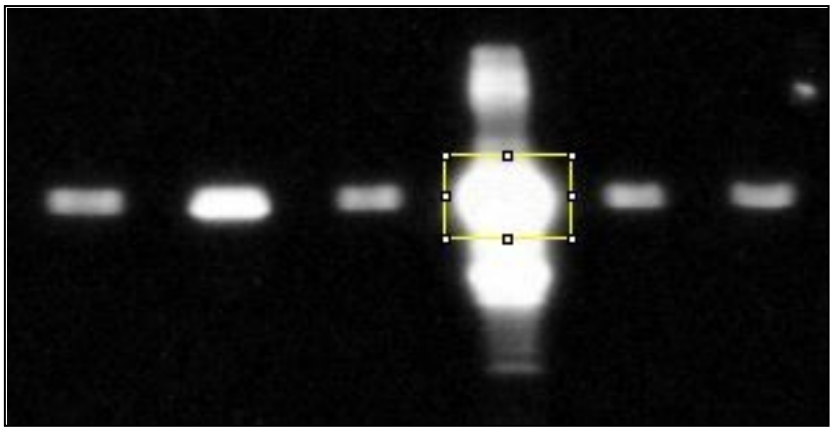

**Figure 2.12 Conducting densitometry on Western Blot protein bands using ImageJ to quantitatively compare protein levels.** The image colours were inverted. A box was drawn around the largest protein band and the mean grey scale was measured. This same box was dragged to each of the other bands to ensure the same sized area was analysed each time. This provided a means to quantitatively compare the amounts of protein in each band on the blot.

Fig. 2.12 illustrates how the measurements taken. The SparQ-Bmi1 band proved difficult to measure as it appeared to have numerous bands. A box was drawn around the band of the expected size for Bmi1 protein and all other measurements were taken using the same sized box.

Table 2.9 quantitatively shows increased Bmi1 protein in bands from either SparQ-Bmi1 or pCDH-Bmi1 transfected cell lysates compared to empty vectors and negative controls (vehicle only and untransfected cells).

| Mean Grey Scale Value | pCDH empty vector (EV) | pCDH-Bmi1 | SparQ EV | SparQ-Bmi1 | TransIT-LT1 only | Untransfected |
|---|---|---|---|---|---|---|
| Bmi1 | 36.97 | 69.416 | 32.404 | 189.447 | 29.995 | 28.331 |
| Beta-actin | 36.487 | 43.687 | 46.234 | 43.746 | 50.369 | 25.798 |
| Ratio (Bmi1/beta-actin) | **1.013** | **1.589** | **0.7001** | **4.330** | **0.596** | **1.098** |

**Table 2.9 Densitometry of Western Blot bands indicate increased Bmi1 protein in transfected HEK293T cells.** Protein bands from Fig 2.11. were analysed via ImageJ and increased mean grey scale values were observed in lysates from cells transfected with either pCDH-Bmi1 or SparQ-Bmi1 (highlighted in red) compared to empty vector and negative controls. Bmi1 bands were compared to beta-actin bands in order to normalise the values. For the mean grey scale (top two rows), a value of zero would represent black (low protein), whereas a value of 255 would represent white (high protein). Data representative of one repeat.

The transient transfections in HEK293T cells with the lentiviral plasmids were a success. The plasmids were able to express both fluorescent genes and over-express Bmi1 and therefore were functioning as intended and ready to be packaged into lentiviruses.

The large difference observed in the levels of Bmi1 produced in pCDH-Bmi1 transfected cells and SparQ-Bmi1 transfected cells could potentially be due to the difference in promoters used in each plasmid to initiate protein transcription. The pCDH-Bmi1 plasmid contains a CMV promoter, whereas the SparQ-Bmi1 contains a modified CMV promoter (CMV5). In a 2008 study, Papagatsias *et al.* (2008) found that the CMV5 promoter activity was higher than the CMV promoter in certain cell lines, but in human dendritic cells, CMV performed best. This suggests that resultant protein expression may be determined not only by the promoter used, but the combination of cell type and the promoter together.

### 2.3.4 Lentiviral-infected HBEC cultures survive and produce RFP and GFP

Having confirmed that the lentiviral plasmids were functional, lentiviruses were produced in HEK293T cells and collected from the cell supernatant as outlined in the methods. To determine whether they were able to infect cells and introduce the gene of interest, preliminary infections with HBECs were prepared. As the titre had not yet been calculated, a range of volumes were applied to the cells based on previous experiments within the research group. In this case the dosage was: 1µl, 2.5µl, 5µl and 7.5µl of virus. Passage 4 HBECs were infected with lentivirus and then imaged ten days post-infection. Only cells given the maximum dose of virus (7.5µl) are shown in Figure 2.13, which reveals a similar morphology between infected and uninfected cells.

As there was no gross change in HBEC culture appearance, fluorescent microscopy was then undertaken to determine whether the fluorescent proteins (RFP and GFP) could be observed in the infected cells (Fig. 2.14 and 2.15). This would confirm that the viruses were functioning and could infect and deliver genes to the primary HBECs. Infections were repeated a total of 3 times with a minimum of 2 wells per condition within each repeat. Infections with empty vector viruses were repeated twice.

Initial experiments included HBECs infected with both SparQ + CymR to observe whether the cells could tolerate the dual infection before further repression experiments were undertaken. Equal volumes of virus were added (7.5µl of each). As cumate was not added, this should have resulted in at least some of the Bmi1 and RFP gene expression being reduced.

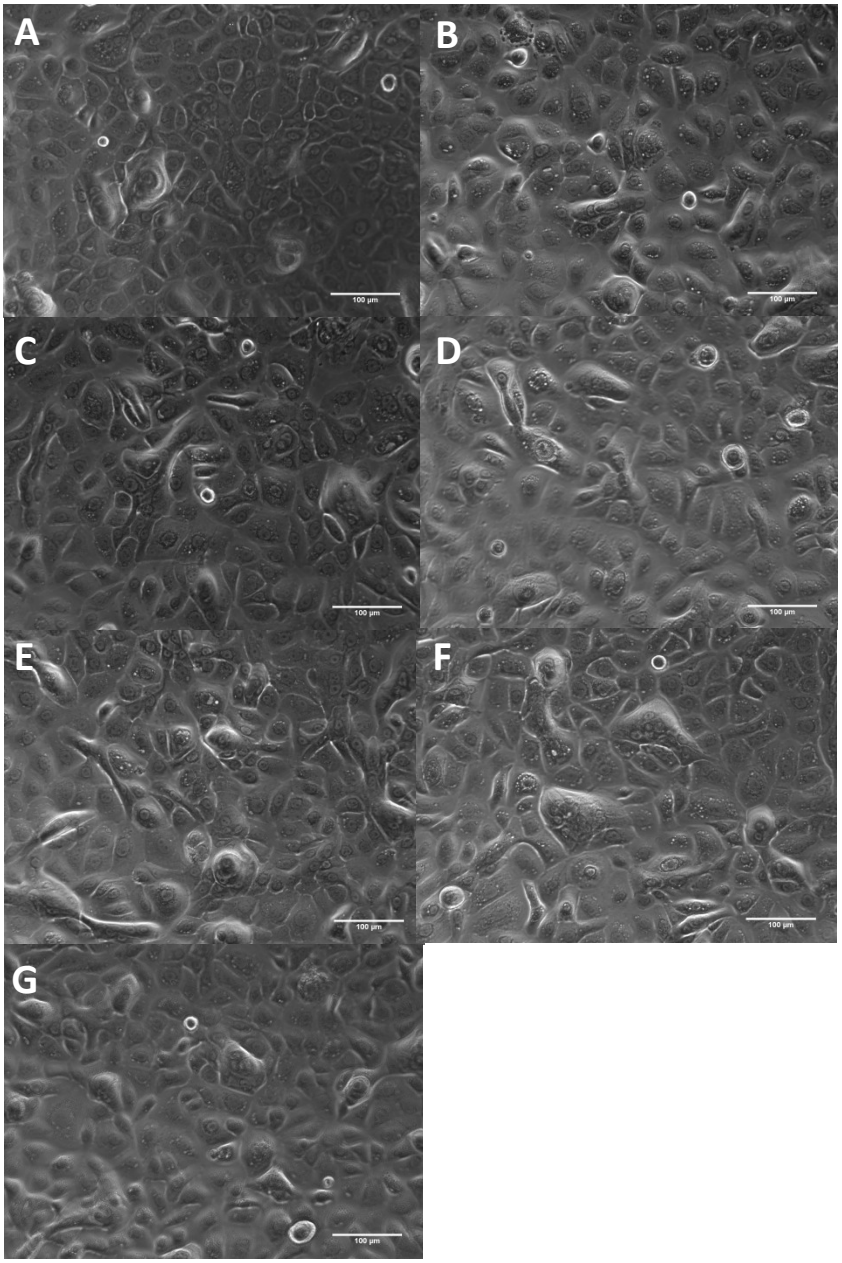


**Figure 2.13 Phase contrast images of HBECs 10 days post- lentivirus infection show similarities in confluency and cell morphology compared to uninfected controls.** Passage 4 HBECs infected with 7.5µl virus: A) pCDH-Bmi1, B) pCDH EV, C) SparQ-Bmi1, D) SparQ EV, E) SparQ-Bmi1 + CymR, F) CymR only and G) none (uninfected control). There were no significant changes in the morphology of infected cell cultures compared to uninfected HBECs. Images taken using x20 objective and Phase plate Ph2. Scale bar shows 100µm.

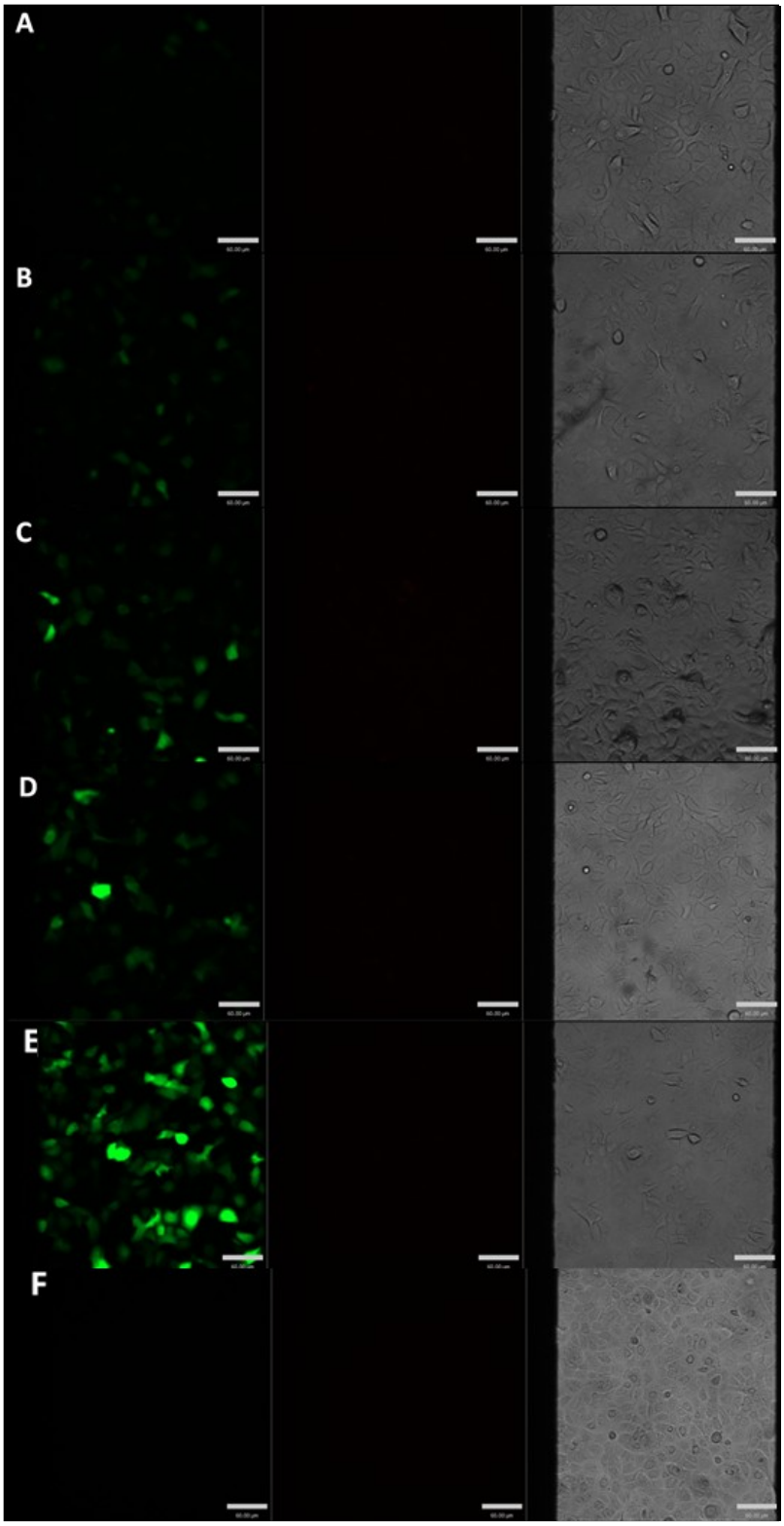


**Figure 2.14 HBECs infected with pCDH-Bmi1 and pCDH EV viruses express GFP.** HBECs were infected with varying volumes of pCDH-Bmi1 virus A) 1µl, B) 2.5µl, C) 5µl, D) 7.5µl; E) pCDH EV 7.5 µl, F) Uninfected cells**.** Scale bar shows 60µm (GFP: exposure 1.68s, gain 4). Representative of 3 replicates in passage 4 HBECs, 10 days post-infection.

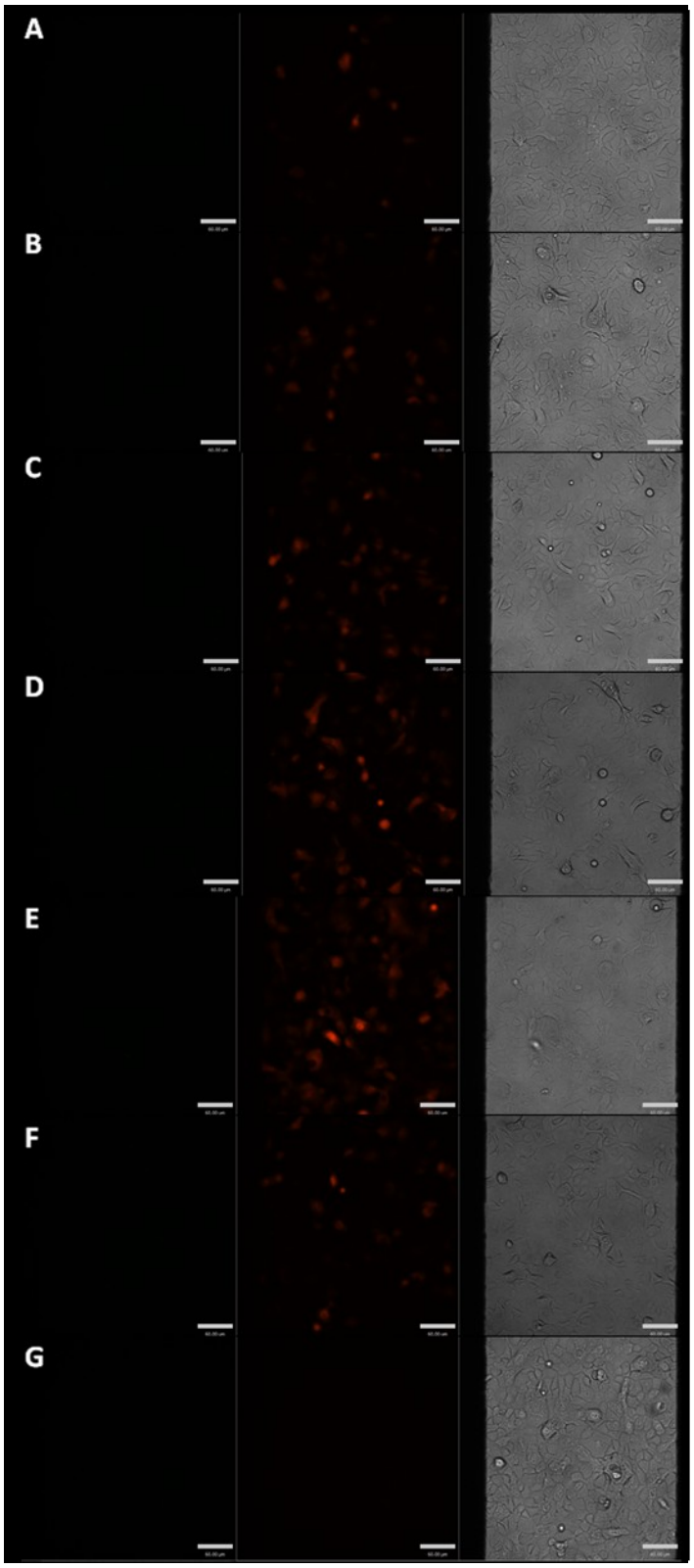


**Figure 2.15 HBECs infected with SparQ-Bmi1 and SparQ EV viruses express RFP.** Passage 4 HBECs were infected with SparQ-Bmi1 A) 1µl, B) 2.5µl, C) 5µl, D) 7.5µl; E) SparQ EV, F) SparQ+CymR, G) CymR only. Scale bar shows 60µm (RFP: exposure 3s, Gain 3). Representative of 3 replicates, 10 days post-infection. The CymR repressor virus does not possess a fluorescent reporter gene.

Fluorescence can be observed in the appropriately infected cells and appears to increase according to viral dose. Uninfected cells and those infected with the CymR virus (which has no fluorescent marker) showed no fluorescence.

Lentiviral infected HBEC cultures visually appeared to be growing as well as uninfected cells although quantitative measures were not taken. Fluorescence showed that the viruses were assembled correctly and capable of both infecting HBECs and integrating the fluorescent genes into the host genome.

### 2.3.5 Quantification of fluorescent protein expression across lentiviral titres

To provide an estimate of the viral dosage which should be used for future experiments and to provide quantitative data for the levels of RFP and GFP, the fluorescent images were analysed using ImageJ to compare the differences between cells infected with a range of viral volumes.

For one repeat, incorrect microscope settings were used (different exposure time) - see red data in Figure 2.16. Unfortunately, this meant that statistical analysis was not possible for this data.

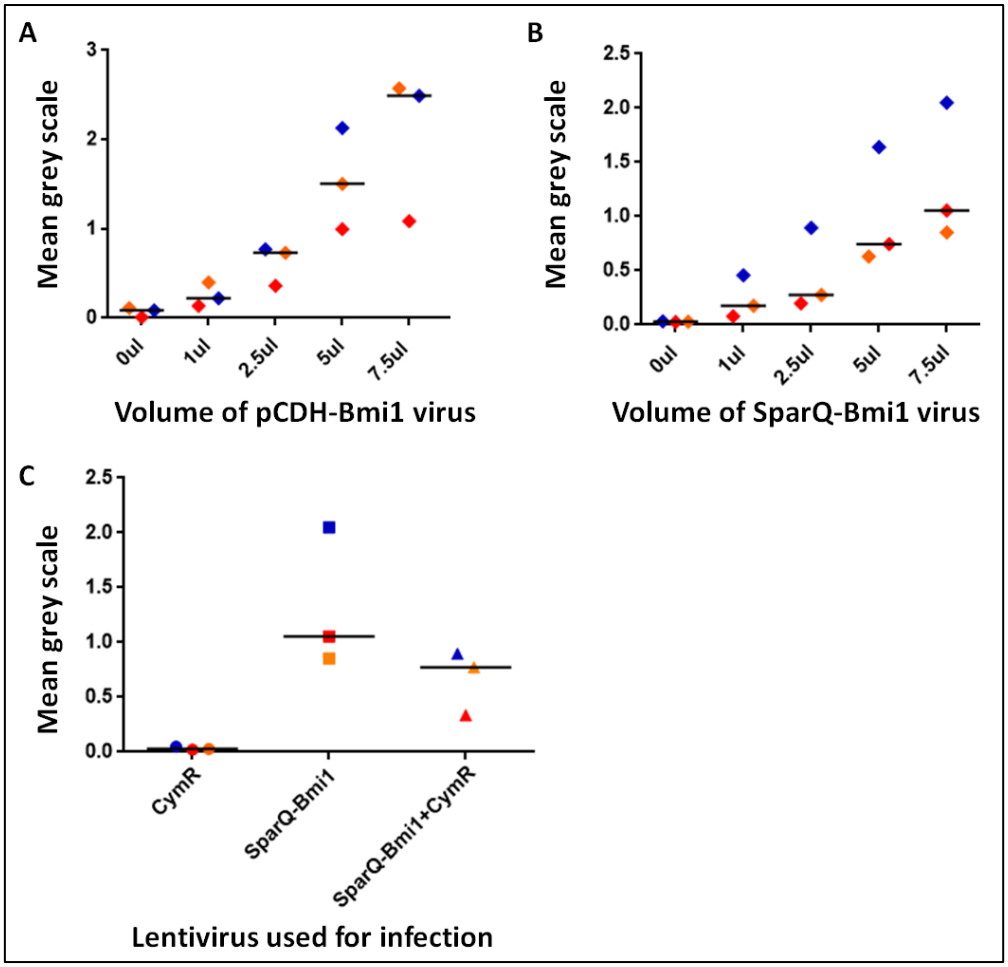


**Figure 2.16 Quantitative analysis of fluorescent images shows a dose-dependent increase of fluorescent signal in HBECs. Inclusion of the repressor system decreases RFP as anticipated.** Passage 4 HBECs have been infected with varying doses of either A) pCDH-Bmi1 virus or B) SparQ-Bmi1 virus. C) shows cells infected with both SparQ-Bmi1 and the repressor virus, CymR. The mean grey scale was determined using ImageJ and raw values plotted into a graph. Each  represents an independent repeat and the horizontal line highlights the median value. The red dot shows the repeat with images taken using different microscope settings.

### 2.3.6 Infected cells demonstrated a dose dependent increase in RFP or GFP

These data demonstrated an increase in fluorescence with increasing viral dose (Fig. 2.16 A and B), implying that a greater number of cells have been infected with the viruses. There appears to be much variation between repeats, even those with the same microscope settings (orange and blue in Figure 2.16 B).

As expected, there was no fluorescence observed in CymR virus only infected cells (which does not contain a fluorescent reporter) and a relatively large increase in cells infected with the SparQ-Bmi1 virus (containing a RFP reporter gene).

### 2.3.7 The SparQ repressor system shows potential but requires more optimisation

Following infection with both the SparQ-Bmi1 and the CymR virus, a decrease in fluorescence would be anticipated (as the repressor would prevent expression of both Bmi1 and RFP). Although statistics could not be performed on this data, there is a trend of decreased fluorescence in cells infected with both SparQ-Bmi1 and CymR virus as compared to SparQ-Bmi1 alone (Fig. 2.16 C). Taking the SparQ-Bmi1 mean grey scale value as 100% in each of the 3 repeats, the value drops to 90.7%, 43.8% and 31.9% when measured in cells infected with SparQ-Bmi1 combined with the CymR repressor virus. However, large variations in the data can also be observed.

### 2.3.8 Establishing a qPCR to measure viral integration into the host genome

Following lentiviral infection of HBECs, qPCR was chosen as the most suitable method to quantify the genes which had been integrated into the host cell genome.

Part of the lentiviral backbone as well as the gene of interest (Bmi1) would have been incorporated into the genome of HBECs infected with the virus. This provides a means of determining the number of gene copies present in the cells and therefore the initial viral titre.

The 5' LTR is a region upstream of the gene of interest and is involved in integrating the gene into the host genome via recombination (Addgene, no date). A section from the 5'-LTR was utilised for primers and probes as it would be present in cells infected with both Bmi1-containing viruses and empty vector viruses as well as the CymR repressor virus, meaning the same standard could be used for all of the viruses produced in this project.

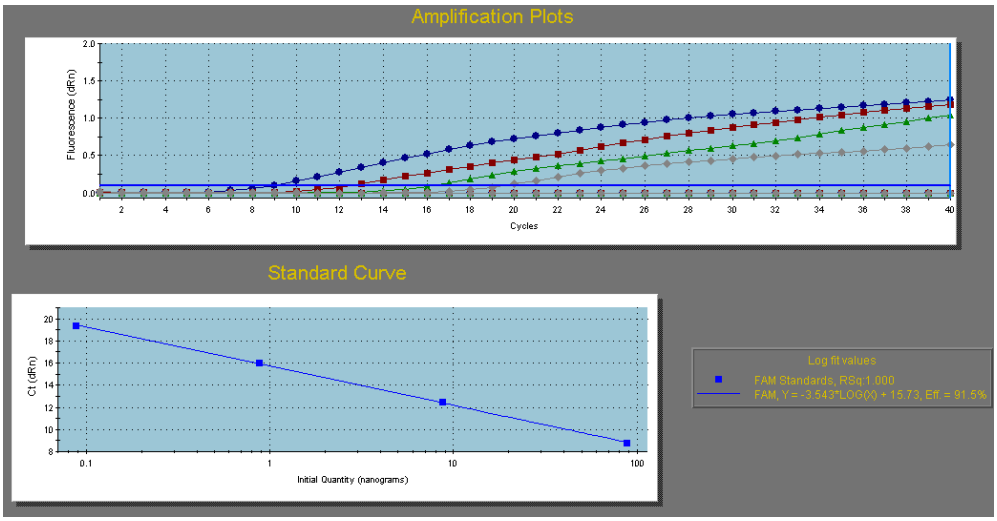


**Figure 2.17 Optimisation of the LTR qPCR assay to be used to determine viral titre.** A standard curve was produced in MxPro software (Agilent) using SparQ-Bmi1 plasmid DNA at known concentrations with LTR primers and Taqman probe. Each sample was a 1 in 10 dilution of the previous dilution; initial quantities: blue = 87.54ng, red = 8.754ng, green = 0.8754ng, silver = 0.08754ng. The efficiency was calculated by MxPro to be 91.5%.

A standard curve was produced using SparQ-Bmi1 plasmid DNA at a range of concentrations, which showed that the assay was functioning as intended. BioRad Laboratories (2006) suggest a qPCR assay should optimally have an amplification efficiency of between 90 and 105%. The efficiency of this assay was 91.5%, meaning the amplification efficiency was satisfactory.

### 2.3.9 Quantification of viral load in infected cell samples using the LTR qPCR does not identify a signal above negative controls

Following lentiviral infection of passage 4 HBECs, DNA samples were collected and extracted 10 days post-infection. The LTR qPCR assay from Section 2.3.8 was then used to determine the initial titre of each virus.

However, when samples were used which had been obtained directly from lentiviral infected cells (for a total of 40 cycles), the assay was unsuccessful on 2 independent occasions as shown in Fig. 2.18. The traces shown in the graph appear later than expected and there is no difference between the samples collected and negative controls which did not include template DNA.

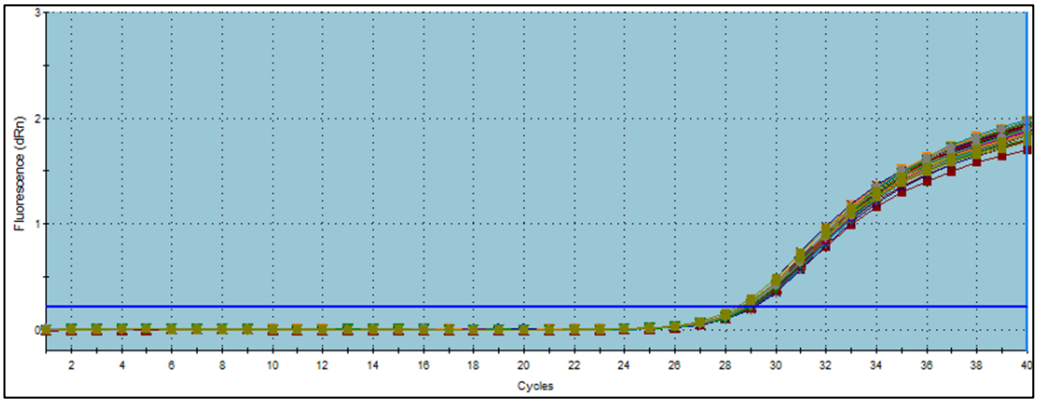


**Figure 2.18 Unsuccessful amplification of Bmi1 via qPCR using LTR primers and probe.** DNA was extracted from lentiviral infected HBECs. Both samples and negative controls showed increases in fluorescence at cycle 29. Representative of 2 replicates run for 40 cycles in total.

The peak for samples and negative controls began at cycle 29, which was much later than those observed in the standard curve (cycles 10-20). This could indicate that the collected DNA possessed the target gene at a much lower quantity, so as to become negligible. Alternatively, there may have been contamination in the water controls, giving a false positive result.

Attempts were also made using a probe targeting an alternative gene, WPRE (common in many lentivectors) with probe and primer sequences used by Barczak *et al.* (2015) and the same qPCR conditions, but without success (data not shown). Ideally, it would be useful to have two distinct gene targets which could be used to independently calculate the viral titre. Further optimisation is required and if still unsuccessful, the project may demand an alternative method of viral titration or to create a CymR cell line prior to SparQ-Bmi1 infection as mentioned previously.

As the qPCR assay did not provide a robust and specific measure of viral integration, it was not possible to determine the viral titre for the lentiviruses produced.

## 2.4 Discussion

### 2.4.1 Key findings

The key aim of this chapter was to develop functional lentiviruses allowing Bmi1 over-expression (in both an inducible and constitutive manner), and to infect primary HBECs with them.

Constitutive and inducible lentiviral plasmids were constructed containing the Bmi1 sequence and were able to over-express the Bmi1 protein and express fluorescent reporter genes following transient transfection in HEK293T cells. These plasmids were then packaged into lentiviruses and were able to successfully infect primary HBECs. The cells survived lentiviral infection and expressed the fluorescent genes which were conferred to them by the viruses. This suggested that the lentiviruses produced were functioning as intended and had delivered genes to the host cell. The fluorescence of the infected cells increased with viral dose and the doses used in this project do not appear to have a detrimental effect on the primary HBECs. The levels of fluorescence observed appeared to begin to plateau at the maximal dose of 7.5μl of virus (they did not continue to increase at a linear rate), therefore there is likely to be an upper threshold where additional virus does not increase fluorescence, but is possibly detrimental to the cells, although whether this also applies to Bmi1 expression is yet to be determined.

For the inducible system, the cells tolerated a dual infection with equal volumes of CymR and SparQ-Bmi1. The presence of the repressor virus did appear to cause some repression of RFP expression although further optimisation is required with more replicates to obtain a more substantial decrease in gene expression.

Having produced functional lentiviruses, the next aim was to titrate the viruses to calculate how much virus was produced and to determine an optimal dose for HBECs. However, titration via qPCR was not achieved and therefore experiments did not move past the preliminary infection stages. There may have been a problem with the method used to collect DNA, contamination of samples, or the qPCR method may have needed to be optimised with different conditions to adapt the assay for collected DNA.

Finally, a bank of genetically modified cells was not accomplished due to the time constraints of the project. However, the foundations to achieve this have been laid and the methodology used here can be applied to HBECs obtained from different donors to account for donor variability.

### 2.4.2 Limitations

The viruses are able to successfully infect primary HBECs and express the fluorescent genes, RFP or GFP. However, as the Bmi1 sequence is present under a separate promoter from GFP in the pCDH-Bmi1 virus and with an IRES for RFP in the SparQ-Bmi1 virus, it has not been confirmed that the Bmi1 sequence is present and being expressed in infected cells. A Western blot has thus far only been obtained for the transiently transfected HEK293T cells and not from the protein of lentiviral infected HBECs. The qPCR assay should have been able to confirm whether the gene had been integrated into the host cell genome, but a Western Blot would still be required to confirm that Bmi1 protein is present and being over-expressed compared to controls.

The Western Blot used for detecting Bmi1 over-expression in transiently transfected HEK293T cells was problematic during the stripping stage and the Bmi1 protein could not be sufficiently removed before probing for beta-actin. Therefore, the beta-actin was run simultaneously on a separate gel. However, although the same samples and volumes were loaded per well, this method does not account for sample loading inaccuracies. Ideally, densitometry would have been performed on samples on the same gel and with more repeats to overcome the variability between samples.

Although the cells did not appear to have suffered a detrimental effect following lentiviral infection, experimental measures were not taken. Following future infections, in-depth study could focus on cell death and proliferation to observe how they change post-infection.

There are now available pre-designed lentiviral titration kits which measure titre using qPCR of the WPRE gene and a reference gene (Ultra Conserved Region 1) as a control (System Biosciences). This may eliminate some of the problems which were encountered in this study and facilitate lentiviral work.

### 2.4.3 Further optimisation required for the inducible system

For the inducible system, the product manual (System Biosciences, n.d.-c) advises infecting with a 1:1 ratio of CymR to SparQ virus (in terms of Multiplicity of Infection which can be determined using the titre). As the viruses have not been titrated yet, this was not possible to do. As an initial experiment, equal volumes were used. This meant doubling the total volume of virus added to the cell in order to maintain the same level of SparQ-Bmi1 to compare with the SparQ-Bmi1 only infected cells.

As an alternative to co-infection, a repressor (CymR) cell line could be produced first using puromycin to select for successfully infected cells which have incorporated the CymR repressor gene. Following selection, the surviving cells could undergo a secondary infection with the inducible SparQ-Bmi1 virus to ensure that the majority of cells are infected with both viruses. This would also avoid problems with titration and finding an optimal dose, as uninfected cells would not survive the process of puromycin selection and flow cytometry could subsequently be used to sort for SparQ-Bmi1 infected HBECs which will express RFP.

Only a small repression of the RFP gene in the SparQ-Bmi1 infected cells was observed when dual infected with CymR (Figure 2.16 C). However, even though equal volumes were used, if the titre of the SparQ-Bmi1 virus was much higher than the CymR virus, there may not be sufficient gene repression to observe the effect. Furthermore, the analysis may have required a larger number of images to be taken for each condition to provide a more representative overview and reduce variation between repeats. Fluorescent image analysis was intended to be used alongside qPCR to calculate the optimal viral dose for each virus and cannot by itself provide an accurate estimate.

### 2.4.4 Over-expression of Bmi1 protein by mRNA delivery as an alternative methodology

An alternative approach to lentiviral delivery which could be utilised in this project is the direct addition of Bmi1 mRNA to cultured cells. This would allow Bmi1 protein to be synthesised without permanent modification to the epithelial cells.

There are several differences between mRNA delivery and lentiviral gene delivery. For gene expression, it is not necessary for exogenous mRNA to enter the cell nucleus and therefore there is quicker expression of protein (Thermofisher Scientific, n.d. -a) and there are unlikely to be unwanted side effects at a genomic level (via insertional mutagenesis, which can be a negative consequence of lentiviral infection). However, there is a risk of host immune defences against the foreign RNA and subsequent degradation of the oligonucleotide (reviewed in Islam *et al.*, 2015).

Kim *et al.* (2015) have developed a nano-particle mRNA delivery system entirely comprised of mRNA (eliminating the use of chemical modification, which is used to protect the mRNA, but can result in damage to the cell). In their study, they were able to produce numerous copies of mRNA which became tangled and self-assembled into mRNA nanoparticles. They state that the mRNA nanoparticles are more resilient to enzymatic degradation

from nucleases. However, a disadvantage is that the system still relies on transfection reagent-aided delivery and gene expression had started to decline after 24 hours (meaning a more restricted window of over-expression compared to the cumate-switch system).

Bangel-Ruland *et al.* (2013) were able to restore function in an epithelial cell line possessing a mutation in the CFTR gene (a common cause in cystic fibrosis) with delivery of wild-type CFTR mRNA by lipofectamine. However, their experiments were not conducted beyond 24 hours. A limitation of transient transfection is that the genetic manipulation is short-lived. Whilst it is advantageous in this project to have reversible gene over-expression, mRNA-based systems appear to offer less control over gene-expression than the Cumate Switch system.

Therefore, for this project the Cumate Switch seems the more appropriate option as Bmi1 over-expression is likely to be required over several days in order to expand the HBECs sufficiently.

### 2.4.5 Summary

This chapter covers the methodology used to generate genetically modified HBECs. The system used incorporates conditional control of Bmi1 over-expression, potentially allowing more precise control than other mechanisms such as RNA delivery.

# 3. Characterisation of modified Bmi1 HBECs using cellular outcomes

## 3.1 Introduction

In preparation of the generation of modified airway epithelial cell lines, there was a need to assess the functionality of epithelial airway cells and characterise them effectively, for example in terms of proliferation, migration, apoptosis and barrier formation. Different techniques could be utilised to compare the modified cells to endogenous wild type cells and this project will focus on barrier formation.

### 3.1.1 Electric Cell Substrate Impedance Sensing

Electric Cell Substrate Impedance Sensing (ECIS) is a non-invasive measure of barrier function across a cell monolayer. Cells are grown on gold-plated electrodes in an array and a small alternating current is applied. The resultant impedance produced by the cells is measured in real time as the cells grow, from which the resistance and capacitance are derived and provided to the user by the ECIS software (Applied Biosystems, 2017a).

At higher frequencies, the majority of the current travels through the cell (Fig. 3.1), which provides an insight into proliferation of the culture and the electrode coverage (Applied Biophysics, 2017a). As the monolayer becomes more confluent, the capacitance should drop as the cells flatten out, attach and spread across the surface - due to the layer of cells having an insulating effect and interfering with the current flow (Xiao & Luong, 2003).

On the other hand, at lower frequencies, the majority of the current flows around the cells which gives an indication of the barrier properties of the monolayer (Applied Biophysics, 2017a). As the barrier develops, the resistance (at low frequencies) across the monolayer is expected to increase due to the formulation of tight junctions. This was highlighted by Heijink *et al*. (2010) who showed that junctional protein, ZO-1 in airway epithelial cells was present at 72 hours when ECIS resistance increased sharply, but not at earlier time points.

Therefore, different aspects of the monolayer can be studied depending on the frequency of current used.

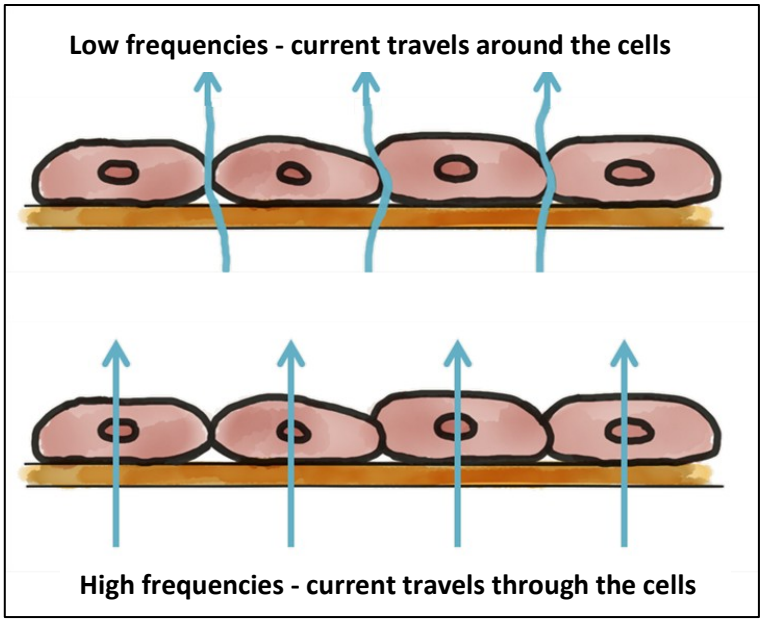


**Figure 3.1 The current applied to the electrodes travels different routes through the monolayer depending on the frequency (based on Applied Biophysics, 2017a).** At lower frequencies, the current travels around the cells through intercellular spaces, which gives an indication of barrier function. At higher frequencies, the current travels through the cell, giving an indication of electrode coverage and confluency.

ECIS provides a way to study airway epithelial cells non-invasively to provide insight into the barrier characteristics and behaviour of the monolayer. It can therefore be used to compare the genetically modified +Bmi1 HBECs against early passage wild type HBECs to evaluate how representative the genetically modified cells are of endogenous non-modified low passage primary cells traditionally used in cell biology experiments, and that the changes incurred by over-expressing Bmi1 do not detrimentally affect the functionality of the cells.

Whilst production of inducible HBECs was occurring in this project, ECIS was performed using previously modified constitutive +Bmi1 HBECs (by Torr *et al*., 2016) to provide an indication of the suitability of this method and initial assessment of Bmi1 over-expression. The cells were previously shown to over-express Bmi1 protein via Western Blot (Torr *et al*., 2016).

### 3.1.2 Air Liquid Interface

Air liquid interface (ALI), as mentioned previously (see Chapter 1), involves growing the cells in submerged culture, but then exposing the apical cell surface to air. For airway epithelial cells, this mimics the *in vivo* environment and drives them to differentiate into the various cell types of the epithelium.

Once differentiated, the trans-epithelial electrical resistance can be measured across the layer to provide insight into the barrier function of the cell monolayer. ALI allows the development of a more complex, representative barrier.

A disadvantage of ECIS is that the measurements cannot be taken when the cells are grown at ALI, only in submerged culture. Therefore, this method of measuring TEER may provide a more representative insight into the epithelial cell layer properties. For example, the airway epithelium is normally coated in a layer of mucus, however this is removed in submerged culture, meaning the conditions do not match those *in vivo* (Ahmad *et al*., 2014).

To establish ALI methodology, Calu3 cells were used due to their ease of culture and ability to develop a high TEER (Stewart *et al*., 2012), as well as to become acquainted with culturing this cell type. ALI will be an integral part of characterising the modified cells in the future and the Calu3 cells are intended to be used for a later stage in the project, CRISPR-Cas9 genome editing (where genes relevant to asthma progression will be knocked out) before attempting this in the modified HBECs. An advantage in using Calu3 cells is that they spontaneously differentiate and are frequently used as an ALI model, however they have been confirmed to be deficient in ciliated cells meaning they are not fully representative of primary airway cells (Stewart *et al*., 2012).

### 3.1.3 Aims of the Chapter

The main aim of this chapter was to utilise ECIS as a method of characterising and studying HBECs, and to offer insight into the effect of elevated Bmi1 expression on cell proliferation and barrier formation. Furthermore, to provide initial characterisation of Bmi1 engineered cells compared to endogenous control cells to evaluate how representative these cells are.

## 3.2 Methods

### 3.2.1 Cell Culture

**HBECs**

HBECs

HBECs were supplied by Clonetics (Lonza) and used for ECIS at passage 3. The donor used was a 43 year old non-smoking Caucasian male, HIV and Hepatitis B negative. All HBECs were cultured as in Section 2.2.2.1.

Genetically modified +Bmi1 HBECs

The genetically modified cell lines used for ECIS were previously produced within the lab group (Torr *et al*., 2016). These HBECs were infected with a pFLRu lentivirus containing Bmi1 under the human ubiquitin C promoter. They are constitutively expressing Bmi1 HBECs, which were donor matched to early passage unmodified cells for ECIS. The passage number is presented as 'a/b' where a is the infection passage (number of passages since infection with virus containing Bmi1) and b is the actual passage (as used by Torr *et al.,* 2016). The genetically modified cells were used for ECIS at passage 7/10 (7 passages since infection, actual passage 10).

**Calu3 cells**

Calu3 cells were grown in DMEM/F12 (+ L glutamine) with 10% FBS, 1% essential amino acids and 1% Pen/Strep and used at passages 22-25. To detach Calu3 cells, they were treated with trypsin EDTA 0.25% (cat no. T4049 Sigma).

Calu3 cells were seeded into 12mm Transwells with 0.4µm pore insert (Corning cat no. 353180) within a 12 well plate (Costar cat no. 3513) at a density of 100,000 cells per well. 0.5ml of media was used in the upper compartment, and 1.5ml of media in the lower. Media was changed in both compartments every 2-3 days. Protocol provided by Emanuela Cingolani.

All cells were incubated at 37°C in 5% $CO_2$.

### 3.2.2 ECIS array preparation and settings

The ECIS Zθ (Applied Biophysics) machine was used for measurements. An 8W10E (Applied Biophysics) array was inserted into the machine, which consisted of 8 wells, each with 10 electrodes.

The array was treated with 200µl of 10mM L-cysteine (Sigma, catalogue number 168149-2.5G) in water for 15 minutes at room temperature to

remove production contaminants. L-cysteine was removed and the array washed three times with 300µl of water. The array was coated with 200µl of 30µg/ml PureCol Bovine Collagen Solution, Type 1 (Catalog #5005-B Advanced Biomatrix) and placed in the incubator overnight. The following day, it was washed with media three times and stored at 4$^{o}$C until further use.

Before seeding, the array was stabilised inside the ECIS machine with 400µl of media. 75,000 cells added to each well in a total volume of 400µl as in Heijink *et al.* (2010). The array was inserted into the ECIS machine and recordings taken continuously over a range of frequencies for 72 hours. Heijink *et al*. (2010) found the optimal frequency to monitor resistance was at 400Hz and capacitance at 40,000Hz for airway epithelial cells. Therefore, a frequency of 400Hz was used and for capacitance a frequency of 32,000Hz (which was the closest available setting, the next being 64,000Hz).

Thanks to Dr. Vincent Pang and Prof. Irene Heijink for advice in this protocol.

### 3.2.3 Statistical analyses of ECIS results

Normalisation of data (to minimise inter-experimental variation) involved either taking one of the wells containing endogenous passage 3 HBECs of each array as 100% or the average of two empty wells (in Repeat 1) as 100%. The results for each of the other wells were taken as a percentage of this value. Multiple wells of a sample were then averaged for plotting. This control well with HBECs was kept in the same position on the array for each biological replicate. Graphs were produced using GraphPad Prism version 7 for Windows (La Jolla California USA, www.graphpad.com).

There were multiple sharp peaks observed in ECIS plots, likely to be caused by disturbances in the incubator (opening and closing of the door) and sensitivity to environmental conditions. The peaks are possibly unavoidable, so were removed from the graph for a smoother trace.

A two-way ANOVA was used with Sidak's post-hoc multiple corrections test to analyse the differences between endogenous and +Bmi1 HBECs over time. At each time point, the data was compared between cell types. This was also performed on normalised data using GraphPad Prism version 7.01 for Windows, GraphPad Software, La Jolla California USA, www.graphpad.com.

### 3.2.4 Air-liquid interface with Calu3 cells

TEER measurements were taken as in Stewart *et al.* (2012). Upon the cells reaching confluency within the transwells, media was removed and replaced

only in the basal compartment to create the air-liquid interface. Before TEER measurements were taken, the apical surface of the cells was washed with PBS and media replaced in both apical and basal compartments. An EVOM2 epithelial volt/ohm (TEER) meter (World precision Instruments, cat. no. 300523) was used to measure resistance. The electrodes were first stabilised in 5ml of pre-heated media without cells. They were then placed either side of the transwell membrane (one in the apical compartment and one in the basal compartment) and the resistance was measured across the monolayer. Care was taken to ensure that measurements were taken so as not to disturb the layer of cells. One measurement was taken per well, with 4 wells in the first repeat and 8 wells in the subsequent two repeats. Three readings were taken and averaged for the control well (no cells). After readings were taken, media was replaced in the basal compartment only. The readings were taken at intervals of 2-3 days over a period of 15 days.

The TEER was then calculated using the following equation:

Calculated TEER ($\Omega$ $cm^2$) = (measurement-control average)*area of membrane (as in Chen *et al*., 2015)

The area of the transwells used in this project was 0.9$cm^2$.

### 3.2.5 Microscopy

A Nikon Diaphot 300 Inverted Microscope was used and images taken using the 10x objective.

## 3.3 Results

I set out to use ECIS as a tool for characterising bronchial epithelial cells and determining whether differences between modified and unmodified HBECs could be observed using this technique.

### 3.3.1 Reproducibility of ECIS measurements in HBECs

For ECIS to be a viable option for characterisation of genetically modified HBECs, the results need to be reproducible and reliable. Therefore, the traces of three independent biological repeats were compared for early passage unmodified cells to determine similarity between them and whether they conformed to the results of existing studies. Cells were seeded at 75,000 cells as per Heijink *et al.* (2010) as they found that lower densities meant that the airway cells did not form appropriate intercellular junctions within the 72 hour timeframe. The experiment was limited to 72 hours as preliminary work (not shown) showed that the ECIS output was hugely affected by media changes. A peak resulting from a media change is also shown by Applied Biophysics (2017c) in their examples of chondrocyte proliferation.

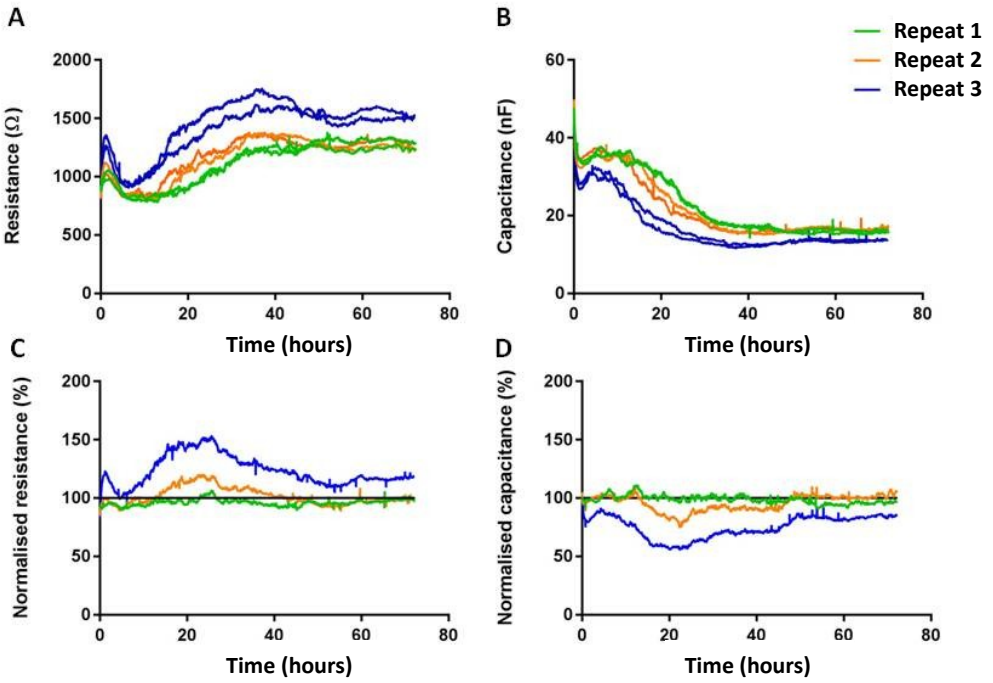


**Figure 3.2 Increased barrier function and cell adherence observed over time in primary HBECs.** Raw A) resistance and B) capacitance plots and C) Normalised resistance and D) capacitance plots. (A-B: Each line represents one well of passage 3 HBECs from the same donor). C-D: All measurements were normalised to an empty well control in Repeat 1 to account for variation across repeats and then averaged. Three independent biological replicates shown.

The initial dynamics of the raw data (Fig. 3.2 A and B) observed in the first 3 hours (a sharp increase in resistance and a sharp dip in capacitance) correlate with the results Heijink *et al*. (2010) obtained - which they describe as a 'hallmark' of primary bronchial epithelial cells and suggest they are potentially caused by changes in cell shape as the cells adhere. Results obtained by Hackett *et al.* (2013) also show an initial peak in resistance in ECIS measurements of primary bronchial epithelial cells, but not other airway cell types (BEAS-2B and 16HBE cells) supporting the idea that this is unique to primary bronchial epithelial cells.

A plateau in capacitance can be observed after 40 hours (Fig. 3.2 B and D), suggesting the cells had reached confluency. However, Heijink *et al.* (2010) observe a much more dramatic drop in capacitance measured at high frequency with primary bronchial epithelial cells.

The resistance across the monolayer begins to increase at approximately 10 hours (Fig. 3.2 A and C) which could suggest settling of the cells and the beginning of junctional protein formation.

The plots for Repeat 1 lie very closely to the control empty well trace. This could potentially be a result of problems in cell counting or seeding, where the cells are at a lower density than intended.

In terms of reproducibility, the plots appear to show that there is more variation between biological replicates than between technical replicates in the same array.

The next stage was to investigate the variation between wells of the same array. For each repeat one well of passage 3 HBECs was used as a control and the other well of passage 3 HBECs was normalised against it, as seen in Fig. 3.3.

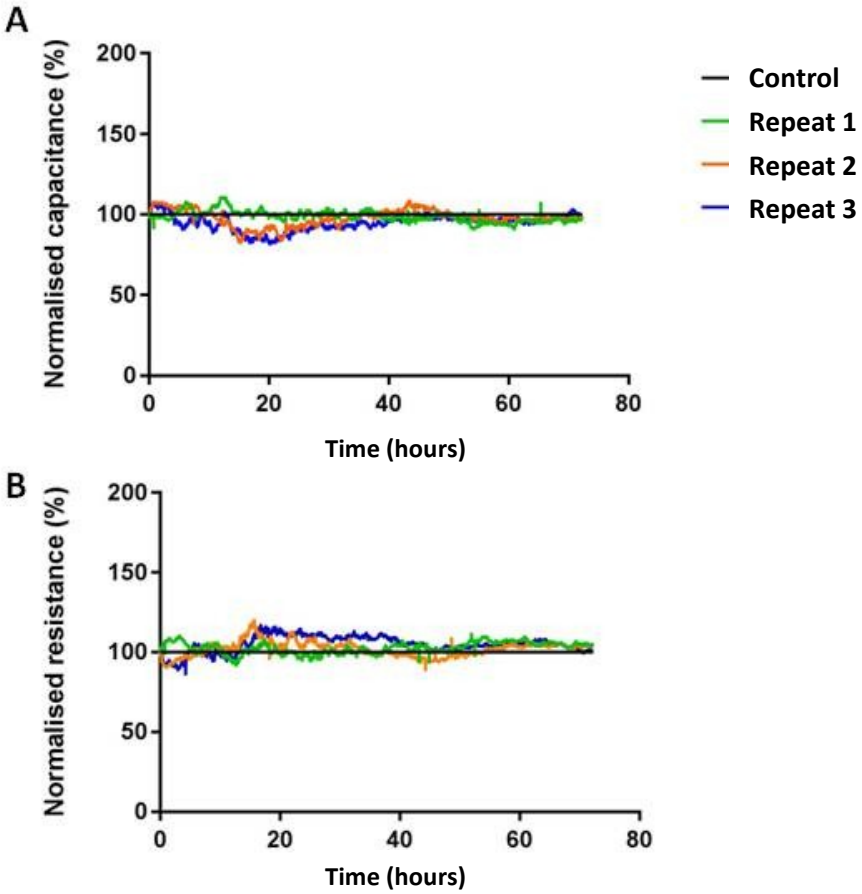


**Figure 3.3 ECIS plots show low variation in measurements on the same array.** Normalised A) Resistance and B) Capacitance. Each result is one well of endogenous passage 3 HBECs normalised to a control well of passage 3 HBECs on the same array. The control well was kept in the same position between repeats. Measurements were taken over 72 hours for 3 independent biological replicates.

Figure 3.3 shows that there is relatively low variation within wells on the same array (when compared to Fig. 3.2 C and D). This suggests that there is less variation in technical repeats than in biological repeats.

### 3.3.2 Comparison of early passage endogenous HBECs and late passage +Bmi1 HBECs using ECIS

Whilst inducible cell lines were being produced, the ECIS system was used to compare previously modified (by Torr *et al*., 2016) late passage HBECs (+Bmi1) to early passage unmodified HBECs of the same donor. If +Bmi1 HBECs are to be used for respiratory research, ideally they should be as representative of unmodified cells as is possible. ECIS has been used here to compare barrier function between the two cell types.

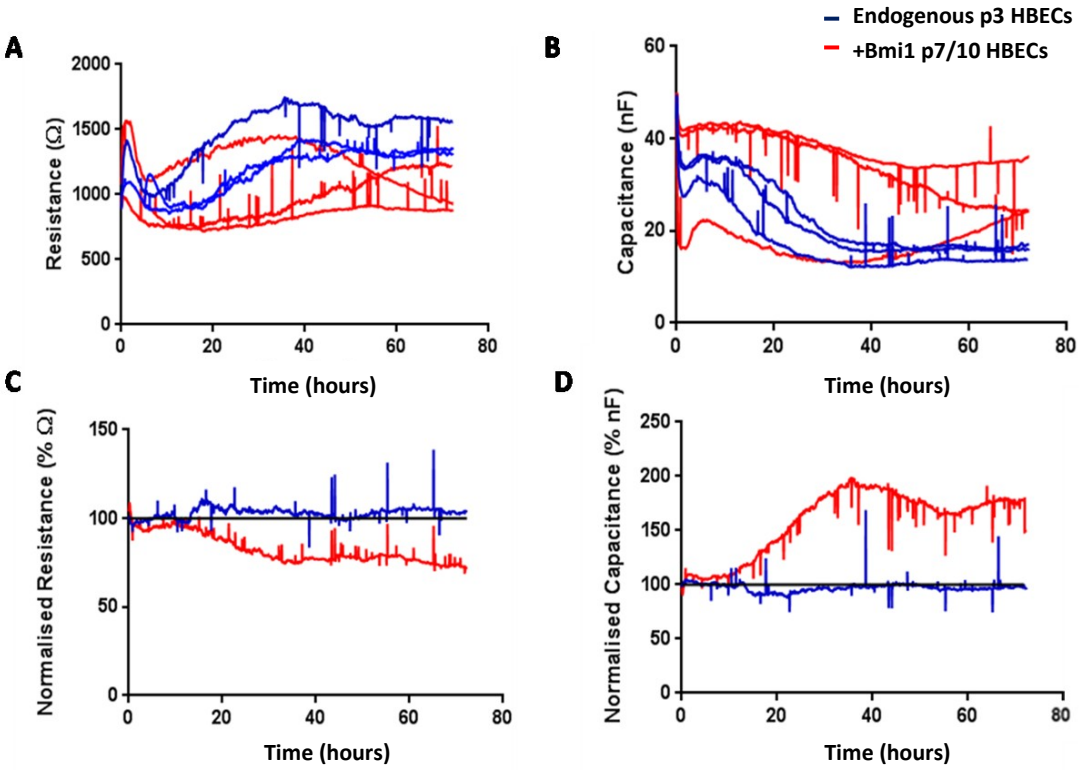


**Figure 3.4 Bmi1-engineered cells show growth and barrier differences compared to endogenous cells of the same donor.** A) Raw resistance, B) Raw capacitance; C) Normalised resistance and normalised capacitance of unmodified passage 3 HBECs (blue) and genetically modified passage 7/10 +Bmi1 HBECs (red) show deviances between cells. Resistance measured at 400Hz and capacitance at 32kHz. In A-B, each line represents the mean of two wells from an independent repeat. In C-D), results were normalised per well to one of the endogenous passage 3 HBEC wells and then averaged. Cells from the same donor were used for both endogenous and genetically modified samples.

The resistance does not increase as quickly in modified HBECs and does not reach the same level of resistance as wild type cells (Fig 3.4 A and C), by 40 hours, the +Bmi1 HBECs were only at 70% of the resistance of wild type cells, which could indicate that the barrier function is affected in the +Bmi1 HBECs or as a result of being at a later passage. The normalised resistance appears to plateau after this time point for both cell types.

Furthermore, the capacitance does not decrease as markedly in the modified cells, suggesting that there is decreased electrode coverage. Again, the raw data (Fig 3.4 B) shows that the modified HBECs do not reach the same level of capacitance as the wild type cells and by 40 hours were at almost double the capacitance (Fig. 3.4 D).

Overall, this could indicate that the genetic modification and/or late passage of the cell line has decreased barrier characteristics and decreased cell attachment. Furthermore, the modified HBECs appear to be more variable than the unmodified cells.

In order to determine when the differences in barrier properties occur between wild type and +Bmi1 HBECs, the resistance and capacitance measurements were taken at various time points over the 72 hours.

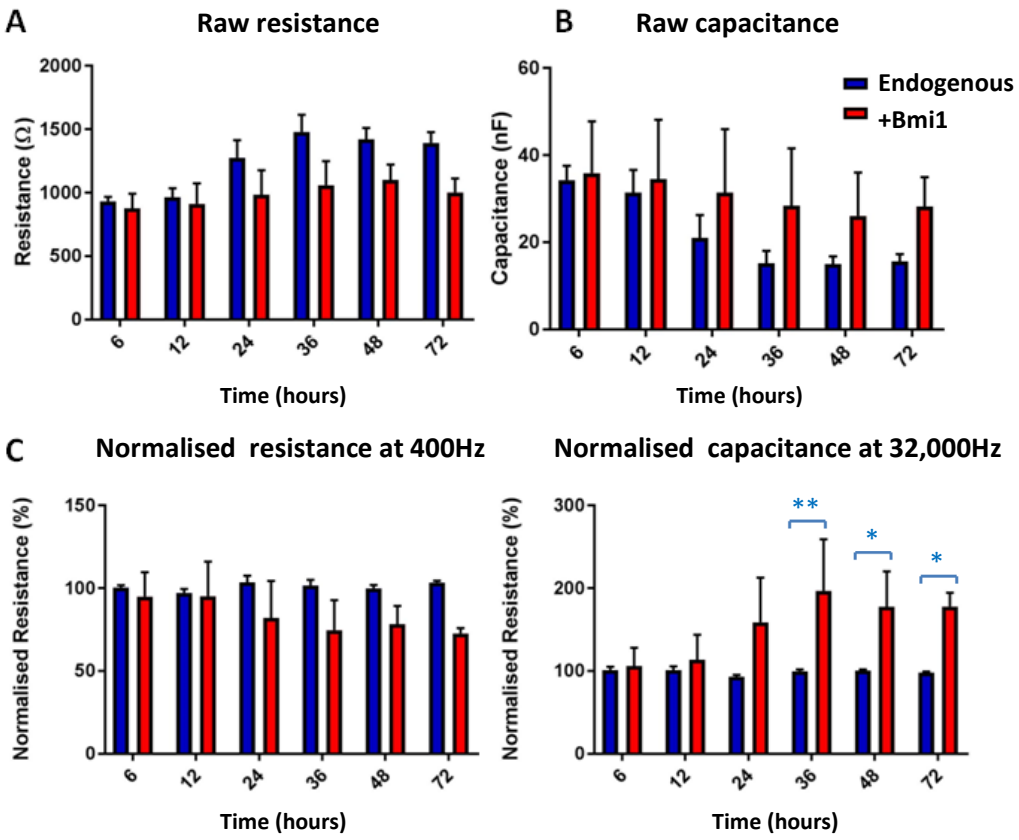


**Figure 3.5 Genetically modified HBECs with elevated Bmi1 show a greater degree of deviation from endogenous HBECs after 24 hours.** The A) resistance, B) capacitance, C) normalised resistance and D) normalised capacitance for 3 independent repeats biological shown. Duplicate wells in each repeat were averaged. Bars indicate the standard error of the mean. A two-way ANOVA was performed on the normalised data with Sidak's multiple comparison test. *: $p \leq 0.05$, **: $p \leq 0.01$, not significant: $P > 0.05$.

Fig 3.5 shows differences in resistance and capacitance between endogenous and genetically modified HBECs. Larger deviations from the wild type are seen after 24 hours, but statistical significance is only observed in the capacitance plot after 36 hours, showing that there is a difference between the cell types in terms of electrode coverage. Overall, the +Bmi1 HBECs show a greater variation between repeats compared to the wild type HBECs.

### 3.3.3 Monitoring barrier resistance in Calu3 cells

A key aim of the current work was to utilise +Bmi1 HBECs with the ALI model; ALI will be an integral part of characterising the modified cells in the future. As a prelude to this, I developed ALI techniques using the Calu3 cell line. In addition, the purpose of this was to become acquainted with culturing this cell type which was to be used for CRISPR-Cas9 genome editing in the later stages of the project, however due to time restraints this element of the project was not completed .

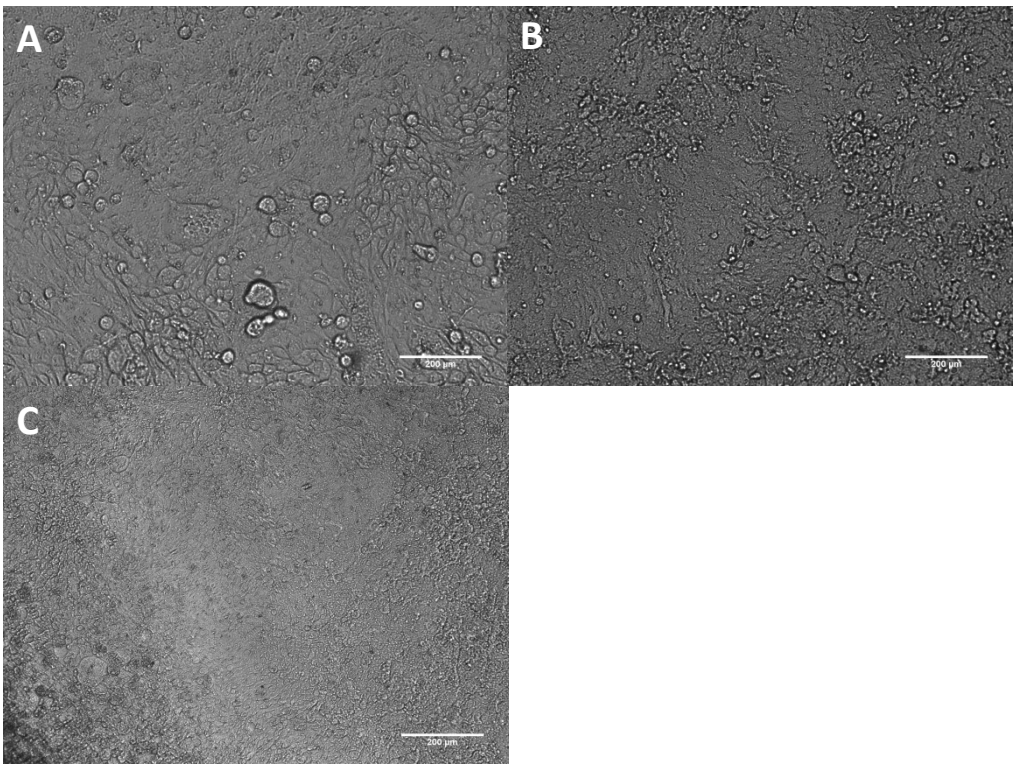


**Figure 3.6 Morphology of Calu3 cells before and after air lift.** A) Submerged Passage 22 Calu3 cells immediately before air lift, B) at day 2 of ALI and C) at day 8 of ALI. Mucus can be observed on the surface of the cells showing differentiation after culture at ALI. Scale bar shows 200μm.

Mucus could be observed on the apical surface of the cells (Fig. 3.6 B), suggesting that the cells had undergone differentiation and goblet cells were present in the culture.

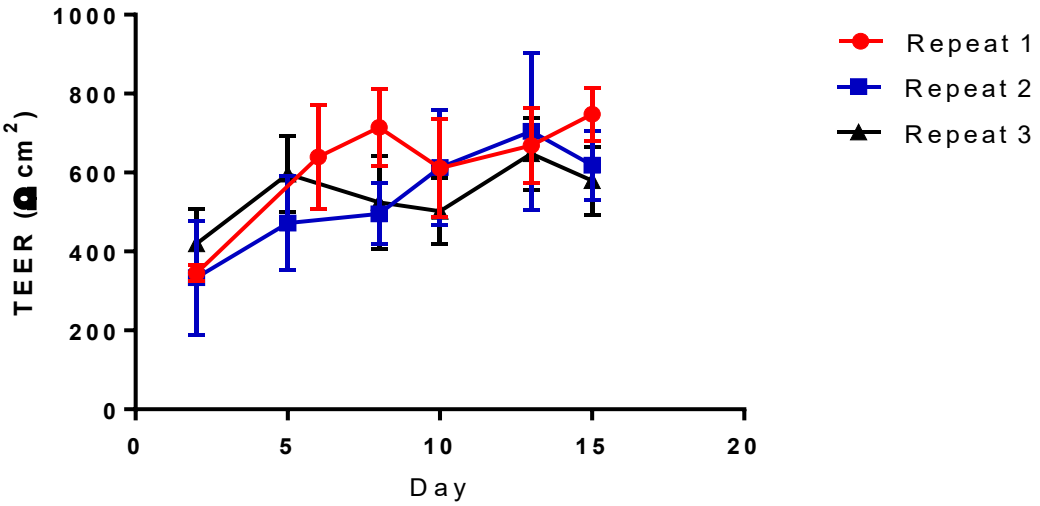


**Figure 3.7 TEER measured at ALI shows an increasing trend over time in Calu3 cells.** Repeat 1: P22, Repeat 2: P24, Repeat 3: P24.

Overall, the TEER gradually increases over time as the monolayer became more substantial and reached levels of > 400Ωcm$^2$, as observed in Stewart *et al.* (2012). Repeat 1 was conducted at a slightly lower passage, which may have accounted for the higher resistance achieved.

## 3.4 Discussion

The aim of this chapter was to establish the ECIS approach in my laboratory and begin to characterise similarities and differences in growth, adhesion and barrier formation between endogenous cells and Bmi1-engineered cells. In particular, to use ECIS with modified and unmodified HBECs and determine if this was a suitable method to use for characterisation.

### 3.4.1 Key findings

ECIS appears to be a sensitive enough method to detect a difference in barrier establishment and function between the modified and unmodified HBECs. The raw ECIS traces obtained for endogenous HBECs agreed with those in existing literature - the peak in resistance and dip in capacitance observed in the first few hours are proposed to be a 'hallmark' of primary bronchial epithelial cells, which is not seen in other airway cells (Heijink *et al.,* 2010). This suggests that ECIS is able to identify between different airway cell types and indicates that this could be a useful marker of bronchial epithelial cells. The 'hallmark' is seen in the genetically modified cells, but to a lesser extent than in WT controls.

Genetically modified HBECs with elevated Bmi1 show decreased resistance compared to endogenous controls which could suggest that barrier function is detrimentally affected. This agrees with results obtained by Torr *et al.* (2016), who found that the previously genetically modified HBECs produced a lower TEER at ALI than endogenous cells; low passage (p5) +Bmi1 cells reached only 56.5% of the TEER that control endogenous cells produced, medium passage (p8) cells reached 88% and high passage (p13) cells, 29.1%. At each stage, the TEER was lower in +Bmi1 cells than endogenous controls. Using ECIS, the normalised resistance of passage 10 HBECs dropped to 70% of the passage 3 WT control after 72 hours (Fig. 3.5 C), which is comparable to the decrease in TEER observed by Torr *et al.* (2016) at passage 8. Further analysis, for example, by using immunofluorescent staining to investigate tight junction proteins would be advantageous to provide a more complete picture. However, as the electrode coverage is also decreased (as indicated by a high capacitance), this could be due to a loss of cells rather than a decrease in the barrier integrity.

Loss of cells could be due to a decrease in adherence to the surface of the plates or as a result of increased apoptosis. As Bmi1 normally promotes cell survival, it would be surprising that over-expression of Bmi1 would directly cause cell death, although the process of gene manipulation may have had some adverse effects on the cells. Alternatively, a study in 2015 (He *et al.*, 2015) found that knockdown of Bmi1 resulted in a decrease in migratory

behaviour in tongue squamous cell carcinoma cells, and another (Li *et al.*, 2014) showed that Bmi1 over-expression enhanced migration and epithelial-mesenchymal transition, suggesting that Bmi1 could promote migratory behaviour. However, these studies were completed in cancerous cell types which may already have a predisposition for migratory behaviour.

Cell loss could potentially be problematic further down the line, and additional experiments will need to be undertaken to determine the extent and cause of the cell loss, particularly as cell adhesion is a vital requirement of epithelial cells in order to form an effective barrier. The ability to switch off Bmi1 over-expression may prove essential for developing the cell model.

At specific time points during ECIS measurements, larger differences were observed between the resistance and capacitance of modified cells compared to wild type cells after 24 hours, however resistance was not found to be statistically different at the time points analysed, whereas capacitance was statistically different after 36 hours, suggesting that by this time the barrier function and electrode coverage had decreased, although it is unclear which mechanisms are behind this.

There was high variation between biological repeats, particularly the genetically modified cells, which could be due to a number of factors, such as human error or the cells being less tolerant to external factors due to their manipulation. An element of this may be unavoidable given that the experiments were performed in a different laboratory.

A range of TEER measurements have been recorded for Calu3 cells in various studies from 100-2500$\Omega cm^2$ (reviewed in Srinivasan *et al*., 2015). The measurements taken in this project fall within that range, however are highly variable between repeats and over time. They are similar to those obtained by Stewart *et al*. (2012); their results also show variability between repeats. The TEER results they achieved were slightly lower but this may be due to the increased passage of their cells (35-37).

The next stage of the project would have been to culture the genetically modified cells produced in this thesis at ALI and on the ECIS array.

### 3.4.2 Potential for the future

ECIS provides a sensitive method of analysing barrier properties in airway epithelial cells and various other studies have used ECIS to study airway epithelial cells.

Singh *et al.* (2007) use ECIS to show that infection with respiratory syncytial virus causes a decrease in the barrier function of primary human bronchial

epithelial cells, although not until 16 hours post-infection. Furthermore, Antony *et al*. (2002) show that exposure to cockroach antigen also causes a significant decrease in the barrier function of bronchial airway epithelial cells after only 3 hours by inducing vascular endothelial growth factor (VEGF) activity, but this can be prevented by treatment with VEGF antibody. The ECIS measurements of primary bronchial epithelial cells from healthy and asthmatic donors show that there is a significant difference between their barrier resistances, and that in response to house dust mite, cells from asthma patients show more of a decrease in barrier resistance (Post *et al*., 2013).

ECIS has also been used to compare the responses of Calu3 and normal human bronchial epithelial cells to the β1-AR agonist, dobutamine (Peitzman *et al.,* 2015). This study found dobutamine caused a significant inhibition of both cell migration and wound repair in normal human bronchial epithelial cells, but not in Calu3 cells. This further illustrates the differences between primary bronchial epithelial cells and airway cell lines and shows how ECIS can differentiate between the two.

Whilst the results of this project show that passage 10 HBECs with elevated Bmi1 had decreased barrier function and cell coverage, the +Bmi1 HBECs used for ECIS in this instance possessed constitutive expression of Bmi1. Once inducible lines are produced, Bmi1 over-expression can be switched off in late passage GM HBECs and compared to early passage endogenous cells. Culturing the cells as high as passage 10 may also not be necessary to sufficiently expand the cells for experiments, and effects may be limited at lower passages.

Applied Biophysics also produce a 96 well plate for experiments (instead of the 8 well plate used in these experiments). The 8 well plate meant experiments were very limited and an empty well control could not always be included. As the results in this chapter indicate that there is less variation within the same array, the 96 well plate may be advantageous and would allow more comparisons, but would only be cost-effective with larger scale experiments.

### 3.4.3 Limitations

ECIS provides an interesting technique of assessing barrier function, with benefits of real time measurements. However, because the cells cannot be exposed to air, as in ALI, they remain undifferentiated basal cells, which is not representative of the *in vivo* environment. Therefore, in the case of airway epithelial cells, ECIS cannot be utilised alone, be should remain a complementary technique alongside other methods such as ALI and TEER.

Heijink *et al.* (2010) reinforce this issue by showing that 16HBE14o- cells provide a relatively low ECIS resistance reading (suggesting poor barrier formation), but a markedly higher TEER reading when grown at ALI.

Another limitation of ECIS is that any disruptions to the cell culture (incubator door opening, cell media changing, removal of the array) resulted in large anomalies in the measurements which lasted a period of several hours in the case of a media change (in preliminary experiments). As the measurements were taken over 72 hours, this meant a large proportion of the data was affected, so in future experiments, media was left unchanged and disruptions minimised as much as possible.

Ideally, images would have been taken to compare confluency with the ECIS capacitance output. However, cells could not easily be imaged following ECIS due to the electrodes on the bottom of the array obscuring the cells.

There were various options available for normalising the data obtained from ECIS. Applied Biophysics (2017c) mention that they minus the starting value of an empty well when plotting data. This was not possible in the repeats obtained as an empty well was not included on every array due to the limited number of wells available. The process used here normalised data at every time point and allows a clear visual comparison between cell types.

Calu3 cells were to be used for CRISPR-Cas9 genome editing. Genes of relevance to asthma progression were to be investigated and the effect on barrier function studied at ALI as a precursor to working with the modified +Bmi1 HBECs. The protocol followed for culturing Calu3 cells at ALI may need to be adapted for HBECs as the cell types grow at different rates. TEER provides a simple measure of barrier resistance, although the act of taking the measurements may affect the result, something which is not an issue for ECIS. In addition, the resistance may alter depending on the temperature of the cells (they need to be outside the incubator for as little time as possible) and the positioning of the electrodes. This could be overcome by maintaining the cells at 37$^{o}$C whilst measurements are taken and always taking measurements from the same location within the wells. A clearer trend may have been observed if the cells were cultured for a longer period of time. This experiment was to practice taking measurements and gain confidence in using Calu3 cells, however for future experiments all repeats should be performed at the same passage.

### 3.4.4 Summary

ECIS provides a complementary technique to utilise alongside ALI TEER measurements, with the considerable advantage of measurements being

taken in real-time without needing to disturb the cells. Whilst ECIS provides a lot of data, it can only be interpreted fully when analysed alongside other experimental techniques, for example protein studies, like Western Blotting and immunohistochemistry to determine the mechanisms behind the changes observed. ECIS has successfully been used to study airway epithelial cells in this study and others and will therefore provide a useful tool for characterising the inducible cell line.

# 4. Transcriptomic analysis of the effect of BMI-1 over expression in a human cell line

## 4.1 Introduction

Transcriptomic analyses can be used to explore the global effects that Bmi1 over-expression has on the genetically modified cells.

The genes which are being expressed by a cell determine its function, behaviour and characteristics and is known as the transcriptome. Recent advances in sequencing and computing technology now mean that it is possible and economically viable not only to sequence the entire transcriptome but also to determine a measure of transcript abundance and calculate differential gene expression between samples using statistical analyses (Mutz *et al.*, 2013).

RNA sequencing (RNA-seq) produces an overview of the transcriptome and can provide a 'snapshot' of the gene expression levels of a particular sample. Collection and sequencing of the RNA from the genetically modified HBECs would provide a wealth of information about how over-expression of Bmi1 affects the primary cells and to determine the utility of the Bmi1 approach as an airway epithelial cell model based on the number and extent of changes observed. RNA sequencing has many benefits, for example it provides a large amount of unbiased information, with low background noise, and is able to function even with incomplete reference genomes (Han *et al*., 2015).

In respiratory research, RNA-seq has been used to highlight how smoking affects the expression of various genes within the airway epithelium and was sensitive enough to identify novel genes associated with smoking (Hackett *et al*., 2012). RNA-seq can thus be used on the genetically modified airway epithelial cells produced in this project and early passage endogenous airway epithelial cells to determine differentially expressed genes and assess how representative the modified cells are.

As discussed in Section 2.1, Fig. 2.4, the genetically modified HBECs were intended to undergo RNA sequencing analysis to determine the effects of Bmi1 over-expression and lentiviral infection. In particular this would have been useful in comparing differential gene expression in endogenous cells and genetically modified but repressed HBECs (Bmi1 over-expression switched off).

However, due to time limitations of the project, RNA sequencing could not be performed on the modified cells and ideally a larger number of donors would be utilised first to create numerous cell lines. Therefore, online RNA sequencing databases were examined for existing studies involving Bmi1 over-expression instead to at least provide an indication of the nature and extent of the changes observed.

### 4.1.1 A Gene Expression Omnibus dataset was chosen for analysis of differential gene expression

Gene Expression Omnibus (GEO; https://www.ncbi.nlm.nih.gov/geo/) (Edgar *et al.*, 2002) is a repository which collates gene expression data from researchers (Barrett & Edgar, 2006), allowing them to share their RNA sequencing data with others for independent analysis.

GEO was searched with keywords 'Bmi1' and 'human' to find datasets which provided RNA sequencing data for human Bmi1 over-expression. Initially, it was intended to perform a meta-analysis of multiple studies, however at the time of research only one study met the needs of this project.

The GEO dataset that was identified as the most relevant (a study by Ferretti *et al*., 2016; GEO accession: GSE71890), contained RNAseq data from a human melanoma cell line (A375 cells) infected with lentiviruses containing either mouse Bmi1 or GFP (mouse and human Bmi1 coding regions are 92% homologous (Kinnon & Fulton, 1999)). A summary of the methods used in their study are shown in Table 4.1.

| | |
|---|---|
| **GEO ID** | GSE71890 |
| **Cell type used** | A375 cells (human melanoma) |
| **Conditions** | +Bmi1 or +GFP (control) |
| **Samples** | 3 independent biological repeats for each condition (total RNA) |
| **RNA preparation** | Illumina protocol |
| **Sequencing system** | Illumina HiSeq 2000 (Homo sapiens) |
| **Paired or single-end sequenced?** | Single-end |
| **Read length** | -50mers |
| **Log transformed?** | No |
| **Normalisation** | EBSeq Median normalisation |
| **Differential expression software** | EBSeq version 1.4.0 |

**Table 4.1 Summary of the RNA-seq methods used by Ferretti *et al.* (2016)**

Their study aimed to investigate the role of Bmi1 over-expression in promotion of metastatic behaviour and therefore their study was targeted towards differential expression of metastatic regulators, such as PTEN and AKT.

However, for this project the RNA sequencing data will be used in a broader investigation into how Bmi1 over-expression could affect a human cell line and to what extent these changes may occur.

The use of alternative statistical approaches to investigate differential expression of mRNA is an evolving field. These approaches use different parameters from the data and have various strengths and weaknesses depending on which parameters are ranked highly and the nature of the dataset.

The authors of the paper use EB Seq (Leng *et al.,* 2013) for the differential expression analysis. This technique appears to prioritise analysing the differential expression of isoforms (Leng *et al*., 2013) and may not be as relevant to my interest.

For this project I have applied two techniques to analyse differential expression, Rank Prod (Carratore *et al.*, 2016) and Cuff Diff (Trapnell *et al.*, 2010, 2013). These outputs will be compared with the genes identified by Ferretti *et al.* (2016) to determine the genes which are consistently ranked differently in cells engineered to over-express Bmi1. Scripture-Adams *et al.* (2014) have also utilised a combination of both CuffDiff and an analysis based on rank products to identify differentially expressed genes, which supports the use of this methodology in this project.

### 4.1.2 RankProd

RankProd is a non-parametric analysis package which identifies differentially expressed genes that are consistently ranked highly amongst repeats (Hong *et al*., 2006).

RankProd relies on the Rank Product method (Breitling *et al.,* 2004). It is primarily aimed at micro-array data and ranks data between a sample and control based on the Fold Change, which is thought to be more reproducible than analyses based on expression level variability (Dembélé & Kastner, 2014). This technique takes into account that biologically relevant changes are usually relatively large and it has been shown to deal well with data of high variance (Breitling *et al.,* 2004).

One of the main benefits is that it allows the user to compare data obtained from different laboratories and using different platforms (Hong *et al.*, 2006), thus would not have been a limiting factor had multiple Bmi1 datasets been found online.

### 4.1.3 CuffDiff

As an alternative methodology, the Bowtie-Cufflinks Pathway (Trapnell *et al.*, 2010, 2013) was utilised. The Bowtie-Cufflinks Pathway is a series of analyses which when combined together assist in comparing differential gene expression between conditions using RNA-seq data (Trapnell *et al.*, 2012). A brief overview of the pathway can be seen in Fig. 4.1. Each step produces files which are fed into the next stage.

The initial stage is a program called TopHat. TopHat was developed to use Illumina output and in conjunction with a software called Bowtie functions to align RNA sequencing reads to a reference genome (CCB, n.d.).

These alignments are then assembled and quantified by Cufflinks (which also filters out background noise) and merged together to form a transcriptome for each condition by Cuffmerge (Trapnell *et al.* 2012)

CuffDiff then uses rigorous statistical tests to compare the expression levels for each condition and identify differential expression based on the abundance of transcripts being equivalent to the level of expression (Trapnell *et al.*, 2012). The statistical analyses are based on a negative-binomial distribution model which is thought to represent the output data most appropriately (Zhang *et al.*, 2014).

The CuffDiff output provides numerous files - the most relevant to this study is gene_exp.diff which provides gene level information about whether there is differential expression. For each gene, a single FPKM (or Fragments Per Kilobase of transcript per Million mapped reads) value is calculated for each condition. When the FPKM value is totalled per gene it provides a measurement of transcript abundance and therefore gene expression (Twine *et al.*, 2011). The calculated FPKM values per condition indicate whether the gene is up or down-regulated. The log2(fold change), p-value and q-value (the "FDR adjusted p-value" (Trapnell, 2016)) are also computed to determine whether there is statistical significance and to what extent the expression is changed.

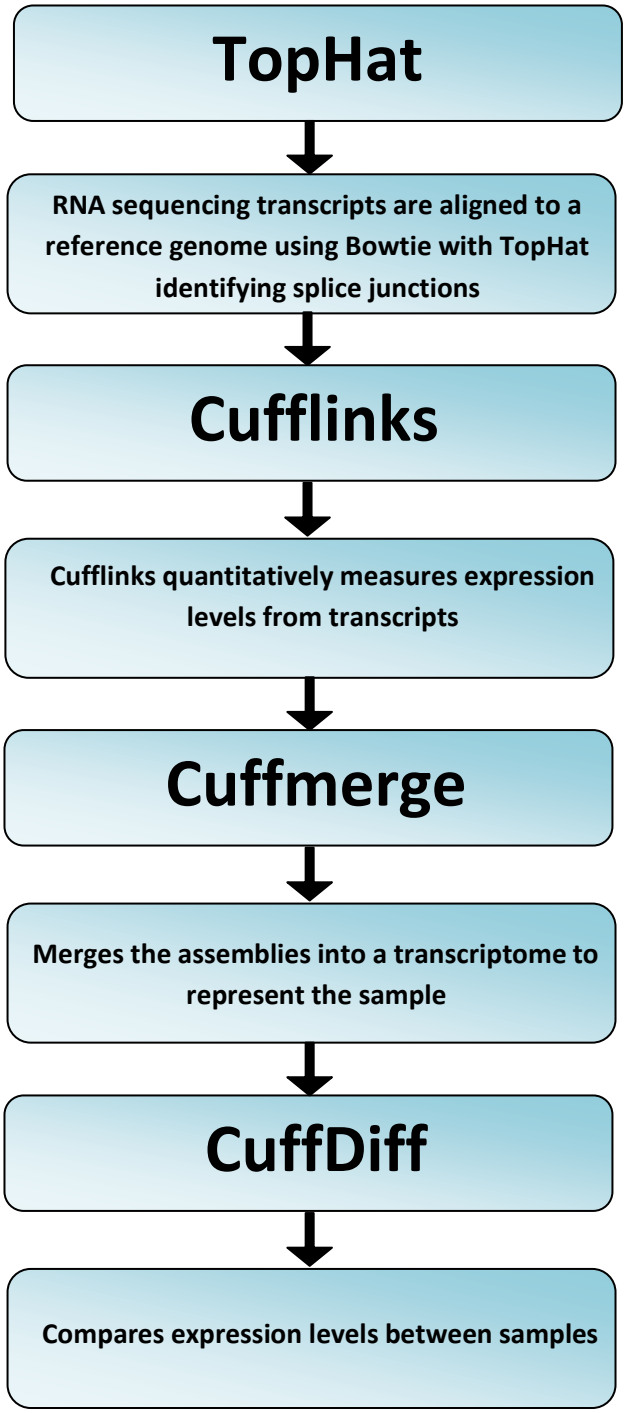


**Figure 4.1 A flowchart of the stages involved in the Bowtie-CuffLinks Pathway (Trapnell *et al.*, 2012) in order to analyse RNA sequencing data for differential gene expression.**

### 4.1.4 Aims of the chapter

The aim of this chapter is to provide initial characterisation of the effects caused by increasing Bmi1 expression in a human cell line and to identify any relevant genes which may be significantly affected by Bmi1 over-expression.

## 4.2 Methods

This work was completed in collaboration with Sangita Bhaker and Alexander Kheirallah.

### 4.2.1 Rank Product Analysis

RankProd (Hong *et al*., 2006) is an R package (R Core Team, 2013) which was utilised to rank differentially expressed genes.

Only the normalised data of the differentially expressed genes identified by Ferretti *et al.* (2016) was available online via Supplementary Information, so a complete normalised dataset (containing all genes) in Excel format was requested and provided by the authors via personal communication.

Any genes which had an RNA-seq test value of zero (in either the Bmi1 samples of the control GFP samples) were excluded from the analysis. The normalised values were saved in a csv file to be accepted by R.

The Rank Prod package was used as described in the Rank Prod Vignette. R version 3.3.3 was used with R studio Desktop 1.0.143.

After inputting the script into R, a table was produced of the genes. Percentage of false predictions (pfp) was the corrected p value and a cut off of pfp≤0.05 was selected to identify significantly altered genes compared to controls.

### 4.2.2 CuffDiff Analysis using the Bowtie-Cufflinks Pathway

Bowtie-Cufflinks Pathway (Trapnell *et al.*, 2010) was used with TopHat version 2.0 and Cufflinks version 2.21 on Ubuntu Linux version 12.04 LTS.

The FASTQ files of raw sequencing data (3 files for each condition) were downloaded directly from the GEO (Edgar *et al.*, 2002) website (GEO accession: GSE71890) and unzipped.

The reference human genome (GRCh37) was downloaded from Ensembl (Aken *et al*., 2016) and the Bowtie-Cufflinks Pathway followed as described in Trapnell *et al.* (2012).

The cuffdiff output includes a range of files including gene_exp.diff which compares differential gene expression but also files with additional information, for example which allow comparisons of isoform expression.

CummeRbund (Goff *et al*., 2013) was used in R Studio Desktop 1.0.143 with R (version 3.2.5) and Bioconductor (version 3.5) in order to create figures as described in Trapnell *et al.* (2012).

### 4.2.3 Comparisons between methods

Venny 2.1 (Oliveros, J.C., 2007-2015) was used to compare gene lists between methods.

Genes which were identified at the same locus by CuffDiff were individually considered during comparisons and those loci which did not have a gene name associated with them were omitted from gene comparisons using Venny.

For RNA-seq analysis, a percentage of false predictions (pfp) value of < 0.05 was used for Rank Prod as used in Henz *et al*. (2007), and False Discovery Rate of < 0.05 was considered significant for CuffDiff, as used in Soneson & Delorenzi (2012).

## 4.3 Results

Using the GEO dataset, two different methods of identifying differentially expressed genes were utilised: Rank Prod and CuffDiff.

### 4.3.1 Rank Product Analysis identifies 380 differentially expressed genes

Rank Prod provides a relatively quick and simple means to study differential mRNA expression based on rankings of 'peak abundance and expression changes' (Wang *et al.*, 2015).

Initial analysis results were heavily skewed by values of zero in the dataset. Therefore, the analysis was redone excluding any genes which included a zero RNA-seq value in the normalised data. The total number of genes this included was 5263 of the 21,712, leaving 16,449 genes for the Rank Prod analysis.

Of the 16,449 genes analysed from the Ferretti *et al*. (2016) dataset, 269 were significantly up-regulated and 111 were significantly down-regulated in response to Bmi1 over-expression (pfp<5%).

Of the significantly up-regulated genes, the fold change ranged from 3.4411 to 91.2409. Of the significantly down-regulated genes, the fold change ranged from 0.1054 to 0.5653, suggesting that the down-regulated genes are affected to a much lesser extent than the up-regulated genes.

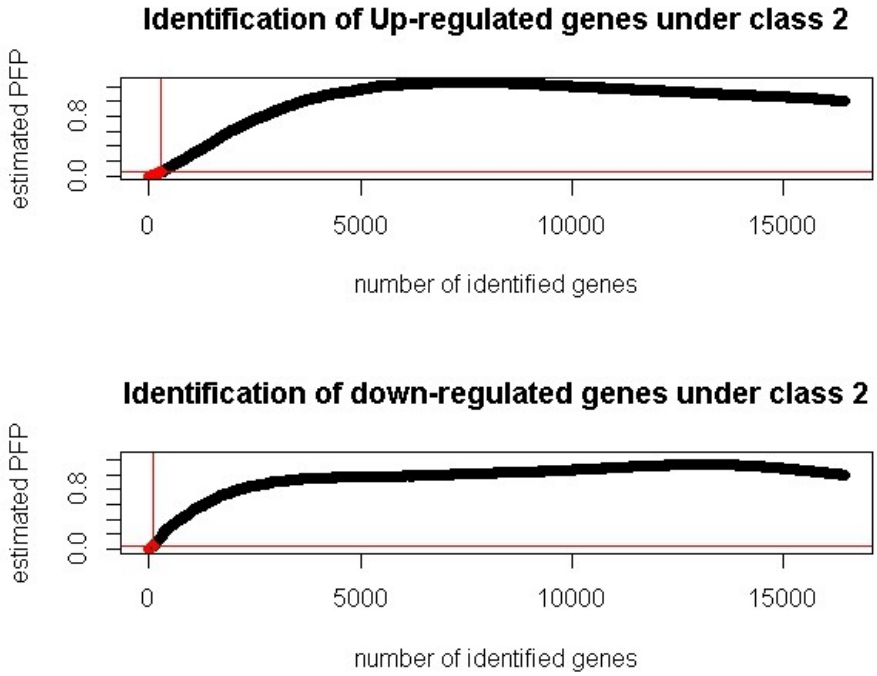


**Figure 4.2 Of the 16,449 genes analysed, only a small proportion are significantly up or down-regulated (estimated pfp<0.05 highlighted in red).** Each dot represents a gene with its RP/RSum value plotted against its estimated percentage false prediction as computed by Rank Prod.

The list of up-regulated genes (pfp<5%) produced by Rank Prod were compared to the up-regulated genes discovered by Ferretti *et al.* (2016). They identified 842 up-regulated genes (q-value<0.05, FC≥1.5) of which 192 were also identified using RankProd and 107 down-regulated genes (q-value<0.05, FC≥1.5), of which 29 were also identified using RankProd.

### 4.3.2 Cuffdiff identifies 1024 genes which are differentially expressed

CuffDiff is an alternative means of determining differentially expressed genes which is widely used to analyse RNA sequencing data (Hayer *et al.,* 2015).

CuffDiff identified 836 genes which were up-regulated and 188 were down-regulated (q<0.05); q is the False Discovery Rate (FDR) adjusted p-value. Multiple genes were sometimes identified at the same locus. Those loci not associated with a gene name have not been included (90 of the 1114 significant loci did not have a gene name associated with them).

Of the 836 up-regulated genes, 287 had a log2Fold Change >1.5 and 50 had a log2Fold Change >3. Of the down-regulated genes, 47 had a log2Fold Change >1.5 and 20 had a log2Fold Change >3.

Bmi1 is identified as being significantly up-regulated (q-value = 0.001636, log2Fold Change = 1.40097, Fold Change = 0.3786744532), however is 246th when the up-regulated genes are ordered by q-value (smallest to largest), and 318th when ordered by log2FoldChange (largest to smallest).

CummeRbund, which is an additional component of the Bowtie-Cufflinks pathway, was used to visualise the CuffDiff output in R globally. There are quality control features included in the CummeRbund package; one of which is a density plot to ensure similar distributions of data between samples. Fig. 4.3 shows the density plots from the CuffDiff output. The over-lapping plots show that the majority of both sets of data share a comparable distribution and therefore were likely to be successfully normalised. A similar size and shaped density plot for each condition also suggests that they were both sequenced to similar read depths (Hart *et al.*, 2013).

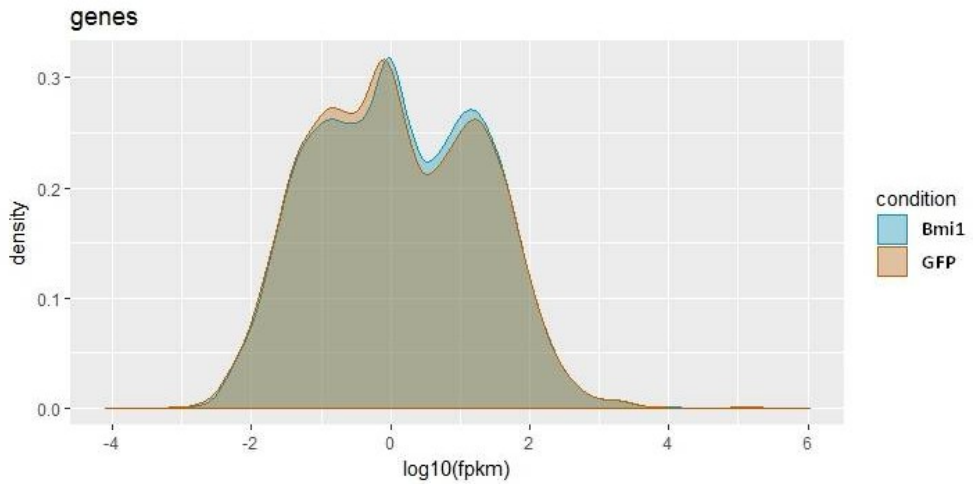


**Figure 4.3 Overlapping density plots log10-transformed FPKM values indicate successful normalisation of samples.** The computed densities of log10-transformed FPKM values for genes from either the condition engineered to over-express Bmi1 (blue) or the control GFP (red). The data distribution of both samples is similar as the majority of genes are not affected between conditions.

CuffDiff has grouped Bmi1 with two other isoforms at the XLOC_005475 (location 10:22604902-22620553) locus, COMMD3 and COMMD3-BMI1. COMMD3 is identified as being in close proximity to the Bmi1 gene on Chromosome 10. COMMD3-BMI1 is a read-through transcript which results in a fusion protein of the two components (Hoffman *et al*., 2017), however there is little published data concerning this fusion product.

As expected, a bar plot of the FPKM results for 'BMI1, COMMD3, COMMD3-BMI1' shows a significantly increased FPKM value in the +Bmi1 sample compared to the GFP control (Fig. 4.4).

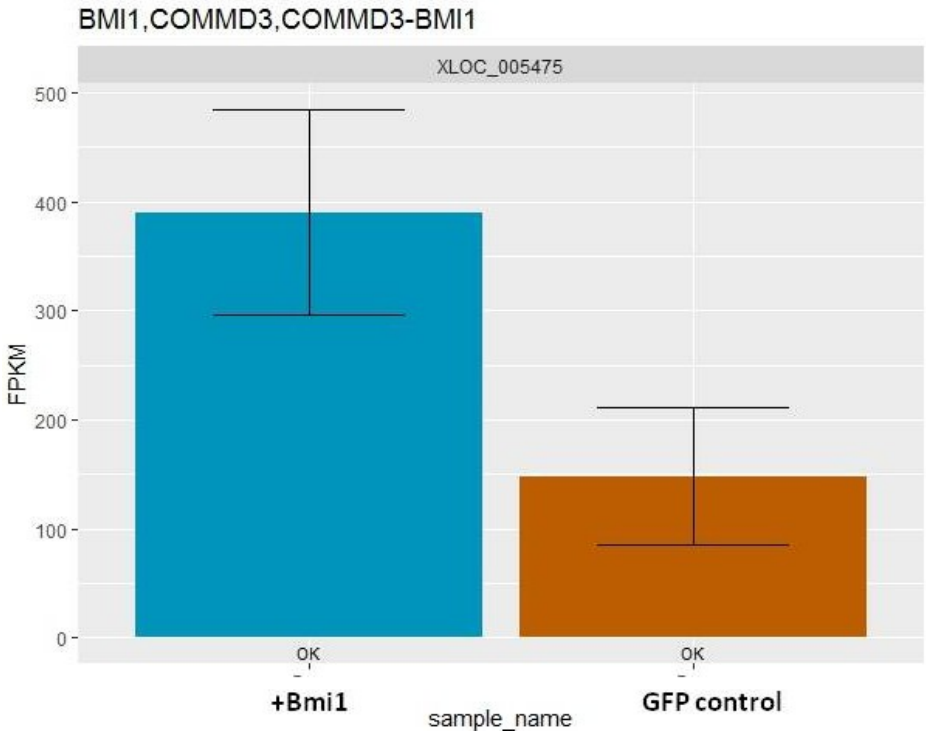


**Figure 4.4 RNA sequencing analysis shows Bmi1 expression is significantly higher in cells engineered to over-express Bmi1 compared to the control GFP sample.** A bar plot of the FPKM values for the 'BMI1, COMMD3, COMMD3-BMI1' locus with 95% confidence intervals shown.

In order to determine that the data shown is a result of Bmi1 over-expression (rather than COMMD3) the FPKM of the gene isoform expression data was compared for each isoform separately in Table 4.2.

| Isoform | +Bmi1 sample | GFP control |
|---|---|---|
| **BMI1** | 5.50825 | 12.825 |
| **BMI1** | 0.372799 | 1.24994 |
| **BMI1** | 1.37896 | 2.24268 |
| **BMI1** | 18.1655 | 3.57194 |
| **BMI1** | 131.565 | 4.79107 |
| **BMI1** | 0.127296 | 0.050107 |
| **BMI1** | 0.0966101 | 0 |
| **BMI1** | 124.888 | 6.8113 |
| **BMI1** | 4.24165 | 15.7034 |
| **BMI1** | 31.2013 | 2.05938 |
| | **317.5453651** | **49.30482** |
| **COMMD3** | 0.886149 | 0.969284 |
| **COMMD3** | 0.16441 | 0 |
| **COMMD3** | 0.571418 | 0.654975 |
| **COMMD3** | 0.409805 | 0.316258 |
| **COMMD3** | 10.9294 | 14.8317 |
| **COMMD3** | 0 | 0.124163 |
| **COMMD3** | 0 | 1.55028 |
| **COMMD3** | 0.084924 | 0 |
| **COMMD3** | 0.552821 | 1.33471 |
| **COMMD3** | 14.5846 | 12.4658 |
| **COMMD3** | 0.53123 | 0.627502 |
| **COMMD3** | 19.2674 | 25.6571 |
| **COMMD3** | 0.467085 | 2.07347 |
| **COMMD3** | 0.894352 | 1.02188 |
| **COMMD3** | 0 | 0.039597 |
| | **49.34359** | **61.66672** |
| **COMMD3-BMI1** | 5.97243 | 5.65276 |
| **COMMD3-BMI1** | 0.952823 | 0 |
| **COMMD3-BMI1** | 0 | 3.10853 |
| **COMMD3-BMI1** | 7.30762 | 16.1907 |
| **COMMD3-BMI1** | 0 | 0 |
| **COMMD3-BMI1** | 0.232363 | 0.498957 |
| **COMMD3-BMI1** | 5.76106 | 6.69222 |
| **COMMD3-BMI1** | 2.73983 | 4.51345 |
| | **22.96613** | **36.65662** |

**Table 4.2 Increase in the FPKM value show that differential expression is attributed to the Bmi1 isoform rather than COMMD3.** The CuffDiff FPKM values were totalled (in red) for the reads assigned to each isoform to ensure that changes in gene expression were due to the contribution of Bmi1.

Table 4.2 shows a large increase in the FPKM value for the Bmi1 isoform in the +Bmi1 samples compared to the GFP control, rather than COMMD3. Therefore, the resultant changes in expression are a result of Bmi1 over-expression. This data is also summarised and presented in Fig. 4.5.

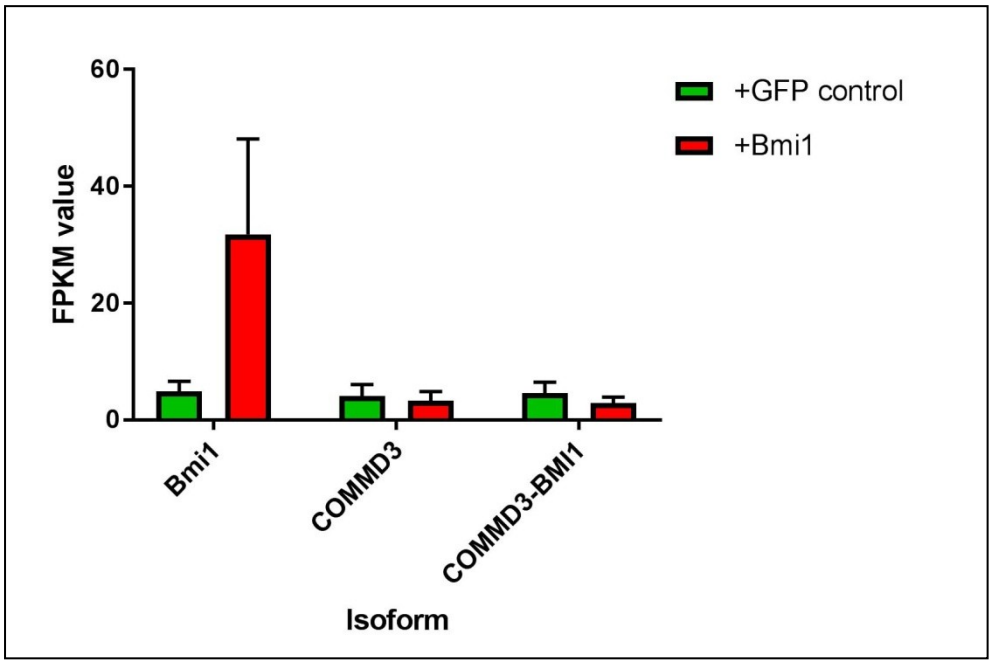


**Fig. 4.5 The mean FPKM values for each isoform at the XLOC_005475 locus show that the Bmi1 isoform has the largest increase between conditions.** Therefore, the signal from this locus is attributed to the Bmi1 isoform. Error bars showing the standard error of the mean.

Furthermore, COMMD3 is not amongst the differentially expressed genes identified by Ferretti *et al.* (2016) whereas Bmi1 is. This allows me to have confidence that the differential gene expression results obtained from CuffDiff are due to the Bmi1 gene and not COMMD3 or COMMD3-BMI1.

### 4.3.3 Overall differential gene expression

In order to get an overview of how Bmi1 over-expression can affect gene expression, all of the gene expression data was plotted into a scatter plot (Fig. 6) and a volcano plot (Fig. 7).

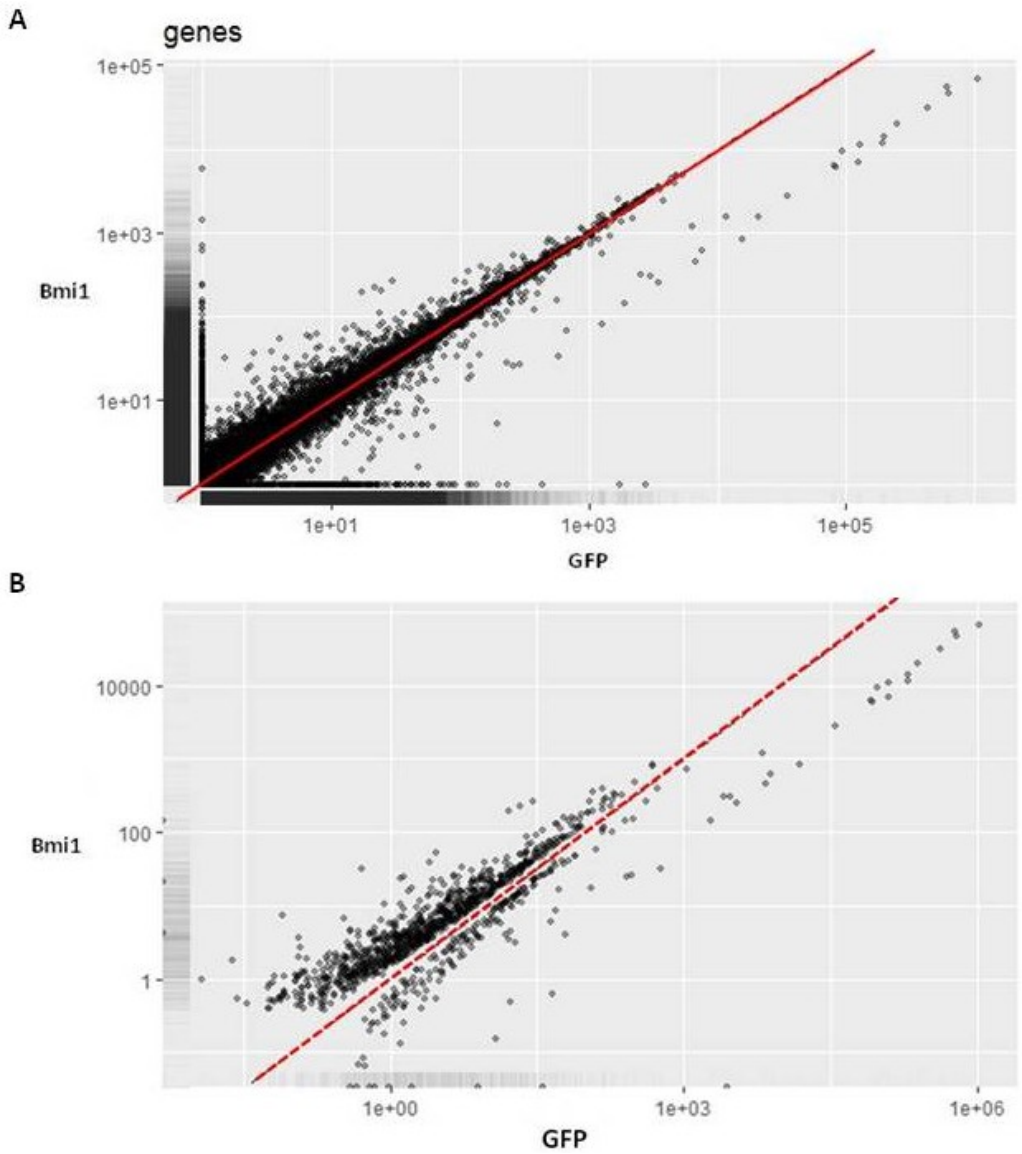


**Figure 4.6 Pairwise comparison of FPKM values assigned to each gene by CuffDiff from samples engineered to over-express Bmi1 compared to a control GFP condition.** A) All genes analysed by CuffDiff and B) only differentially expressed genes (1114 loci where q<0.05) are shown. Each dot represents the FPKM value of a single locus plotted on a log10 scale. The line represents the same level of expression between samples, Therefore, any dots which deviate from the line show differential expression at that locus. A position below the line indicates higher expression in the control GFP sample, whereas above the line represents higher expression in the +Bmi1 sample.

As can be seen in Fig 4.6 B, there are a greater number of genes over-expressed in the +Bmi1 sample compared to the GFP control. However, those which are expressed more highly in the control (and thus down-regulated with Bmi1 over-expression) deviate more from the line, suggesting a larger difference between conditions.

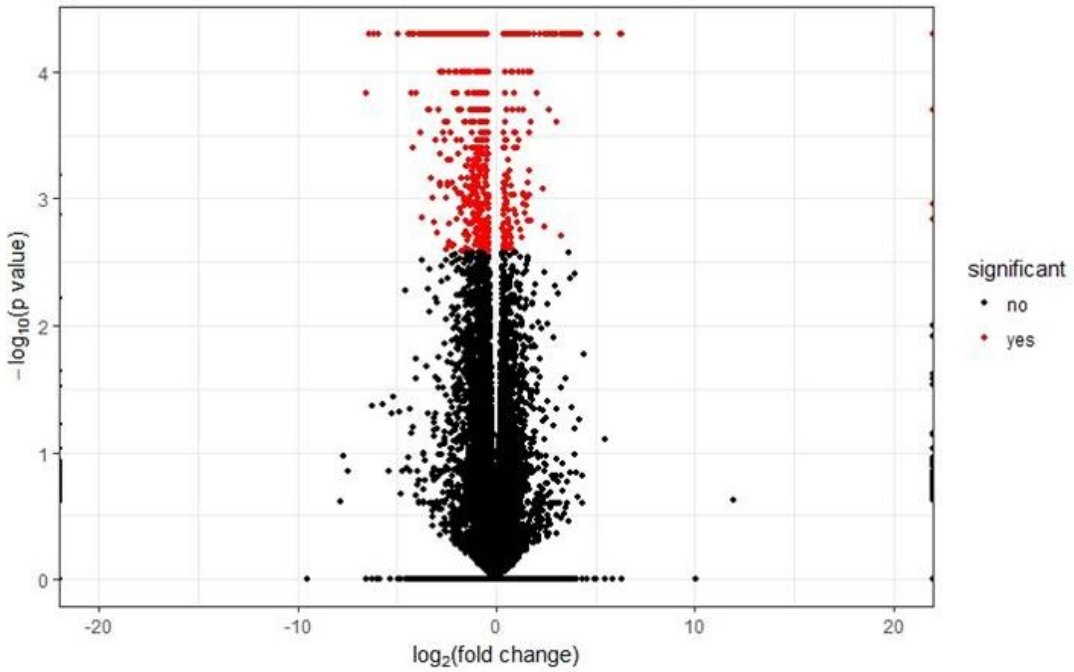


**Figure 4.7 Volcano plot showing higher fold changes in genes up-regulated in +Bmi1 samples (alpha <0.05).** The dots on the left of zero $\log_2$(fold change) indicate loci for which expression is lower in the GFP control, whereas those on the right show those which are higher in the GFP control when compared to the +Bmi1 sample.

Fig. 4.7 also provides a graphical overview of the differential gene expression between the +Bmi1 and GFP control condition, showing that for significant genes, the log2(fold change) has a similar distribution for up and down-regulated genes. Note - for Fig. 4.7, Bmi1 was used as the reference gene by default, so the dots represent the effect on GFP compared to Bmi1.

As Fan *et al.* (2008) and others have shown, both p16 and alternative reading frame p14 (CDKN2A) are inhibited by Bmi1. Therefore, the FPKM values were investigated for CDK2NA and compared between samples.

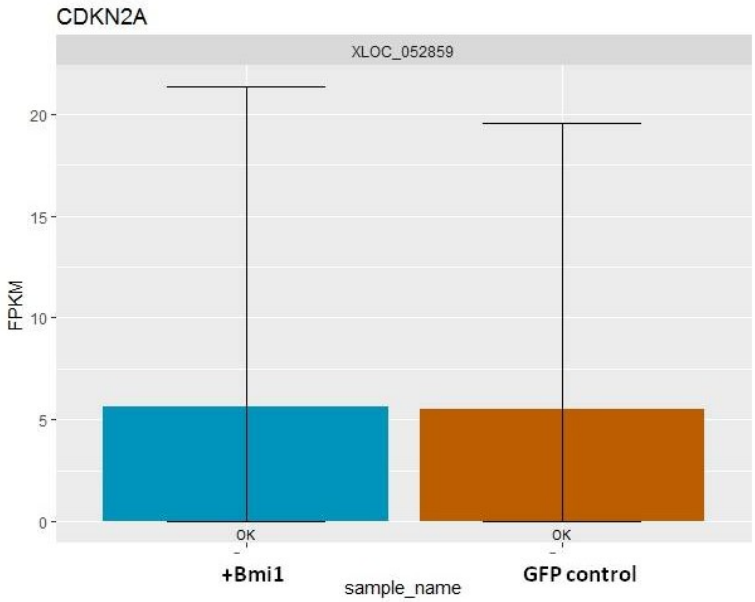


**Figure 4.8 CDKN2A expression was not significantly different in +Bmi1 samples compared to the GFP control.** The FPKM values were unchanged suggesting that the Bmi1 over-expression did not alter the expression of the p16 or p14 gene. Error bars show 95% confidence intervals.

As with the Ferretti *et al.* (2016) paper and Rank Prod, p16 was not identified by CuffDiff as being significantly differentially expressed (Fig. 4.8).

### 4.3.4 Differentially expressed genes which are consistently significant

CuffDiff identified a large number of significantly differentially expressed genes. Therefore, the list of genes was compared with those found to also be significantly different by Ferretti *et al.* (2016) using EBSeq, and those found using Rank Prod in Section 4.3.1. This produced a list of genes which have been consistently ranked as significant via the various methods and are therefore more likely to be of consequence biologically.

Bmi1 was amongst those, as expected, and statistical comparisons can be seen in Table 4.3.

| | Statistical significance | Fold Change | Log2(Fold Change) |
|---|---|---|---|
| CuffDiff | q=0.00005 | 2.6407907678 | 1.40097 |
| Rank Prod | pfp =0.01246 | 5.737235 | 2.520356 |
| EB Seq (Ferretti *et al.* (2016) | FDR = 0 | 5.7372 | 2.5204 |

**Table 4.3 Comparison of the statistical values computed for the Bmi1 gene from RNA sequencing data.** Data from the two different methods explored in this project and EB Seq which was used by the authors of the data (Ferretti *et al.,* 2016) shown. Data represents samples over-expressing Bmi1 compared to GFP controls.

Comparisons were performed using the differentially expressed genes which were identified by Ferretti *et al.* (2016), RankProd and CuffDiff to determine those which were consistently significant across all three. Multiple genes which were identified at the same locus with CuffDiff were treated separately for the purpose of these comparisons.

144 up-regulated genes were shared by the three methods and 14 down-regulated genes as shown in Fig. 4.9 A and B. A large proportion of the significant genes are not shared between methods.

**A**

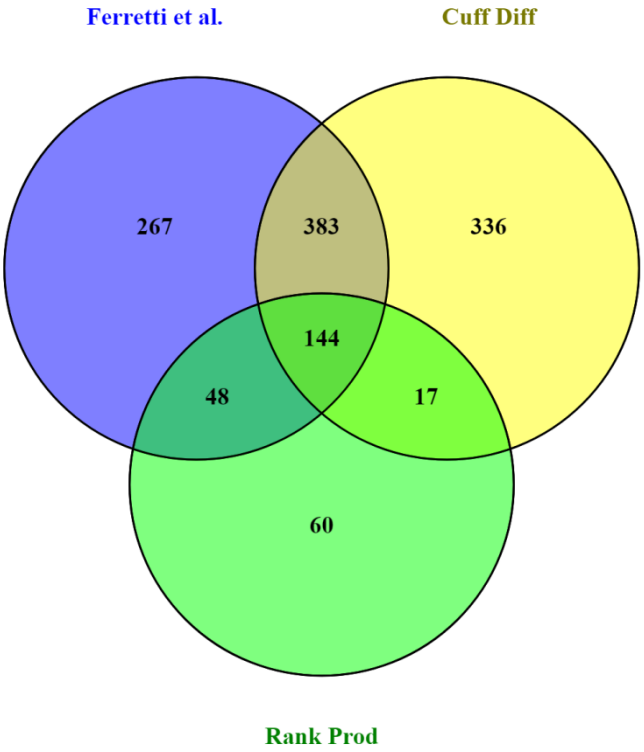


**B**

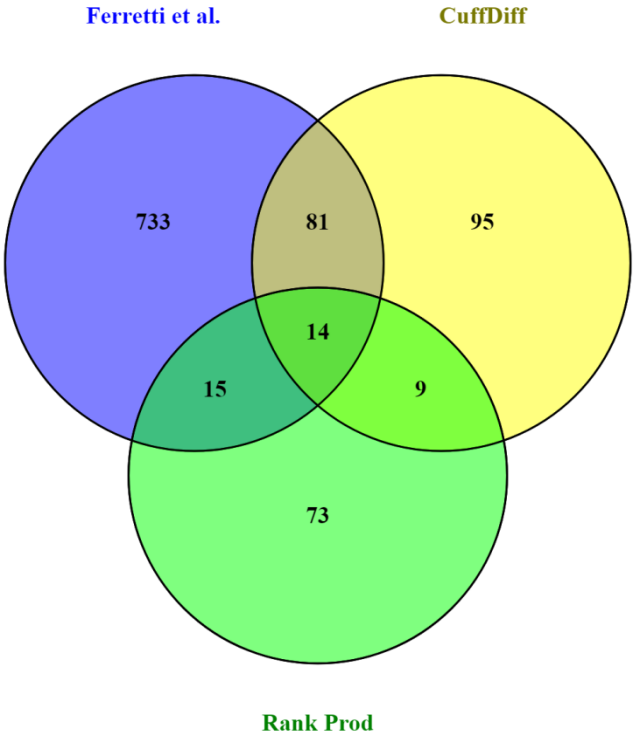


**Figure 4.9 A) 144 genes are significantly up-regulated and B) 14 genes are significantly down-regulated in all three methods.** Genes which were significantly different in the Ferretti *et al.* (2016) paper (q<0.05), Rank Prod (pfp<0.05) and CuffDiff (FDR<0.05).

To determine how these differentially expressed genes may affect the cells, their functions have been investigated.

In order to narrow down the gene list for up-regulated genes, after the comparison (144 in total), the results were ordered by log2(FC) of the CuffDiff output and the top 20 up and down-regulated genes are listed in Table 4.4 and Table 4.5 respectively. The complete list of 144 genes significantly up-regulated in all three methods can be found in the Appendix (Table S3).

Amongst the up-regulated genes in Table 4.4, are genes which are associated with cell growth and some which were linked to cancer and metastases, such as ELFN2 and IGF2.

In a recent study, cells were derived from either a lower gingival carcinoma primary lesion or a secondary cervical lymph node metastasis (in the same donor) and the gene differences studied to determine factors contributing to metastasis (Fujinaga *et al.*, 2014). ELFN2 was identified as one of the top 5 genes up-regulated (in terms of fold change) in the secondary tumour, suggesting that it may play a role in promoting a metastatic state.

IGF2 is elevated in multiple cancers (Livingstone, 2013). For example, IGF2 mRNA is found to be up-regulated in liver tumours compared to equivalent non-tumour tissue and is believed to accelerate tumour development (Martinez-Quetglas *et al.*, 2015). It is thought to act via the MAPK pathway to promote genes involved in proliferation and is transcriptionally suppressed via p53 (reviewed in Livingstone, 2013).

Additionally, there are genes associated with the extra-cellular matrix, such as ADAMTS2 and FN1, which may also enable metastatic behaviour and affect cell adhesion.

Surprisingly, there are also genes which are thought to be suppressed in certain cancers (IGFBPL1, NPTX1, NPTX2 and CHD5).

Amongst the down-regulated genes are BEX4, which is a suspected tumour suppressor (Chien *et al*., 2005) and RBM11 which is involved in neuron and germ cell differentiation (Pedrotti *et al.*, 2011) and therefore its down-regulation may assist in maintaining plasticity. Again, there are unexpected genes down-regulated, such as PDGFD, which is highly expressed in breast cancer (Liu *et al.* 2011).

| Gene Name | q-value | Log2 (Fold Change) | Function | Citation |
|---|---|---|---|---|
| **MEGF6** (Multiple EGF Like Domains 6) | 0.001636 | 6.39519 | Calcium ion binding protein | Jonchére *et al.,* 2010 |
| **IGF2** (Insulin Like Growth Factor 2) | 0.001636 | 6.19085 | Growth factor. Over-expressed in hepatocellular carcinoma | Martinez-Quetglas *et al*., 2016 |
| **CACNG7** (Calcium Voltage-Gated Channel Auxiliary Subunit Gamma 7) | 0.001636 | 4.94881 | Calcium channel subunit | Burgess *et al.*, 2001 |
| **SNCB** (Synuclein Beta) | 0.001636 | 4.42134 | Suspected role in synaptic function | Galvin *et al.*, 2001 |
| **TSPAN18** (Tetraspanin 18) | 0.001636 | 4.3113 | Membrane protein prevents neural crest migration | Fairchild *et al*., 2014 |
| **IL8** (Interleukin 8) | 0.001636 | 4.1529 | Involved in neutrophil activation and migration | Hull *et al.*, 2001 |
| **IGFBPL1** (Insulin Like Growth Factor Binding Protein Like 1) | 0.0044 | 4.03275 | Silenced in breast cancer | Smith *et al.,* 2007 |
| **PXDN** (Peroxidasin) | 0.001636 | 3.90804 | Hydrogen peroxide metabolism. Required for normal eye development. | Khan *et al*., 2011 |
| **CHD5** (Chromodomain-helicase-DNA-binding protein 5) | 0.001636 | 3.82857 | Tumour suppressor | Bagchi *et al.,* 2007 |
| **ADAMTS2** (ADAM Metallopeptidase With Thrombospondin Type 1 Motif 2) | 0.008055 | 3.81937 | Metalloproteinase involved with the extracellular matrix | Wang *et al.,* 2006 |
| **NPTX1** (Neuronal pentraxin 1) | 0.030194 | 3.72742 | Neuronal lineage differentiation<br>Hypermethylated (silenced) in lung tumours | Boles *et al.*, 2014<br>Zhou *et al.*, 2015 |
| **NPTX2** (Neuronal pentraxin 2) | 0.001636 | 3.55689 | Inhibits pancreatic cancer cell invasion | Zhang *et al*., 2011 |

**Table 4.4 (continued on next page) Top 20 genes based on log2(fold change) which are significantly up-regulated in all three methods.** The 144 significant genes identified by the three methods were ordered by log2(fold change) from CuffDiff output and the 20 genes with highest log2(fold change) are shown.

| Gene Name | q-value | Log2 (Fold Change) | Function | Citation |
|---|---|---|---|---|
| **FN1** (Fibronectin 1) | 0.001636 | 3.54521 | Connective tissue protein, role in cell adhesion | Pankov & Yamada, 2002 |
| **GPRC5C** (G Protein-Coupled Receptor Class C Group 5 Member C) | 0.001636 | 3.53963 | G-protein coupled receptor | Gonzales *et al.* 2009 |
| **CRLF1** (Cytokine Receptor Like Factor 1) | 0.005641 | 3.41413 | Development of the nervous system. Associated with Crisponi Syndrome. | Crisponi *et al*. 2007 |
| **ELFN2** (Extracellular leucine rich repeat and fibronectin type III domain containing 2) | 0.001636 | 3.37959 | Inhibits protein phosphatases and related to cancer/metastasis | Fujinaga *et al*., 2014 |
| **C2CD4C** (C2 calcium dependent domain containing 4C) | 0.001636 | 3.3397 | May play a role in pancreatic cell development | Omori *et al.,* 2016 |
| **CRABP2** (Cellular Retinoic Acid Binding Protein 2) | 0.001636 | 3.31755 | Vitamin A carrier. Involved in myoblast differentiation | Yuan *et al.*, 2013 |
| **HMX3** (H6 Family Homeobox 3) | 0.01682 | 3.22849 | Transcription factor involved in CNS development | Wang *et al.*, 2004 |
| **ARHGEF16** (Rho Guanine Nucleotide Exchange Factor 16) | 0.001636 | 3.20128 | Promotes phagocytosis of apoptotic cells | Lee *et al.*, 2014 |

**Table 4.4 (continued). Top 20 genes based on log2(fold change) which are significantly up-regulated in all three methods.** The 144 significant genes identified by the three methods were ordered by log2(fold change) from CuffDiff output and the 20 genes with highest log2(fold change) are shown.

| Gene Name | q-value | Log2 (Fold Change) | Function | Citation |
|---|---|---|---|---|
| **SPRR2D** (Small Proline Rich Protein 2D) | 0.03912 | -3.29462 | Scavenger of reactive oxygen species | Tan & Wahli, 2014 |
| **DNAH9** (Dynein Axonemal Heavy Chain 9) | 0.001636 | -1.94813 | Movement of organelles and cilia/flagella | Bartoloni *et al*., 2001 |
| **RBM11** (RNA Binding Motif Protein 11) | 0.03177 | -1.76602 | Splicing regulator. Involved in neuron and germ cell differentiation | Pedrotti *et al.,* 2012 |
| **CXorf57** (Chromosome X Open Reading Frame 57) | 0.008055 | -1.71235 | Uncharacterised | |
| **CALB2** (Calbindin 2) | 0.001636 | -1.66213 | Calcium binding protein | Bezprozvanny , 2009 |
| **DTNA** (Dystrobrevin Alpha) | 0.001636 | -1.62256 | Membrane protein which interacts with the cytoskeleton | Requena *et al.*, 2015 |
| **PTPRO** (Protein Tyrosine Phosphatase, Receptor Type O) | 0.003077 | -1.62105 | Suspected tumour suppressor | Motiwala *et al.*, 2004 |
| **GCA** (Grancalcin) | 0.001636 | -1.42881 | Calcium binding protein. Found in neutrophils at high levels. | Jia *et al.*, 2000 |
| **KCNJ2** (Potassium Voltage-Gated Channel Subfamily J Member 2) | 0.00163577 | -1.42672 | Associated with Short QT syndrome of the heart | Priori *et al.,* 2005 |
| **FBXL7** (F-Box And Leucine Rich Repeat Protein 7) | 0.001636 | -1.40241 | Causes mitotic arrest by ubiquitinates the kinase, Aurora A | Coon *et al*., 2012 |
| **PDGFD** (Platelet Derived Growth Factor D) | 0.020825 | -1.35739 | Highly expressed in breast cancer | Liu *et al.*, 2011 |
| **BEX4** (Brain Expressed X-Linked 4) | 0.00163577 | -1.3307 | Suspected tumour suppressor | Chien *et al.,* 2005 |
| **SLC1A3** (Solute Carrier Family 1 Member 3) | 0.001636 | -1.23698 | Glutamate transporter | Berger & Hediger, 2006 |
| **TAC1** (Tachykinin Precursor 1) | 0.001636 | -0.001636 | Modifies immune response | Cunningham *et al*., 2007 |

**Table 4.5 The 14 genes which are significantly down-regulated in all three methods.** The 14 significant genes identified across all three methods as down-regulated were investigated to determine function and relevance to Bmi1 over-expression. The q-value and log2(fold change) results from CuffDiff are displayed.

### 4.3.5 Genes associated with barrier function were not consistently differentially expressed

For this project, Bmi1 will be over-expressed in airway epithelial cells. As mentioned in Chapter 1, barrier function is crucial to the airway epithelium and various genes contribute to the 'tightness' of the barrier. This Bmi1 cell model will be used in airway epithelial studies and so over-expression of Bmi1 should not confer a disadvantage to barrier formation.

Contributing factors to barrier function include the formation of intercellular junctions such as tight junctions, adherens junctions and gap junctions.

Therefore, genes important to epithelial barrier function were investigated to determine if they were significantly affected by Bmi1 over-expression and the analysis from all three methods can be observed in Table 4.6.

Significant differential expression was not identified by all three methods for any of the genes selected to represent barrier function. Nextin and TJP1 were found to be significantly up-regulated in CuffDiff and by Ferretti *et al.* (2016), but not by Rank Prod. There were also four other genes identified as significant by only one of the methods.

| Gene Name | Function/relation to epithelial cells | Citation | CuffDiff q-value | Rank Prod pfp value (up, down) | Significant in Ferretti *et al*. (2016)? |
|---|---|---|---|---|---|
| **TJP1** (Zona-occludens 1) | Necessary for tight junction assembly | Fanning *et al*. (2012) | 0.00307742 (log2FC= 0.725829) | 1.25, 1.074 | No |
| **TJP2** (Zona-occludens 2) | Necessary for tight junction assembly | Fanning *et al*. (2012) | 0.00163577 (log2FC= 0.663609) | 0.4744, 1.081 | Yes (FDR=0, log2FC= 0.6248) |
| **TJP3** (Zona-occludens 3) | Joins tight junction components to actin | Kiener *et al.* (2008) | 0.759208 | 0.01046, 1.01 | No |
| **CDH1** (E-cadherin) | Required for the formation of adherent junctions | Pecina-Slaus (2003) | 1 NO TEST | 0.3988, 1.081 | No |
| **OCLN** (Occludin) | A component of epithelial tight junctions | Furuse *et al*. (1993) | 1 NO TEST | 1.252, 1.09 | No |
| **F11R** (Junctional Adhesion Molecule 1) | Component of tight junctions | Ozaki *et al*. (1999) | 0.997556 | 0.9741, 1.136 | No |
| **MMP7** (Matrix Metallopeptidase 7) | Loss of MMP7 results in loss of barrier function | Grindel *et al*. (2014) | 1 NO TEST | NA, NA | No |
| **PCDH1** (Protocadherin 1) | Involved in cell adhesion | Faura Tellez *et al*. (2016) | 0.502805 | 0.7, 1.107 | No |
| **EHD2** (EH Domain Containing 2) | Involved in endocytosis | Guilherme *et al.* (2004) | 0.595165 | 0.6853, 1.107 | No |
| **CGN** (Cingulin) | Tight junction component | Citi *et al.* (1988) | 0.997556 | 0.1509, 1.039 | Yes (FDR = 0, log2FC= 1.2333) |
| **PVRL1** (Nectin) | Intercellular adhesion molecule | Takai & Nakanishi (2003) | 0.047277 (log2FC= 0.582497) | 0.4227, 1.076 | Yes (FDR = 0, log2FC= 0.6822) |
| **AFDN** (Afadin) | Nectin-binding molecule | Takai & Nakanishi (2003) | 0.336703 | 0.9739, 1.136 | No |
| **GJB2** (Gap Junction Protein Beta 2) | Gap Junction component | Sohl & Willecke (2004) | 1 NO TEST | NA, NA | No |
| **SCNN1A** | Epithelial sodium channel | Xue *et al*. (2002) | 0.997556 | 0.3727, 1.077 | No |
| **VCL** (Vinculin) | Formation of epithelial cell-cell contacts | Maddugo da *et al.,* (2007) | 0.799719 | 1.015, 1.137 | No |

**Table 4.6 (continued on next page) A table of comparison to determine whether genes implicated in barrier function/maintenance of barrier integrity are differentially expressed with Bmi1 over-expression.** Statistical results generated by CuffDiff and Rank Prod along with those produced by Ferretti *et al*. (2016) using their RNA sequencing dataset. Statistically significant results highlighted in red (q-value, pfp or FDR<0.05). Rank Prod provides a pfp value for both up and down-regulation.

| Gene Name | Function/relation to epithelial cells | Citation | CuffDiff q-value | Rank Prod pfp value (up, down) | Identified as significant by Ferretti *et al*. (2016)? |
|---|---|---|---|---|---|
| **CLDN1** (Claudin-1) | The claudin family has a role in tight junction formation | Lal-Nag & Morin (2009) | 0.252528 | 1.012, 0.1362 | Yes (FDR= 0.0162, log2FC= -0.9294) |
| **CLDN2** (Claudin-2) | - | - | 1 NO TEST | 1.012, 0.1362 | No |
| **CLDN3** (Claudin-3) | - | - | 1 NO TEST | NA, NA | No |
| **CLDN4** (Claudin-4) | - | - | 0.997556 | 1.178, 0.9661 | No |
| **CLDN5** (Claudin-5 | - | - | 1 NO TEST | 1.012, 0.1162 | No |
| **CLDN6** (Claudin-6) | - | - | 1 NO TEST | NA, NA | No |
| **CLDN7** (Claudin-7) | - | - | 0.997556 | 0.9361, 0.5846 | No |
| **CLDN8** (Claudin-8) | - | - | 1 NO TEST | NA, NA | No |
| **CLDN9** (Claudin-9) | - | - | 1 NO TEST | NA, NA | No |
| **CLDN10** (Claudin-10) | - | - | 1 NO TEST | 0.5277, 0.8409 | No |
| **CLDN11** (Claudin-11) | - | - | 0.901885 | 0.4638, 1.087 | No |
| **CLDN12** (Claudin-12) | - | - | 0.877669 | 1.043, 0.5955 | No |
| **CLDN14** (Claudin-14) | - | - | 1 NO TEST | 1.228, 0.2649 | No |
| **CLDN15** (Claudin-15) | - | - | 0.997556 | 1.198, 0.9701 | No |
| **CLDN16** (Claudin-16) | - | - | 1 NO TEST | 0.7099, 0.6815 | No |
| **CLDN17** (Claudin-17) | - | - | 1 NO TEST | NA, NA | No |
| **CLDN18** (Claudin-18) | - | - | 1 NO TEST | 1.055, 0.8037 | No |
| **CLDN19** (Claudin-19) | - | - | 1 NO TEST | 1.232, 0.4437 | No |
| **CLDN20** (Claudin-20) | - | - | 0.997556 | 0.3484, 1.064 | No |
| **CLDN22** (Claudin-22) | - | - | 0.998058 | NA, NA | No |
| **CLDN23** (Claudin-23) | - | - | 0.701297 | 0.7279, 1.121 | No |
| **CLDN24** (Claudin-24) | - | - | 1 NO TEST | NA, NA | No |

**Table 4.6 (continued) A table of comparison to determine whether genes implicated in barrier function/maintenance of barrier integrity are differentially expressed with Bmi1 over-expression.** Statistical results generated by CuffDiff and Rank Prod along with those produced by Ferretti *et al*. (2016) using their RNA sequencing dataset. Statistically significant results highlighted in red (q-value, pfp or FDR<0.05). Rank Prod provides a pfp value for both up and down-regulation.

### 4.3.6 Genes associated with asthma were not consistently differentially expressed

As the cell model is intended to be used for respiratory research and more specifically to study asthma, a search was also performed for genes related to asthma pathogenesis and susceptibility, to determine whether they are affected by Bmi1 over-expression.

| Gene Name | Function/ relation to asthma | Citation | CuffDiff q-value | Rank Prod pfp value (up,down) | Significant in Ferretti *et al*. (2016)? |
|---|---|---|---|---|---|
| **GATA3** (GATA Binding Protein 3) | SNP associated with adult asthma | Hirota *et al*. (2011) | 0.0425696 (log2FC= 0.987773) | 0.3257, 1.061 | Yes (FDR=0, log2FC= 0.8405) |
| **IL33** (Interleukin 33) | Polymorphisms implicated in asthma susceptibility | Ferreira *et al*. (2014) | 1 NO TEST | NA, NA | No |
| **IKZF4** (IKAROS Family Zinc Finger 4) | SNP associated with adult asthma | Hirota *et al*. (2011) | 0.979568 | 1.067, 0.9163 | No |
| **C11orf30** | Associated with increased total serum IgE in asthma | Li *et al.* (2012a) | 0.997556 | 1.189, 1.015 | No |
| **HLA-DQB1** (major histocompatibility complex, class II, DQ beta 1) | Polymorphisms implicated in asthma susceptibility | Ferreira *et al*. (2014) | 1 NO TEST | 1.04, 1.138 | No |
| **HLA-DQA1** (major histocompatibility complex, class II, DQ alpha 1) | Polymorphisms implicated in asthma susceptibility | Gao *et al.* (2003) | 1 NO TEST | 1.017, 1.138 | No |
| **TSLP** (Thymic Stromal Lymphopoietin) | SNP associated with adult asthma | Hirota *et al*. (2011) | 1 NO TEST | 1.013, 0.0975 | No |
| **CLEC16A** (C-Type Lectin Domain Family 16 Member A) | Implicated in the cause of asthma | Ferreira *et al*. (2014) | 0.650082 | 1099, 1.139 | No |
| **IL13** (Interleukin 13) | Cytokine involved in asthma pathogenesis | Corren (2013) | 1 NO TEST | NA, NA | No |
| **ZBTB10** (Zinc finger and BTB domain containing 10) | Implicated in the cause of asthma | Ferreira *et al*. (2014) | 0.997556 | 1.234, 1.08 | No |
| **ORMDL3** (Orosomucoid like 3) | Polymorphisms implicated in asthma susceptibility | Wan *et al.* (2012) | 0.997556 | 1.175, 1.125 | No |
| **IL1RL1/IL18R1** (Interleukin 1 receptor-like 1, interleukin-18 receptor 1) | Polymorphisms implicated in asthma susceptibility | Ferreira *et al*. (2014) | 1 NO TEST | 0.5096, 0.557 | No |
| **OPN3** (Opsin 3) | Unknown function, involved in asthma pathophysiology | White *et al.* (2008) | 0.753521 | 1.123, 0.9715 | No |

**Table 4.7 (continued on next page) A table of comparison to determine whether certain asthma-associated genes are differentially expressed with Bmi1 over-expression.** Statistical results generated by CuffDiff and Rank Prod along with those produced by Ferretti *et al*. (2016) using their RNA sequencing dataset. Statistically significant results highlighted in red (q-value, pfp or FDR<0.05). Rank Prod provides a pfp value for both up and down-regulation.

| Gene Name | Function/ relation to asthma | Citation | CuffDiff q-value | Rank Prod pfp value (up, down) | Significant in Ferretti *et al*. (2016)? |
|---|---|---|---|---|---|
| **PDE4D** (Phosphodiesterase 4D) | Identified by GWAS to cause asthma susceptibility | Himes *et al.* (2009) | 0.353706 | 1.061, 0.8075 | No |
| **GSTP1** (Glutathione S-Transferase Pi 1) | Susceptibility gene in childhood asthma | Kamada *et al.* (2007) | 0.997556 | 1.159, 0.9922 | No |
| **GSTM1** (Glutathione S-transferase Mu 1) | Increased asthma risk with polymorphisms in GSTM1 | Liang *et al.* (2013) | 0.548529 | 0.9309, 1.132 | No |
| **NOS1** (Nitric Oxide Synthase 1) | Polymorphisms linked to asthma | Martinez *et al.* (2007) | 1 NO TEST | 0.9252, 1.139 | No |
| **STAT6** ( Signal transducer and activator of transcription 6) | Elevated in asthma | Walford & Doherty (2013) | 0.997556 | 1.12, 1.139 | No |
| **IL12B** ( Interleukin 12B) | Linked to severe asthma phenotype | Randolph *et al.* (2004) | 1 NO TEST | 0.202 , 1.036 | No |

**Table 4.7 (continued) A table of comparison to determine whether certain asthma-associated genes are differentially expressed with Bmi1 over-expression.** Statistical results generated by CuffDiff and Rank Prod along with those produced by Ferretti *et al*. (2016) using their RNA sequencing dataset. Statistically significant results highlighted in red (q-value, pfp or FDR<0.05). Rank Prod provides a pfp value for both up and down-regulation.

Table 4.7 shows that none of the genes investigated were significantly differentially expressed in all three methods. Although, GATA3 was significantly up-regulated in both CuffDiff and EB Seq analyses (but not Rank Prod). This may be because it has a relatively small fold change so is excluded by Rank Prod analysis.

## 4.4 Discussion

Prior to generating RNA sequencing data with genetically modified HBECs over-expressing Bmi1, an online dataset was utilised to provide initial investigation into the effects and magnitude of changes caused by elevating Bmi1 in a human cell line. The analysis of existing data from a GEO dataset provides a basic awareness of how Bmi1 may be interacting within human cells and may indicate any caveats in the use of Bmi1 to extend lifespan in airway epithelial cells.

As there are multiple options available to compare differential gene expression, two different methods were utilised and then compared with the original method used by the authors of the data. The purpose of this was not to determine which method of analysis is better, but to identify which genes are consistently highlighted by various analyses as being significantly differentially expressed in samples of elevated Bmi1 expression.

In all three methods Bmi1 was identified as significantly up-regulated, as expected, which provides confidence in the RNA sequencing data and the methods of analyses. Rank Prod also provided very similar statistical data (pfp and FC) as Ferretti *et al*. (2016) using EB Seq.

As Bmi1 is increased, it would be expected that p16 (which is inhibited by Bmi1) expression would be decreased. p16 was not identified as significantly up or down-regulated in any of the three methods. However, it is possible that the effects of Bmi1 may be masked by the use of a cancerous cell line. If expression is already low in the cell line, then any further inhibition may not be significantly identified. The A375 cell line was originally derived from a melanoma (Giard *et al.*, 1973), and Bmi1 has been found to be elevated in some melanomas and melanoma cell lines (Mihic-Probst *et al*. 2007); so it is possible Bmi1 is already at a high baseline level in the cell line, which may limit the effects of further Bmi1 elevation.

Alternatively, a study by Yip *et al.* (2013) whereby Bmi1 was over-expressed in nasopharyngeal epithelial cells for immortalisation did not immediately detect significant decreases in p16, but only at later (30) passages post-infection. As it is unknown at which passage post-infection Ferretti *et al*. (2016) conducted their RNA sequencing, it could be that changes in p16 expression had not yet had time to occur.

Amongst the up-regulated genes identified in Table 4.4 are genes which are involved with growth and cell development, and additionally associated with the extracellular matrix and cell adhesion. This may be due to the apparent role of Bmi1 in promoting metastasis (He *et al*., 2015). By conducting

pathway analyses, Ferretti *et al.* (2016) identified genetic pathways associated with migration, Wnt signalling and tumour progression, highlighting an invasive function for Bmi1 in melanoma. Also, amongst these up-regulated genes are some which are suppressed in cancers, which seems counter-intuitive in Bmi1 over-expressing cells, as Bmi1 is often highly expressed in tumours (see Chapter 1).

An investigation into genes relevant to asthma and barrier function did not identify any genes which were significantly up or down-regulated in all three methods of analysis. This did not highlight any specific reason that Bmi1 would not be suitable for extending the cell lifespan of airway epithelial cells for use in asthma research. However, a lot of the genes which were explored resulted in a "NO TEST" output from CuffDiff (17 out of the 37 barrier-related genes and 8 of the 19 asthma-associated genes). This indicates that there were "not enough alignments for testing" (Trapnell, 2016). Therefore, there may be differential gene expression relevant to asthma and airway epithelium which could not be identified using this dataset and also other genes which were not included in the search.

Furthermore, none of the genes involved in stemness which Yip *et al.* (2013) investigated and found to be up-regulated in Bmi1 transduced cells were also identified by CuffDiff as being significantly differentially expressed (data not shown) which could again be due to the cell type used.

### 4.4.1 Limitations

The Ferretti *et al.* (2016) paper provides a useful dataset, however as the cell type used is a cancerous non-airway epithelial line, there may be limited relevance to this project. Furthermore, the modifications existing in the cancerous cell line may mask those caused by over-expression of Bmi1, meaning differential expression cannot be observed.

As mentioned in the previous section, genes of interest could not be included in the statistical analyses due to the lack of alignments, which may mean that an important gene was missed. Also, although the barrier function genes investigated were not found to be differentially expressed, this may only be relevant to this cell line - Bmi1 over-expression may have a different effect in airway epithelial cells where barrier function is more of a priority. Furthermore, as this study uses comparisons of multiple analyses, there is the chance that if one of these methods is too stringent a gene of interest may be excluded from the results.

The Ferretti *et al*. (2016) paper used for RNASeq analysis in this project had only 3 replicates. Liu *et al.* (2014) show that increasing the number of

biological replicates increases the power of such studies significantly. Therefore, when RNA sequencing is performed on the modified HBECs produced in this project, a higher number of replicates would be beneficial. Ferretti *et al.* (2016) also used single-end RNA-seq which may not be as reliable as paired-end sequencing that is performed from both ends of the template strand. Furthermore, CuffDiff is optimised for use with reads of 75bp (CCB, n.d) and may not be optimal for single-end reads (Zhang *et al.,* 2014) therefore there must be careful consideration of the advantages and disadvantages of sequencing parameters and analysis software used.

### 4.4.2 Summary

Overall, a large number of genes are altered by Bmi1 over-expression. However, this number is reduced when cross-examining the results of different methods of analyses, with 144 genes being consistently identified as up-regulated and 14 genes consistently identified as down-regulated.

This research supports the development of an inducible system where Bmi1 over-expression can be reduced to endogenous levels in order to minimise the effect on global gene expression.

Although there are limitations in using this dataset, it provides an initial estimation of how Bmi1 over-expression may affect the cells and thus far has not identified any consistently significant effect on genes of respiratory interest, in particular those associated with barrier function.

# 5. General Discussion

This project set out to develop a sustainable primary human airway cell model for respiratory research, which can be used over an extended period of time but remains representative of cells recently isolated from the human lung, without the loss of endogenous features. The airway epithelium is the first line of defence against insults and often the site of interaction with drug therapies, therefore airway epithelial cells are incredibly important to study. As mentioned in Chapter 1, there are a number of disadvantages to existing cell lines and primary cells used for respiratory research. A key problem in research is that primary cells *in vitro* quickly de-differentiate and lose their characteristics over a restricted number of passages. This limits the number of cells which can be grown *in vitro* and rules out large scale studies which could be used to investigate novel drug therapies for asthma and other respiratory diseases. Additionally, the isolation of cells from patients is invasive and causes discomfort to the donor with risk of injury.

## 5.1 Progress of the project

This project aimed to overcome some of these problem by introducing Bmi1 over-expression to primary HBECs using an inducible system to control gene expression and temporarily extend cell lifespan. Lentiviruses have been used to deliver the Bmi1 sequence to primary HBECs in a manner which allows control over gene expression. The effect of elevated Bmi1 on the barrier properties of HBECs has been studied using ECIS and RNA-seq analysis has been performed on existing data to provide insight into the global effects of elevated Bmi1.

### 5.1.1 Lentiviral gene delivery in primary HBECs

Lentiviral plasmids were constructed containing the Bmi1 sequence and packaged into functional lentiviruses which were used to infect primary early passage HBECs. Whilst there is significant interest in the use of Bmi1 for extending cell lifespan and success in other cell types, there are relatively few studies over-expressing Bmi1 in airway epithelial cells. Those that do incorporate Bmi1 into airway epithelial cells have shown positive results.

Munye *et al.* (2017) have used Bmi1 transduced airway epithelial cells and found that they retained both normal morphology and karyotype and were also still capable of differentiating at ALI, which correlates with the data shown by Torr *et al*. (2016) achieved previously in our research group. Bmi1 has also been shown to significantly extend the lifespan of human bronchial epithelial cells *in vitro* (Fulcher *et al.*, 2009), which supports the rationale of using Bmi1 in this project to delay senescence of airway epithelial cells.

Genetic modification of HBECs to extend lifespan will allow expansion of the cells in culture. However, the cells should be minimally divergent from endogenous HBECs in order to be a representative alternative. Therefore, a means to control gene expression and revert back to endogenous expression levels is advantageous.

The important aspect of this project is the incorporation of the Cumate Switch System which allows control over Bmi1 gene expression. Gene induction, then a return to endogenous levels, has been performed in dendritic cells using the SV40 T-large antigen and a doxycycline based induction system (Richter *et al*., 2013). Their study showed that the conditionally extended cells could be expanded and were able to revert to a normal primary cell phenotype following a removal of induction. In this study, this concept is applied to airway epithelial cells in order to overcome the limitations of primary cell culture.

Successful delivery of the Bmi1 lentiviruses to primary HBECs has been achieved, along with various quality control stages throughout the project, however elevated Bmi1 protein still needs to be confirmed in the transduced HBECs and prolonged cell culture needs to be undertaken to ensure cell lifespan is extended. The genetic modification of cells from asthmatic donors would also be included to generate an asthmatic epithelial cell line.

#### 5.1.1.1 Limitations of alternative genes in airway epithelial cells

Current methods which have been used to extend the lifespan of cells have significant deficiencies.

The E6 and E7 genes from the human papillomavirus have been introduced into primary bronchial epithelial cells to create the cell line, VA10, which after culture for 2 years retained basal cell markers but showed chromosome instability at passage 35 (Halldorssen *et al*., 2007). Additionally, Ramirez *et al.* (2004) show that immortalisation of HBECs using E6 and E7 resulted in more genetic changes compared to those transduced with a combination of hTERT and Cdk4. Also, human MECs which had been immortalised either by hTERT or hTERT with Bmi1 showed normal ploidy, in contrast to alternative techniques using E6 or E7 viral genes (Haga *et al.,* 2007), suggesting that the latter may be more detrimental to the cell development and could lead to genetic instability.

As mentioned above, there has been some success with hTERT. However, in some cases hTERT over-expression has been linked with the development of

potentially malignant mutations over numerous passages (Milyavsky *et al.,* 2003). In addition to this, Campisi (2003) and Farwell *et al.* (2000) suggest that expression of hTERT alone in epithelial cells is not sufficient to extend lifespan, but requires a separate mechanism by which to prevent terminal differentiation. Lundberg *et al*. (2002) showed that primary tracheobronchial epithelial cells underwent senescent even with ectopic hTERT expression. They also show that telomere length was not correlated with the initiation of senescence, suggesting that telomeres are not the only determining factor. Kiyono *et al.* (1998) have previously suggested that inactivation of the Rb/p16INK4a pathway is also required to delay senescence.

It is worth noting that in an alternative methodology, Smith *et al.* (2016) have immortalised primary human airway epithelial cells by using retroviral-delivered hTERT combined with shRNA targeting the CDKN2A locus (encoding p16/p14$^{ARF}$) in a single construct. Transduced cells showed lower p16 and p14 protein expression and were able to reach 70 population doublings, whilst those with only p16 shRNA reached 45 and untransduced cells did not extend beyond 10 population doublings. Their modified cells showed chromosome stability and provide a model they intend to use to study lung cancer development.

In relation to this project, lentivirus delivery is preferable over retrovirus delivery due to the ability to infect non-dividing cells. However, combination of hTERT with a method to down-regulate p16 does show promise, and may be superior to hTERT alone, which was used previously in our research group without success (Torr *et al*., 2016). Fulcher *et al.* (2009) state that human bronchial epithelial cells transduced with both Bmi1 and hTERT retained a diploid karyotype at passage 14 and the ability to form a pseudostratified monolayer, showing potential for their combination in airway cells.

### 5.1.2 Modified HBECs show differences in barrier function with ECIS

ECIS was investigated as a methodology to study barrier function and to determine its suitability for comparing genetically modified HBECs to endogenous controls. In other studies, ECIS has been used to differentiate between cancerous and non-cancerous epithelial cells and the method was capable of distinguishing the differences in cell-spreading between the two cell types (Yang *et al*., 2011).

In this project, ECIS proves to be a sensitive technique and was able to detect differences in the cell adhesion and barrier properties between

endogenous and previously modified HBECs with constitutive over-expression of Bmi1.

Surprisingly, the results indicated that there was a significant decrease in the confluence and electrode coverage of modified cells; Bmi1 acts to increase cell proliferation (Huang *et al.*, 2011), so a proliferative advantage would be expected in the modified cells. In support of this, Torr *et al.* (2016) showed that HBECs with elevated Bmi1 expression had significantly increased viability at passage 8-10.

The ECIS results also show a decrease in barrier resistance - perhaps due to the role of Bmi1 in metastasis (Guo *et al*. 2011); an invasive behaviour would require a reduction in cell-cell interaction (Martin & Jiang, 2009). However, these deviations may not necessarily be due to Bmi1 expression, but because the cells were at much a later passage than the endogenous cells or because there was a loss of cells. Torr *et al*. (2016) show that at passage 8, the previously modified HBECs (constitutive over-expression of Bmi1) do form TEER at ALI but to a lesser extent than endogenous (early passage) controls; TEER had dropped to 88% (of wild-type control, 100%). The ECIS results obtained confirm and extend this study, examining the effect of Bmi1 on cell homeostasis.

Although a considerable difference was observed between the two cell types, it would be more informative to look at how the cells behave when +Bmi1 over-expression is repressed as this will be the condition under which investigations will take place and it will be necessary for the modified cells to be as representative of endogenous HBECs as possible.

Heijink *et al.* (2010) show a marked increase in barrier function of primary bronchial epithelial cells when media was changed for hormone/growth factor-deprived medium. This may indicate that culture conditions can be optimised to produce a more significant change in ECIS measurements.

A disadvantage to this technique is that, as the cell monolayer is undifferentiated, measurements are not taken from a mature, differentiated epithelial layer, so do not resemble the *in vivo* situation. In submerged conditions, they will comprise of basal cells rather than a pseudo-stratified layer including ciliated and goblet cell types. Applied Biophysics (2017) have since developed a transwell adaptor allowing media conditions to be controlled on both the apical and basal surfaces and TEER measurements to be continually taken. This may potentially allow growth of cells at air-liquid interface whilst non-invasively recording the resistance across the monolayer and could be looked into for future work.

Once Bmi1 is elevated in HBECs, it would be interesting to use ECIS to compare the +Bmi1 modified cell lines to existing airway epithelial cell lines as well as primary cells, to evaluate their strengths and weaknesses in barrier formation.

### 5.1.3 Transciptomic analysis did not identify consistent differential expression of barrier or asthma-associated genes correlated in samples with elevated Bmi1

As RNA-seq could not be completed within the time frame of this project, previously published RNA-seq data (Ferretti *et al.*, 2016) was used to provide insight into the potential global effects of Bmi1 over-expression in a human cell line.

Methods of RNA-seq analysis vary depending on the parameters of the data they prioritise, therefore the comparisons of two different methods of analysis along with analysis by the original authors of the data (Ferretti *et al.*, 2016) determined genes which were consistently ranked as differentially expressed, on the assumption that these genes are likely to be true representations of those affected by Bmi1 over-expression.

A large number of genes were identified by CuffDiff (1024 genes), and to a lesser extent by Rank Prod (380 genes), which is unsurprising given that 1536 genes are thought to be affected by Bmi1 (Meng *et al*., 2010). However, this number was decreased by combining the three analyses to identify genes consistently differentially expressed and resulted in 144 genes significantly up-regulated and 14 significantly down-regulated. Of the top 20 genes which were up-regulated (ordered by fold change), there were numerous genes which played a role in cell growth and others which were associated with migration and the extracellular matrix, which is unsurprising given the role Bmi1 is thought to play in promoting cancer metastasis (He *et al*., 2015).

For the top 20 up-regulated genes, the log2(fold change) ranged from 3.20128 to 6.39519, whereas the down-regulated genes ranged from -0.001636 to -3.29462. However, the changes may not be as considerable if they do not have a lasting effect on the cells once Bmi1 over-expression is repressed in the inducible system. As the expression levels of some genes are greatly affected by elevated Bmi1, it is all the more important to incorporate the inducible switch and revert these changes to endogenous levels.

Genes involved in barrier integrity were not significantly identified as being differentially expressed, this would suggest that the decrease in barrier

function observed using ECIS may be due to other factors, for example detachment of cells from the electrode, as indicated by the increase in capacitance on ECIS plots.

As discussed in Chapter 4.4.1, the use of a cancer (melanoma) cell line could potentially be masking the function of Bmi1 (as p16 expression was not significantly down-regulated), which may also have resulted in other genes of importance being masked. Xu *et al*. (2013) show that there is an upper-limit for genetic manipulation, where additional gene over-expression does not necessarily result in further downstream effects. Alternatively, the timing of sequencing post modification with Bmi1 may not have allowed for relevant changes to occur (Yip *et al.*, 2013). This highlights the issue of deciding at how many passages post-infection samples should be collected for sequencing to provide a representative overview for this project.

Overall, Bmi1 over-expression does affect the expression of a large number of genes provides support for the need of an inducible switch system and suggests that the effects of Bmi1 will have to be taken into consideration when using this cell model, particularly if they are not reversible once Bmi1 over-expression is repressed. The techniques used in analysing the RNA sequencing data generated a vast amount of information which will prove useful in comparing endogenous low passage HBECs to +Bmi1 genetically modified HBECs and to cells which have Bmi1 over-expression repressed (via removal of cumate).

This dataset, although with limitations, provides preliminary information on the nature and extent of differential expression caused by elevated Bmi1 in a human cell line. Thus far the results do not discourage the use of Bmi1 over-expression in producing an airway cell model for respiratory research; a consistent significant effect on representative barrier function and asthma-associated genes was not identified with Bmi1 over-expression which could show utility for this model in asthma-related research.

It is evident though, that further conclusions on Bmi1 over-expression cannot be made until samples from this project undergo RNA-sequencing. Despite a large number of genes being altered by Bmi1 over-expression, the success of the project as an airway cell model may hinge on the nature of differential expression specifically in airway epithelial cells and whether these changes are able to revert following removal of induction in the inducible system.

## 5.2 Short-term extensions of the project

There are a number of ways in which the current work can be built upon.

### 5.2.1 Optimisation of cumate dose to induce Bmi1 over-expression

The addition of cumate will be used to induce Bmi1 gene expression and control the level of this expression. Once the cells have been infected with both the Bmi1-lentivirus and the CymR repressor virus, varying doses of cumate will have to be tested to obtain optimal gene control and to determine the tightness of this control. When gene over-expression is switched off, there will be a delay in the decrease of Bmi1 protein depending on the half-life of the protein and mRNA (Schmidt-Supprian & Rajewsky, 2007). Studies will have to be carried out to determine how long it will take to return Bmi1 over-expression levels to the endogenous state following removal of cumate and whether there is any 'leaky' expression due to incomplete repression.

The Cumate Switch system shows promise as a method of temporally controlling Bmi1 expression and has been used successfully in other studies.

Lu *et al*. (2014) use the Cumate Switch system to deliver miR-126 to a breast cancer cell line, MDA-MB-231. They perform RT-PCR to assess the over-expression of miR-126 when in the presence of varying doses of cumate at different time points. Their results appear to show that the cumate induction time has a greater effect than increasing the dosage of cumate, which led them to settle on a final dose of 300µg/mL cumate for 24 hours to produce a physiologically relevant increase in miR-126. This suggests that the Cumate Switch system allows precise control and that an appropriate dose and time period can be selected depending on the experimental requirements.

Additionally, Akiyama *et al.*, (2013) use the Cumate Switch system in order to induce "acute" expression of XBP1s in pancreatic cells and monitor protein expression levels in response to this at various time points. Addition of cumate to their cells lifts repression and allows high levels of XBP1s protein to be detected by Western Blot 24 hours later, although earlier time points are not shown.

Both of these studies show a rapid change in response to cumate, allowing controlled expression of their sequence of interest. This will play an important factor in the future of this project, as Bmi1 over-expression and repression will need to be precisely controlled and it highlights the importance of optimising the cumate dose in HBECs.

### 5.2.2 Extensive characterisation of genetically modified HBECs

As with any genetic modification, there is a risk of introducing unwanted side-effects. Extensive characterisation will be necessary using a range of techniques including TEER, ECIS, RNA sequencing as mentioned previously, but also additional characterisation methods such as karyotyping, immunofluorescent staining and microarray analysis to provide a comprehensive picture of how the cell lines differ from endogenous human airway epithelial cells. This will help to evaluate the suitability of the engineered cells for respiratory research.

The work thus far has been restricted to just one donor. This has removed the complication of increased variability in these experiments. However, to extend the project a minimum of 6 donors ideally would be used to generate modified cell lines in order to overcome donor variation and differences in growth rates which may skew experimental data.

## 5.3 Overall limitations to the project

Whilst this project aims to minimise unwanted side-effects, there are certain limitations which need to be taken into consideration.

Telomerase (encoded by the hTERT gene in humans) plays an important role in protecting chromosome ends from degrading and determines the replicative potential of cells (Sahin & DePinho, 2010). Telomere degradation is thought to induce p53 pathway signalling (Saretzki *et al.*, 1999) and ultimately cell cycle arrest. Therefore, without additional telomerase expression, there will be a limit to the number of replications that the modified HBECs will be able to undergo. Although, some studies indicate that Bmi1 can induce telomerase activity (Dimri *et al.*, 2002). Yip *et al.* (2013) show that Bmi1 alone could not immortalise nasopharyngeal epithelial cells. However the aim of this project has not been to immortalise the cells but to give them a temporary proliferative advantage. Experiments will need to be performed to determine at which passage the cells can no longer be utilised.

Biehs *et al*. (2013) found that not only did Bmi1 regulate the Ink4a/Arf locus, but also suppressed expression of Hox genes in order to maintain an undifferentiated state in adult stem cells. Therefore, there may be an effect on the ability of the genetically modified airway cells to mature. It will be necessary to ensure that the HBECs retain their ability to differentiate following removal of cumate and a return to endogenous levels of Bmi1 expression. However, even with constitutive Bmi1 over-expression, Torr e*t al.* (2016) showed that HBECs with elevated Bmi1 were able to differentiate

and form a pseudostratified epithelium at passages 10-15 when cultured at ALI.

The use of lentiviruses, whilst beneficial in providing stable gene transfer by integrating the gene of interest into the host genome, also comes with the risk of disruptive insertional mutagenesis. The site of insertion could be within an endogenous gene, preventing it from being expressed or having other downstream effects. With lentiviruses it is possible to achieve multiple integrations per cell genome which increases the risk of normal gene expression being disrupted (Woods *et al*., 2003). However, lentiviruses are a very commonly used method of gene delivery and alternatives such as RNA-delivery do not offer the long-term modification required for this project. There has to be a compromise on the gene delivery method depending on the required outcome of the project.

Additionally, there have been concerns over the cytotoxicity of GFP expression, as well as the damaging effects of photoactivation required for imaging (Ansari *et al.*, 2016). Therefore, the fluorescent reporter genes present in the lentiviruses produced in this project, while useful during the preliminary stages for ease of detection, may be detrimental to the HBECs and have negative side-effects. Once proof of concept is achieved, it may be beneficial to remove the reporter genes from the system. Moreover, the presence of GFP and RFP in the cell lines may limit the use of fluorescent reporters in further analyses (for example, immunofluorescence studies).

Although there are limitations of the work completed so far, this project builds on previous work by Torr *et al.*, (2016) and lays the foundation for producing a Human Bronchial Epithelial Cell line which can temporarily delay senescence.

## 5.4 Potential future research using this epithelial cell model

One interesting avenue of study would be to investigate the long term exposure of both common and novel asthma drug treatments directly with the airway epithelium and the impact they have on the cells which are generally the first point of contact. Furthermore, toxicity screening on a large scale would assist in determining viable options to be used in therapy.

Current airway cell models used for drug studies have various limitations, as summarised by Forbes (2000), for example the lack of mucus in the 16HBE14o- cell line and reduced intercellular junctions in BEAS2B cells. Studies using primary HBECs are generally limited in time span (Brockman-Schneider *et al*., 2014), so there is a need for a representative model which allows longer-term study of drug interactions.

One particular aspect of the asthmatic airway epithelium is the abnormal wound response (as described in Chapter 1) which could be targeted with therapeutics. ECIS machines also have the potential to conduct wounding assays - unfortunately, the type of array used in this project was not compatible for this purpose (the wounding assay requires a single electrode per well, rather than ten). This process growing cells in an array consisting of a single electrode, and when confluent passing a current pulse through the electrode to damage the cells covering it (Applied Biophysics, 2017b). This allows real-time monitoring of the resultant migration and wound healing response, and has advantages over typical scratch wound assays in that the wound is reproducible and uniform (Applied Biophysics, 2017c). Taliaferro-Smith *et al.* (2009) use the wound assay function of ECIS to assess the effect of adiponectin treatment on the migratory and invasive behaviour of cancer cells. In this project, ECIS could be used to assess the success of drug therapies in aiding wound recovery and provide better understanding of how asthma disrupts the healthy epithelial wound response. ECIS provides a wide range of applications and shows a lot of potential for studying the airway epithelium.

Finally, genome deletion methods such as CRISPR-Cas9 could be utilised to target and delete relevant asthma-related genes to provide insight into their mechanisms on a much larger scale. Genome editing was intended to be part of this project and established in Calu3 cells before progressing onto genetically modified HBECs due to the difficulty in transfecting and modifying primary cells.

## 5.5 Conclusion

This project provides novel insight into extending cell lifespan in a controlled manner which could potentially be applied to other airway cell types. This research is beneficial as it provides a means to study human airway epithelial cells over a longer term and will enable researchers to produce larger numbers of cells to study; the limited availability of human airway epithelial cells can be a restricting factor to many experiments.

Clearly Bmi1 has an impact on a wide range of genes and pathways, and undoubtedly there will be many genes affected by Bmi1-overexpression in the modified HBECs, but the true extent with regards to this project cannot be investigated until RNA sequencing is performed on the modified cell lines. This will provide a clearer picture of which genes are differentially expressed and whether they will have a significant impact on the functionality of the airway epithelial cells. However, the defining feature of this project is that Bmi1 over-expression can be temporally controlled and

with that the potential to revert the gene expression levels of modified HBECs to that of endogenous cells.

The work so far suggests that this is a promising method to extend airway cell lifespan, although extensive characterisation is still required to ensure the cells remain representative. There are numerous applications for a representative airway epithelial cell model, particularly in the study of respiratory disease and identification of novel drug therapies.

# 6. References


ADDGENE. n.d. *Lentiviral Guide* [Online]. Available: http://www.addgene.org/viral-vectors/lentivirus/lenti-guide/ [Accessed 2nd February 2017].

AHMAD, S., AHMAD, A., NEEVES, K. B., HENDRY-HOFER, T., LOADER, J. E., WHITE, C. W. & VERESS, L. 2014. In vitro cell culture model for toxic inhaled chemical testing. *J Vis Exp*.

AKEN, B. L., AYLING, S., BARRELL, D., CLARKE, L., CURWEN, V., FAIRLEY, S., FERNANDEZ BANET, J., BILLIS, K., GARCÍA GIRÓN, C., HOURLIER, T., HOWE, K., KÄHÄRI, A., KOKOCINSKI, F., MARTIN, F. J., MURPHY, D. N., NAG, R., RUFFIER, M., SCHUSTER, M., TANG, Y. A., VOGEL, J. H., WHITE, S., ZADISSA, A., FLICEK, P. & SEARLE, S. M. 2016. The Ensembl gene annotation system. *Database (Oxford),* 2016.

AKIRA, S., TAKEDA, K. & KAISHO, T. 2001. Toll-like receptors: critical proteins linking innate and acquired immunity. *Nat Immunol,* 2**,** 675-80.

AKIYAMA, M., LIEW, C. W., LU, S., HU, J., MARTINEZ, R., HAMBRO, B., KENNEDY, R. T. & KULKARNI, R. N. 2013. X-box binding protein 1 is essential for insulin regulation of pancreatic α-cell function. *Diabetes,* 62**,** 2439-49.

AKRAM, K. M., LOMAS, N. J., SPITERI, M. A. & FORSYTH, N. R. 2013. Club cells inhibit alveolar epithelial wound repair via TRAIL-dependent apoptosis. *Eur Respir J,* 41**,** 683-94.

ALTSCHUL, S. F., MADDEN, T. L., SCHÄFFER, A. A., ZHANG, J., ZHANG, Z., MILLER, W. & LIPMAN, D. J. 1997. Gapped BLAST and PSI-BLAST: a new generation of protein database search programs. *Nucleic Acids Res,* 25**,** 3389-402.

AMIN, K. 2012. The role of mast cells in allergic inflammation. *Respiratory Medicine,* 106 (1), 9-14.

ANDERSON, J. M. & VAN ITALLIE, C. M. 2009. Physiology and function of the tight junction. *Cold Spring Harb Perspect Biol,* 1**,** a002584.

ANDREADIS, S., LAVERY, T., DAVIS, H. E., LE DOUX, J. M., YARMUSH, M. L. & MORGAN, J. R. 2000. Toward a more accurate quantitation of the activity of recombinant retroviruses: alternatives to titer and multiplicity of infection. *J Virol,* 74**,** 3431-9.

ANSARI, A. M., AHMED, A. K., MATSANGOS, A. E., LAY, F., BORN, L. J., MARTI, G., HARMON, J. W. & SUN, Z. 2016. Cellular GFP Toxicity and Immunogenicity: Potential Confounders in *in Vivo* Cell Tracking Experiments. *Stem Cell Rev,* 12**,** 553-559.

ANTONY, A. B., TEPPER, R. S. & MOHAMMED, K. A. 2002. Cockroach extract antigen increases bronchial airway epithelial permeability. *J Allergy Clin Immunol,* 110**,** 589-95.

APPLIED BIOPHYSICS. 2017a. *ECIS Theory.* [Online]. Available: http://www.biophysics.com/ecis-theory.php [Accessed 17th April 2017].

APPLIED BIOPHYSICS. 2017b. *Applications. Automated cell migration assay.* [Online]. Available: http://www.biophysics.com/woundhealingpubs.php [Accessed 18th April 2017].

APPLIED BIOPHYSICS. 2017c. *Applications. Cell proliferation.* [Online]. Available: http://www.biophysics.com/cellmeasurements.php [Accessed 17th April 2017].

ARMBRUSTER, B. N., LINARDIC, C. M., VELDMAN, T., BANSAL, N. P., DOWNIE, D. L. & COUNTER, C. M. 2004. Rescue of an hTERT mutant defective in telomere elongation by fusion with hPot1. *Mol Cell Biol,* 24**,** 3552-61.

ATLAS, P. n.d. *Bmi1* [Online]. Available: http://www.proteinatlas.org/ENSG00000168283-BMI1/tissue/bronchus [Accessed 4th June 2017].

BAGCHI, A., PAPAZOGLU, C., WU, Y., CAPURSO, D., BRODT, M., FRANCIS, D., BREDEL, M., VOGEL, H. & MILLS, A. A. 2007. CHD5 is a tumor suppressor at human 1p36. *Cell,* 128**,** 459-75.

BANGEL-RULAND, N., TOMCZAK, K., FERNÁNDEZ FERNÁNDEZ, E., LEIER, G., LECIEJEWSKI, B., RUDOLPH, C., ROSENECKER, J. & WEBER, W. M. 2013. Cystic fibrosis transmembrane conductance regulator-mRNA delivery: a novel alternative for cystic fibrosis gene therapy. *J Gene Med,* 15**,** 414-26.

BARCZAK, W., SUCHORSKA, W., RUBIŚ, B. & KULCENTY, K. 2015. Universal real-time PCR-based assay for lentiviral titration. *Mol Biotechnol,* 57**,** 195-200.

BARNES, P. J. 2001a. Molecular mechanisms of corticosteroids in allergic diseases. *Allergy,* 56**,** 928-36.

BARNES, P. J. 2001b. Th2 cytokines and asthma: an introduction. *Respir Res,* 2**,** 64-5.

BARNETT, S. B. & NURMAGAMBETOV, T. A. 2011. Costs of asthma in the United States: 2002-2007. *J Allergy Clin Immunol,* 127**,** 145-52.

BARRETT, T. & EDGAR, R. 2006. Gene expression omnibus: microarray data storage, submission, retrieval, and analysis. *Methods Enzymol,* 411**,** 352-69.

BARTOLONI, L., BLOUIN, J. L., MAITI, A. K., SAINSBURY, A., ROSSIER, C., GEHRIG, C., SHE, J. X., MARRON, M. P., LANDER, E. S., MEEKS, M., CHUNG, E., ARMENGOT, M., JORISSEN, M., SCOTT, H. S., DELOZIER-BLANCHET, C. D.,

GARDINER, R. M. & ANTONARAKIS, S. E. 2001. Axonemal beta heavy chain dynein DNAH9: cDNA sequence, genomic structure, and investigation of its role in primary ciliary dyskinesia. *Genomics,* 72**,** 21-33.

BERGER, U. V. & HEDIGER, M. A. 2006. Distribution of the glutamate transporters GLT-1 (SLC1A2) and GLAST (SLC1A3) in peripheral organs. *Anat Embryol (Berl),* 211**,** 595-606.

BEZPROZVANNY, I. 2009. Calcium signaling and neurodegenerative diseases. *Trends Mol Med,* 15**,** 89-100.

BIEHS, B., HU, J. K., STRAULI, N. B., SANGIORGI, E., JUNG, H., HEBER, R. P., HO, S., GOODWIN, A. F., DASEN, J. S., CAPECCHI, M. R. & KLEIN, O. D. 2013. BMI1 represses Ink4a/Arf and Hox genes to regulate stem cells in the rodent incisor. *Nat Cell Biol,* 15**,** 846-52.

BIORAD-LABORATORIES. 2006. *Real-Time PCR Applications Guide.* [Online]. Available: http://www.bio-rad.com/pdf/Bulletin_5279B.pdf [Accessed 5th April 2017].

BOLES, N. C., HIRSCH, S. E., LE, S., CORNEO, B., NAJM, F., MINOTTI, A. P., WANG, Q., LOTZ, S., TESAR, P. J. & FASANO, C. A. 2014. NPTX1 regulates neural lineage specification from human pluripotent stem cells. *Cell Rep,* 6**,** 724-36.

BRADDING, P. 2008. Asthma: eosinophil disease, mast cell disease, or both? *Allergy Asthma Clin Immunol,* 4**,** 84-90.

BRADDING, P., WALLS, A. F. & HOLGATE, S. T. 2006. The role of the mast cell in the pathophysiology of asthma. *J Allergy Clin Immunol,* 117**,** 1277-84.

BREITLING, R., ARMENGAUD, P., AMTMANN, A. & HERZYK, P. 2004. Rank products: a simple, yet powerful, new method to detect differentially regulated genes in replicated microarray experiments. *FEBS Lett,* 573**,** 83-92.

BROCKMAN-SCHNEIDER, R. A., PICKLES, R. J. & GERN, J. E. 2014. Effects of vitamin D on airway epithelial cell morphology and rhinovirus replication. *PLoS One,* 9**,** e86755.

BURGESS, D. L., GEFRIDES, L. A., FOREMAN, P. J. & NOEBELS, J. L. 2001. A cluster of three novel Ca2+ channel gamma subunit genes on chromosome 19q13.4: evolution and expression profile of the gamma subunit gene family. *Genomics,* 71**,** 339-50.

BUSSE, W., CORREN, J., LANIER, B. Q., MCALARY, M., FOWLER-TAYLOR, A., CIOPPA, G. D., VAN AS, A. & GUPTA, N. 2001. Omalizumab, anti-IgE recombinant humanized monoclonal antibody, for the treatment of severe allergic asthma. *J Allergy Clin Immunol,* 108**,** 184-90.

CAMELO, A., DUNMORE, R., SLEEMAN, M. A. & CLARKE, D. L. 2014. The epithelium in idiopathic pulmonary fibrosis: breaking the barrier. *Front Pharmacol,* 4**,** 173.

CAMPISI, J. 2003. Analysis of tumor suppressor gene-induced senescence. *Methods Mol Biol,* 223**,** 155-72.

CARAYOL, N., VACHIER, I., CHANEZ, P., VIGNOLA, A. M. & CHIAPPARA, G. 2002. Corticosteroid-induced epithelial shedding in asthma. *Am J Respir Crit Care Med,* 166**,** 1290-1; author reply 1291.

CARRATORE, F.D., <fxhong@jimmy.harvard.edu> AJFH, WITTNER, B., BREITLING, R. & BATTKE, F. (2016).*RankProd: Rank Product method for identifying differentially expressed genes with application in meta-analysis*. R package version 3.2.0.

CAZZOLA, M., CALZETTA, L. & MATERA, M. G. 2011. β(2) -adrenoceptor agonists: current and future direction. *Br J Pharmacol,* 163**,** 4-17.

CCB. n.d. *TopHat* [Online]. Available: https://ccb.jhu.edu/software/tophat/manual.shtml [Accessed 30th May 2017].

CHANG, T. W. 2000. The pharmacological basis of anti-IgE therapy. *Nat Biotechnol,* 18**,** 157-62.

CHEN, S., EINSPANIER, R. & SCHOEN, J. 2015. Transepithelial electrical resistance (TEER): a functional parameter to monitor the quality of oviduct epithelial cells cultured on filter supports. *Histochem Cell Biol,* 144**,** 509-15.

CHIEN, J., STAUB, J., AVULA, R., ZHANG, H., LIU, W., HARTMANN, L. C., KAUFMANN, S. H., SMITH, D. I. & SHRIDHAR, V. 2005. Epigenetic silencing of TCEAL7 (Bex4) in ovarian cancer. *Oncogene,* 24**,** 5089-100.

CHOWDHURY, B. A. & DAL PAN, G. 2010. The FDA and safe use of long-acting beta-agonists in the treatment of asthma. *N Engl J Med,* 362**,** 1169-71.

CITI, S., SABANAY, H., JAKES, R., GEIGER, B. & KENDRICK-JONES, J. 1988. Cingulin, a new peripheral component of tight junctions. *Nature,* 333**,** 272-6.

COCKRELL, A. S. & KAFRI, T. 2007. Gene delivery by lentivirus vectors. *Mol Biotechnol,* 36**,** 184-204.

CONNOLLY, J. B. 2002. Lentiviruses in gene therapy clinical research. *Gene Ther,* 9**,** 1730-4.

COON, T. A., GLASSER, J. R., MALLAMPALLI, R. K. & CHEN, B. B. 2012. Novel E3 ligase component FBXL7 ubiquitinates and degrades Aurora A, causing mitotic arrest. *Cell Cycle,* 11**,** 721-9.

COPPÉ, J. P., DESPREZ, P. Y., KRTOLICA, A. & CAMPISI, J. 2010. The senescence-associated secretory phenotype: the dark side of tumor suppression. *Annu Rev Pathol,* 5**,** 99-118.

CORREN, J. 2013. Role of interleukin-13 in asthma. *Curr Allergy Asthma Rep,* 13**,** 415-20.

COZENS, A. L., YEZZI, M. J., KUNZELMANN, K., OHRUI, T., CHIN, L., ENG, K., FINKBEINER, W. E., WIDDICOMBE, J. H. & GRUENERT, D. C. 1994. CFTR expression and chloride secretion in polarized immortal human bronchial epithelial cells. *Am J Respir Cell Mol Biol,* 10**,** 38-47.

CRISPONI, L., CRISPONI, G., MELONI, A., TOLIAT, M. R., NURNBERG, G., USALA, G., UDA, M., MASALA, M., HOHNE, W., BECKER, C., MARONGIU, M., CHIAPPE, F., KLETA, R., RAUCH, A., WOLLNIK, B., STRASSER, F., REESE, T., JAKOBS, C., KURLEMANN, G., CAO, A., NURNBERG, P. & RUTSCH, F. 2007. Crisponi syndrome is caused by mutations in the CRLF1 gene and is allelic to cold-induced sweating syndrome type 1. *Am J Hum Genet,* 80**,** 971-81.

CUNNINGHAM, S., O'DOHERTY, C., PATTERSON, C., MCDONNELL, G., HAWKINS, S., MARROSU, M. G. & VANDENBROECK, K. 2007. The neuropeptide genes TAC1, TAC3, TAC4, VIP and PACAP(ADCYAP1), and susceptibility to multiple sclerosis. *J Neuroimmunol,* 183**,** 208-13.

CURRAN, D. R. & COHN, L. 2010. Advances in mucous cell metaplasia: a plug for mucus as a therapeutic focus in chronic airway disease. *Am J Respir Cell Mol Biol,* 42**,** 268-75.

DEMBÉLÉ, D. & KASTNER, P. 2014. Fold change rank ordering statistics: a new method for detecting differentially expressed genes. *BMC Bioinformatics,* 15**,** 14.

DEY, A., MUSTAFI, S. B., SAHA, S., KUMAR DHAR DWIVEDI, S., MUKHERJEE, P. & BHATTACHARYA, R. 2016. Inhibition of BMI1 induces autophagy-mediated necroptosis. *Autophagy,* 12**,** 659-70.

DIMRI, G. P., MARTINEZ, J. L., JACOBS, J. J., KEBLUSEK, P., ITAHANA, K., VAN LOHUIZEN, M., CAMPISI, J., WAZER, D. E. & BAND, V. 2002. The Bmi-1 oncogene induces telomerase activity and immortalizes human mammary epithelial cells. *Cancer Res,* 62**,** 4736-45.

DOHERTY, T., BROIDE, D. 2015. Group 2 Innate Lymphoid Cells: New Players in Human Allergic Diseases. *Journal of investigational allergology & clinical immunology*. 25, (1), 1-11.

DORSCHEID, D. R., WOJCIK, K. R., SUN, S., MARROQUIN, B. & WHITE, S. R. 2001. Apoptosis of airway epithelial cells induced by corticosteroids. *Am J Respir Crit Care Med,* 164**,** 1939-47.

DVORAK, A., TILLEY, A. E., SHAYKHIEV, R., WANG, R. & CRYSTAL, R. G. 2011. Do airway epithelium air-liquid cultures represent the in vivo airway epithelium transcriptome? *Am J Respir Cell Mol Biol,* 44**,** 465-73.

EDGAR, R., DOMRACHEV, M. & LASH, A. E. 2002. Gene Expression Omnibus: NCBI gene expression and hybridization array data repository. *Nucleic Acids Res,* 30**,** 207-10.

EICKELBERG, O., ROTH, M., LÖRX, R., BRUCE, V., RÜDIGER, J., JOHNSON, M. & BLOCK, L. H. 1999. Ligand-independent activation of the glucocorticoid receptor by beta2-adrenergic receptor agonists in primary human lung fibroblasts and vascular smooth muscle cells. *J Biol Chem,* 274**,** 1005-10.

ENSEMBL. 2017. *Gene: BMI1* [Online]. Available: http://www.ensembl.org/Homo_sapiens/Gene/Summary?db=core [Accessed 1st February 2017].

FAHY, J. V. 2001. Remodeling of the airway epithelium in asthma. *Am J Respir Crit Care Med,* 164**,** S46-51.

FAIRCHILD, C. L., CONWAY, J. P., SCHIFFMACHER, A. T., TANEYHILL, L. A. & GAMMILL, L. S. 2014. FoxD3 regulates cranial neural crest EMT via downregulation of tetraspanin18 independent of its functions during neural crest formation. *Mech Dev,* 132**,** 1-12.

FAN, C., HE, L., KAPOOR, A., GILLIS, A., RYBAK, A. P., CUTZ, J. C. & TANG, D. 2008. Bmi1 promotes prostate tumorigenesis via inhibiting p16(INK4A) and p14(ARF) expression. *Biochim Biophys Acta,* 1782**,** 642-8.

FANNING, A. S., VAN ITALLIE, C. M. & ANDERSON, J. M. 2012. Zonula occludens-1 and -2 regulate apical cell structure and the zonula adherens cytoskeleton in polarized epithelia. *Mol Biol Cell,* 23**,** 577-90.

FARWELL, D. G., SHERA, K. A., KOOP, J. I., BONNET, G. A., MATTHEWS, C. P., REUTHER, G. W., COLTRERA, M. D., MCDOUGALL, J. K. & KLINGELHUTZ, A. J. 2000. Genetic and epigenetic changes in human epithelial cells immortalized by telomerase. *Am J Pathol,* 156**,** 1537-47.

FAURA TELLEZ, G., WILLEMSE, B. W., BROUWER, U., NIJBOER-BRINKSMA, S., VANDEPOELE, K., NOORDHOEK, J. A., HEIJINK, I., DE VRIES, M., SMITHERS, N. P., POSTMA, D. S., TIMENS, W., WIFFEN, L., VAN ROY, F., HOLLOWAY, J. W., LACKIE, P. M., NAWIJN, M. C. & KOPPELMAN, G. H. 2016. Protocadherin-1 Localization and Cell-Adhesion Function in Airway Epithelial Cells in Asthma. *PLoS One,* 11**,** e0163967.

FERREIRA, M. A., MATHESON, M. C., TANG, C. S., GRANELL, R., ANG, W., HUI, J., KIEFER, A. K., DUFFY, D. L., BALTIC, S., DANOY, P., BUI, M., PRICE, L., SLY, P. D., ERIKSSON, N., MADDEN, P. A., ABRAMSON, M. J., HOLT, P. G., HEATH, A. C., HUNTER, M., MUSK, B., ROBERTSON, C. F., LE SOUËF, P., MONTGOMERY, G. W., HENDERSON, A. J., TUNG, J. Y., DHARMAGE, S. C., BROWN, M. A., JAMES, A., THOMPSON, P. J., PENNELL, C., MARTIN, N. G., EVANS, D. M., HINDS, D. A., HOPPER, J. L. & COLLABORATORS, A. A. G. C. 2014. Genome-wide association analysis identifies 11 risk variants associated with the asthma with hay fever phenotype. *J Allergy Clin Immunol,* 133**,** 1564-71.

FERRETTI, R., BHUTKAR, A., MCNAMARA, M. C. & LEES, J. A. 2016. BMI1 induces an invasive signature in melanoma that promotes metastasis and chemoresistance. *Genes Dev,* 30**,** 18-33.

FIXMAN, E. D., STEWART, A. & MARTIN, J. G. 2007. Basic mechanisms of development of airway structural changes in asthma. *Eur Respir J,* 29**,** 379-89.

FOLKERTS, G. & NIJKAMP, F. P. 1998. Airway epithelium: more than just a barrier! *Trends Pharmacol Sci,* 19**,** 334-41.

FORBES, I. 2000. Human airway epithelial cell lines for in vitro drug transport and metabolism studies. *Pharm Sci Technolo Today,* 3**,** 18-27.

FUJINAGA, T., KUMAMARU, W., SUGIURA, T., KOBAYASHI, Y., OHYAMA, Y., IKARI, T., ONIMARU, M., AKIMOTO, N., JOGO, R. & MORI, Y. 2014. Biological characterization and analysis of metastasis-related genes in cell lines derived from the primary lesion and lymph node metastasis of a squamous cell carcinoma arising in the mandibular gingiva. *Int J Oncol,* 44**,** 1614-24.

FULCHER, M. L., GABRIEL, S. E., OLSEN, J. C., TATREAU, J. R., GENTZSCH, M., LIVANOS, E., SAAVEDRA, M. T., SALMON, P. & RANDELL, S. H. 2009. Novel human bronchial epithelial cell lines for cystic fibrosis research. *Am J Physiol Lung Cell Mol Physiol,* 296**,** L82-91.

FURUSE, M., HIRASE, T., ITOH, M., NAGAFUCHI, A., YONEMURA, S. & TSUKITA, S. 1993. Occludin: a novel integral membrane protein localizing at tight junctions. *J Cell Biol,* 123**,** 1777-88.

GALVIN, J. E., LEE, V. M. & TROJANOWSKI, J. Q. 2001. Synucleinopathies: clinical and pathological implications. *Arch Neurol,* 58**,** 186-90.

GANESAN, S., COMSTOCK, A. T. & SAJJAN, U. S. 2013. Barrier function of airway tract epithelium. *Tissue Barriers,* 1**,** e24997.

GAO, J., LIN, Y., QIU, C., LIU, Y. & MA, Y. 2003. Association between HLA-DQA1, -DQB1 gene polymorphisms and susceptibility to asthma in northern Chinese subjects. *Chin Med J (Engl),* 116**,** 1078-82.

GARCÍA-ESCUDERO, V., GARCÍA-GÓMEZ, A., GARGINI, R., MARTÍN-BERMEJO, M. J., LANGA, E., DE YÉBENES, J. G., DELICADO, A., ÁVILA, J., MORENO-FLORES, M. T. & LIM, F. 2010. Prevention of Senescence Progression in Reversibly Immortalized Human Ensheathing Glia Permits Their Survival After Deimmortalization. *Mol Ther,* 18**,** 394-403.

GERAERTS, M., WILLEMS, S., BAEKELANDT, V., DEBYSER, Z. & GIJSBERS, R. 2006. Comparison of lentiviral vector titration methods. *BMC Biotechnol,* 6**,** 34.

GIARD, D. J., AARONSON, S. A., TODARO, G. J., ARNSTEIN, P., KERSEY, J. H., DOSIK, H. & PARKS, W. P. 1973. In vitro cultivation of human tumors:

establishment of cell lines derived from a series of solid tumors. *J Natl Cancer Inst,* 51**,** 1417-23.

GODFREY, R. W. 1997. Human airway epithelial tight junctions. *Microsc Res Tech,* 38**,** 488-99.

GOFF, L., TRAPNELL, C. and KELLEY, D. (2013). *cummeRbund: Analysis, exploration, manipulation, and visualization of Cufflinks high-throughput sequencing data.*. R package version 2.18.0.

GONZALES, P. A., PISITKUN, T., HOFFERT, J. D., TCHAPYJNIKOV, D., STAR, R. A., KLETA, R., WANG, N. S. & KNEPPER, M. A. 2009. Large-scale proteomics and phosphoproteomics of urinary exosomes. *J Am Soc Nephrol,* 20**,** 363-79.

GRAINGE, C. L. & DAVIES, D. E. 2013. Epithelial injury and repair in airways diseases. *Chest,* 144**,** 1906-1912.

GRAINGER, C. I., GREENWELL, L. L., LOCKLEY, D. J., MARTIN, G. P. & FORBES, B. 2006. Culture of Calu-3 cells at the air interface provides a representative model of the airway epithelial barrier. *Pharm Res,* 23**,** 1482-90.

GRINDEL, B. J., MARTINEZ, J. R., PENNINGTON, C. L., MULDOON, M., STAVE, J., CHUNG, L. W. & FARACH-CARSON, M. C. 2014. Matrilysin/matrix metalloproteinase-7(MMP7) cleavage of perlecan/HSPG2 creates a molecular switch to alter prostate cancer cell behavior. *Matrix Biol,* 36**,** 64-76.

GUILHERME, A., SORIANO, N. A., BOSE, S., HOLIK, J., BOSE, A., POMERLEAU, D. P., FURCINITTI, P., LESZYK, J., CORVERA, S. & CZECH, M. P. 2004. EHD2 and the novel EH domain binding protein EHBP1 couple endocytosis to the actin cytoskeleton. *J Biol Chem,* 279**,** 10593-605.

GUO, B. H., FENG, Y., ZHANG, R., XU, L. H., LI, M. Z., KUNG, H. F., SONG, L. B. & ZENG, M. S. 2011. Bmi-1 promotes invasion and metastasis, and its elevated expression is correlated with an advanced stage of breast cancer. *Mol Cancer,* 10**,** 10.

HACKETT, N. R., BUTLER, M. W., SHAYKHIEV, R., SALIT, J., OMBERG, L., RODRIGUEZ-FLORES, J. L., MEZEY, J. G., STRULOVICI-BAREL, Y., WANG, G., DIDON, L. & CRYSTAL, R. G. 2012. RNA-Seq quantification of the human small airway epithelium transcriptome. *BMC Genomics,* 13**,** 82.

HACKETT, T. L., DE BRUIN, H. G., SHAHEEN, F., VAN DEN BERGE, M., VAN OOSTERHOUT, A. J., POSTMA, D. S. & HEIJINK, I. H. 2013. Caveolin-1 controls airway epithelial barrier function. Implications for asthma. *Am J Respir Cell Mol Biol,* 49**,** 662-71.

HACKETT, T. L., SINGHERA, G. K., SHAHEEN, F., HAYDEN, P., JACKSON, G. R., HEGELE, R. G., VAN EEDEN, S., BAI, T. R., DORSCHEID, D. R. & KNIGHT, D. A. 2011. Intrinsic phenotypic differences of asthmatic epithelium and its

inflammatory responses to respiratory syncytial virus and air pollution. *Am J Respir Cell Mol Biol,* 45**,** 1090-100.

HAGA, K., OHNO, S., YUGAWA, T., NARISAWA-SAITO, M., FUJITA, M., SAKAMOTO, M., GALLOWAY, D. A. & KIYONO, T. 2007. Efficient immortalization of primary human cells by p16INK4a-specific short hairpin RNA or Bmi-1, combined with introduction of hTERT. *Cancer Sci,* 98**,** 147-54.

HALLDORSSON, S., ASGRIMSSON, V., AXELSSON, I., GUDMUNDSSON, G. H., STEINARSDOTTIR, M., BALDURSSON, O. & GUDJONSSON, T. 2007. Differentiation potential of a basal epithelial cell line established from human bronchial explant. *In Vitro Cell Dev Biol Anim,* 43**,** 283-9.

HAN, Y., GAO, S., MUEGGE, K., ZHANG, W. & ZHOU, B. 2015. Advanced Applications of RNA Sequencing and Challenges. *Bioinform Biol Insights,* 9**,** 29-46.

HART, P.H. 2001. Regulation of the inflammatory response in asthma by mast cell products. *Immunology and Cell Biology*, 79, 149–153.

HART, T., KOMORI, H. K., LAMERE, S., PODSHIVALOVA, K. & SALOMON, D. R. 2013. Finding the active genes in deep RNA-seq gene expression studies. *BMC Genomics,* 14**,** 778.

HAYASHI, T. 2012. Molecular Mechanisms of Metaplasia, Differentiation and Hyperplasia of Goblet Cellin Allergic Asthma. *Journal of Allergy & Therapy* [Online], 3. Available: http://www.omicsonline.org/molecular-mechanisms-of-metaplasia-differentiation-and-hyperplasia-of-goblet-cellin-allergic-asthma-2155-6121.1000121.php?aid=9875.

HAYER, K. E., PIZARRO, A., LAHENS, N. F., HOGENESCH, J. B. & GRANT, G. R. 2015. Benchmark analysis of algorithms for determining and quantifying full-length mRNA splice forms from RNA-seq data. *Bioinformatics,* 31**,** 3938-45.

HE, Q., LIU, Z., ZHAO, T., ZHAO, L., ZHOU, X. & WANG, A. 2015. Bmi1 drives stem-like properties and is associated with migration, invasion, and poor prognosis in tongue squamous cell carcinoma. *Int J Biol Sci,* 11**,** 1-10.

HEIJINK, I., VAN OOSTERHOUT, A., KLIPHUIS, N., JONKER, M., HOFFMANN, R., TELENGA, E., KLOOSTER, K., SLEBOS, D. J., TEN HACKEN, N., POSTMA, D. & VAN DEN BERGE, M. 2014. Oxidant-induced corticosteroid unresponsiveness in human bronchial epithelial cells. *Thorax,* 69**,** 5-13.

HEIJINK, I. H., BRANDENBURG, S. M., NOORDHOEK, J. A., POSTMA, D. S., SLEBOS, D. J. & VAN OOSTERHOUT, A. J. 2010. Characterisation of cell adhesion in airway epithelial cell types using electric cell-substrate impedance sensing. *Eur Respir J,* 35**,** 894-903.

HEIJINK, I. H., KIES, P. M., KAUFFMAN, H. F., POSTMA, D. S., VAN OOSTERHOUT, A. J. & VELLENGA, E. 2007. Down-regulation of E-cadherin in human bronchial epithelial cells leads to epidermal growth factor receptor-dependent Th2 cell-promoting activity. *J Immunol,* 178**,** 7678-85.

HENZ, S. R., CUMBIE, J. S., KASSCHAU, K. D., LOHMANN, J. U., CARRINGTON, J. C., WEIGEL, D. & SCHMID, M. 2007. Distinct expression patterns of natural antisense transcripts in Arabidopsis. *Plant Physiol,* 144**,** 1247-55.

HIMES, B. E., HUNNINGHAKE, G. M., BAURLEY, J. W., RAFAELS, N. M., SLEIMAN, P., STRACHAN, D. P., WILK, J. B., WILLIS-OWEN, S. A., KLANDERMAN, B., LASKY-SU, J., LAZARUS, R., MURPHY, A. J., SOTO-QUIROS, M. E., AVILA, L., BEATY, T., MATHIAS, R. A., RUCZINSKI, I., BARNES, K. C., CELEDÓN, J. C., COOKSON, W. O., GAUDERMAN, W. J., GILLILAND, F. D., HAKONARSON, H., LANGE, C., MOFFATT, M. F., O'CONNOR, G. T., RABY, B. A., SILVERMAN, E. K. & WEISS, S. T. 2009. Genome-wide association analysis identifies PDE4D as an asthma-susceptibility gene. *Am J Hum Genet,* 84**,** 581-93.

HIROTA, T., TAKAHASHI, A., KUBO, M., TSUNODA, T., TOMITA, K., DOI, S., FUJITA, K., MIYATAKE, A., ENOMOTO, T., MIYAGAWA, T., ADACHI, M., TANAKA, H., NIIMI, A., MATSUMOTO, H., ITO, I., MASUKO, H., SAKAMOTO, T., HIZAWA, N., TANIGUCHI, M., LIMA, J. J., IRVIN, C. G., PETERS, S. P., HIMES, B. E., LITONJUA, A. A., TANTISIRA, K. G., WEISS, S. T., KAMATANI, N., NAKAMURA, Y. & TAMARI, M. 2011. Genome-wide association study identifies three new susceptibility loci for adult asthma in the Japanese population. *Nat Genet,* 43**,** 893-6.

HOFFMANN, T. J., PASSARELLI, M. N., GRAFF, R. E., EMAMI, N. C., SAKODA, L. C., JORGENSON, E., HABEL, L. A., SHAN, J., RANATUNGA, D. K., QUESENBERRY, C. P., CHAO, C. R., GHAI, N. R., AARONSON, D., PRESTI, J., NORDSTRÖM, T., WANG, Z., BERNDT, S. I., CHANOCK, S. J., MOSLEY, J. D., KLEIN, R. J., MIDDHA, M., LILJA, H., MELANDER, O., KVALE, M. N., KWOK, P. Y., SCHAEFER, C., RISCH, N., VAN DEN EEDEN, S. K. & WITTE, J. S. 2017. Genome-wide association study of prostate-specific antigen levels identifies novel loci independent of prostate cancer. *Nat Commun,* 8**,** 14248.

HOLGATE, S. T. 2011. The sentinel role of the airway epithelium in asthma pathogenesis. *Immunol Rev,* 242**,** 205-19.

HOLLAND, P. M., ABRAMSON, R. D., WATSON, R. & GELFAND, D. H. 1991. Detection of specific polymerase chain reaction product by utilizing the 5'----3' exonuclease activity of Thermus aquaticus DNA polymerase. *Proc Natl Acad Sci U S A,* 88**,** 7276-80.

HONG, F., BREITLING, R., MCENTEE, C. W., WITTNER, B. S., NEMHAUSER, J. L. & CHORY, J. 2006. RankProd: a bioconductor package for detecting differentially expressed genes in meta-analysis. *Bioinformatics,* 22**,** 2825-7.

HUANG, R., CHEUNG, N. K., VIDER, J., CHEUNG, I. Y., GERALD, W. L., TICKOO, S. K., HOLLAND, E. C. & BLASBERG, R. G. 2011. MYCN and MYC regulate tumor proliferation and tumorigenesis directly through BMI1 in human neuroblastomas. *FASEB J,* 25**,** 4138-49.

HUGHES, P., MARSHALL, D., REID, Y., PARKES, H. & GELBER, C. 2007. The costs of using unauthenticated, over-passaged cell lines: how much more data do we need? *Biotechniques,* 43**,** 575, 577-8, 581-2 passim.

HULL, J., ACKERMAN, H., ISLES, K., USEN, S., PINDER, M., THOMSON, A. & KWIATKOWSKI, D. 2001. Unusual haplotypic structure of IL8, a susceptibility locus for a common respiratory virus. *Am J Hum Genet,* 69**,** 413-9.

ISLAM, M. A., REESOR, E. K., XU, Y., ZOPE, H. R., ZETTER, B. R. & SHI, J. 2015. Biomaterials for mRNA delivery. *Biomater Sci,* 3**,** 1519-33.

JACOBS, J. J., KIEBOOM, K., MARINO, S., DEPINHO, R. A. & VAN LOHUIZEN, M. 1999. The oncogene and Polycomb-group gene bmi-1 regulates cell proliferation and senescence through the ink4a locus. *Nature,* 397**,** 164-8.

JIA, J., HAN, Q., BORREGAARD, N., LOLLIKE, K. & CYGLER, M. 2000. Crystal structure of human grancalcin, a member of the penta-EF-hand protein family. *J Mol Biol,* 300**,** 1271-81.

JONCHÈRE, V., RÉHAULT-GODBERT, S., HENNEQUET-ANTIER, C., CABAU, C., SIBUT, V., COGBURN, L. A., NYS, Y. & GAUTRON, J. 2010. Gene expression profiling to identify eggshell proteins involved in physical defense of the chicken egg. *BMC Genomics,* 11**,** 57.

KABATA, H., MORO, K., KOYASU, S., ASANO, K. 2015. Group 2 innate lymphoid cells and asthma. *Allergology International*, 64, (3), 227-234.

KAMADA, F., MASHIMO, Y., INOUE, H., SHAO, C., HIROTA, T., DOI, S., KAMEDA, M., FUJIWARA, H., FUJITA, K., ENOMOTO, T., SASAKI, S., ENDO, H., TAKAYANAGI, R., NAKAZAWA, C., MORIKAWA, T., MORIKAWA, M., MIYABAYASHI, S., CHIBA, Y., TAMURA, G., SHIRAKAWA, T., MATSUBARA, Y., HATA, A., TAMARI, M. & SUZUKI, Y. 2007. The GSTP1 gene is a susceptibility gene for childhood asthma and the GSTM1 gene is a modifier of the GSTP1 gene. *Int Arch Allergy Immunol,* 144**,** 275-86.

KAUR, G. & DUFOUR, J. M. 2012. Cell lines: Valuable tools or useless artifacts. *Spermatogenesis,* 2**,** 1-5.

KHAN, K., RUDKIN, A., PARRY, D. A., BURDON, K. P., MCKIBBIN, M., LOGAN, C. V., ABDELHAMED, Z. I., MUECKE, J. S., FERNANDEZ-FUENTES, N., LAURIE, K. J., SHIRES, M., FOGARTY, R., CARR, I. M., POULTER, J. A., MORGAN, J. E., MOHAMED, M. D., JAFRI, H., RAASHID, Y., MENG, N., PISETH, H., TOOMES, C., CASSON, R. J., TAYLOR, G. R., HAMMERTON, M., SHERIDAN, E., JOHNSON, C. A., INGLEHEARN, C. F., CRAIG, J. E. & ALI, M. 2011. Homozygous mutations in PXDN cause congenital cataract, corneal opacity, and developmental glaucoma. *Am J Hum Genet,* 89**,** 464-73.

KIENER, T. K., SELPTSOVA-FRIEDRICH, I. & HUNZIKER, W. 2008. Tjp3/zo-3 is critical for epidermal barrier function in zebrafish embryos. *Dev Biol,* 316**,** 36-49.

KIM, H., PARK, Y. & LEE, J. B. 2015. Self-assembled Messenger RNA Nanoparticles (mRNA-NPs) for Efficient Gene Expression. *Sci Rep,* 5**,** 12737.

KIM, R. H., LIEBERMAN, M. B., LEE, R., SHIN, K. H., MEHRAZARIN, S., OH, J. E., PARK, N. H. & KANG, M. K. 2010. Bmi-1 extends the life span of normal human oral keratinocytes by inhibiting the TGF-beta signaling. *Exp Cell Res,* 316**,** 2600-8.

KINNON, S. & FULTON, R. 1999. Nucleotide sequence of the feline Bmi-1 coding region. *DNA Seq,* 10**,** 335-8.

KIYONO, T., FOSTER, S. A., KOOP, J. I., MCDOUGALL, J. K., GALLOWAY, D. A. & KLINGELHUTZ, A. J. 1998. Both Rb/p16INK4a inactivation and telomerase activity are required to immortalize human epithelial cells. *Nature,* 396**,** 84-8.

KNIGHT, D. A. & HOLGATE, S. T. 2003. The airway epithelium: structural and functional properties in health and disease. *Respirology,* 8**,** 432-46.

KOJIMA, T., GO, M., TAKANO, K., KUROSE, M., OHKUNI, T., KOIZUMI, J., KAMEKURA, R., OGASAWARA, N., MASAKI, T., FUCHIMOTO, J., OBATA, K., HIRAKAWA, S., NOMURA, K., KEIRA, T., MIYATA, R., FUJII, N., TSUTSUMI, H., HIMI, T. & SAWADA, N. 2013. Regulation of tight junctions in upper airway epithelium. *Biomed Res Int,* 2013**,** 947072.

KUILMAN, T., MICHALOGLOU, C., MOOI, W. J. & PEEPER, D. S. 2010. The essence of senescence. *Genes Dev,* 24**,** 2463-79.

KURIEN, B. T. & SCOFIELD, R. H. 2006. Western blotting. *Methods,* 38**,** 283-293.

LAL-NAG, M. & MORIN, P. J. 2009. The claudins. *Genome Biol,* 10**,** 235.

LARKIN, M. A., BLACKSHIELDS, G., BROWN, N. P., CHENNA, R., MCGETTIGAN, P. A., MCWILLIAM, H., VALENTIN, F., WALLACE, I. M., WILM, A., LOPEZ, R., THOMPSON, J. D., GIBSON, T. J. & HIGGINS, D. G. 2007. Clustal W and Clustal X version 2.0. *Bioinformatics,* 23**,** 2947-8.

LEE, J., PARK, B., KIM, G., KIM, K., PAK, J., YE, M. B., PARK, S. G. & PARK, D. 2014. Arhgef16, a novel Elmo1 binding partner, promotes clearance of apoptotic cells via RhoG-dependent Rac1 activation. *Biochim Biophys Acta,* 1843**,** 2438-47.

LENG, N., DAWSON, J. A., THOMSON, J. A., RUOTTI, V., RISSMAN, A. I., SMITS, B. M., HAAG, J. D., GOULD, M. N., STEWART, R. M. & KENDZIORSKI, C. 2013. EBSeq: an empirical Bayes hierarchical model for inference in RNA-seq experiments. *Bioinformatics,* 29**,** 1035-43.

LESSARD, J. & SAUVAGEAU, G. 2003. Bmi-1 determines the proliferative capacity of normal and leukaemic stem cells. *Nature,* 423**,** 255-60.

LI, H., SONG, F., CHEN, X., LI, Y., FAN, J., WU, X. 2014. Bmi-1 regulates epithelial-to-mesenchymal transition to promote migration and invasion of breast cancer cells. Int J Clin Exp Pathol, 7, (6), 3057–3064.

LI, X., AMPLEFORD, E. J., HOWARD, T. D., MOORE, W. C., LI, H., BUSSE, W. W., CASTRO, M., ERZURUM, S. C., FITZPATRICK, A. M., GASTON, B., ISRAEL, E., JARJOUR, N. N., TEAGUE, W. G., WENZEL, S. E., HAWKINS, G. A., BLEECKER, E. R. & MEYERS, D. A. 2012a. The C11orf30-LRRC32 region is associated with total serum IgE levels in asthmatic patients. *J Allergy Clin Immunol,* 129**,** 575-8, 578.e1-9.

LI, Y., WANG, Y. & LIU, X. 2012b. The role of airway epithelial cells in response to mycobacteria infection. *Clin Dev Immunol,* 2012**,** 791392.

LIANG, S., WEI, X., GONG, C., WEI, J., CHEN, Z., CHEN, X., WANG, Z. & DENG, J. 2013. Significant association between asthma risk and the GSTM1 and GSTT1 deletion polymorphisms: an updated meta-analysis of case-control studies. *Respirology,* 18**,** 774-83.

LIU, J., LIAO, S., HUANG, Y., SAMUEL, R., SHI, T., NAXEROVA, K., HUANG, P., KAMOUN, W., JAIN, R. K., FUKUMURA, D. & XU, L. 2011. PDGF-D improves drug delivery and efficacy via vascular normalization, but promotes lymphatic metastasis by activating CXCR4 in breast cancer. *Clin Cancer Res,* 17**,** 3638-48.

LIU, Y., ZHOU, J. & WHITE, K. P. 2014. RNA-seq differential expression studies: more sequence or more replication? *Bioinformatics,* 30**,** 301-4.

LIVINGSTONE, C. 2013. IGF2 and cancer. *Endocr Relat Cancer,* 20**,** R321-39.

LU, Y. Y., SWEREDOSKI, M. J., HUSS, D., LANSFORD, R., HESS, S. & TIRRELL, D. A. 2014. Prometastatic GPCR CD97 is a direct target of tumor suppressor microRNA-126. *ACS Chem Biol,* 9**,** 334-8.

LUNDBERG, A. S., HAHN, W. C., GUPTA, P. & WEINBERG, R. A. 2000. Genes involved in senescence and immortalization. *Curr Opin Cell Biol,* 12**,** 705-9.

LUNDBERG, A. S., RANDELL, S. H., STEWART, S. A., ELENBAAS, B., HARTWELL, K. A., BROOKS, M. W., FLEMING, M. D., OLSEN, J. C., MILLER, S. W., WEINBERG, R. A. & HAHN, W. C. 2002. Immortalization and transformation of primary human airway epithelial cells by gene transfer. *Oncogene,* 21**,** 4577-86.

MADDUGODA, M. P., CRAMPTON, M. S., SHEWAN, A. M. & YAP, A. S. 2007. Myosin VI and vinculin cooperate during the morphogenesis of cadherin cell cell contacts in mammalian epithelial cells. *J Cell Biol,* 178**,** 529-40.

MAQSOOD, M. I., MATIN, M. M., BAHRAMI, A. R. & GHASROLDASHT, M. M. 2013. Immortality of cell lines: challenges and advantages of establishment. *Cell Biol Int,* 37**,** 1038-45.

MARTIN, T. A. & JIANG, W. G. 2009. Loss of tight junction barrier function and its role in cancer metastasis. *Biochim Biophys Acta,* 1788**,** 872-91.

MARTINEZ-QUETGLAS, I., PINYOL, R., DAUCH, D., TORRECILLA, S., TOVAR, V., MOEINI, A., ALSINET, C., PORTELA, A., RODRIGUEZ-CARUNCHIO, L., SOLÉ, M., LUJAMBIO, A., VILLANUEVA, A., THUNG, S., ESTELLER, M., ZENDER, L. & LLOVET, J. M. 2016. IGF2 Is Up-regulated by Epigenetic Mechanisms in Hepatocellular Carcinomas and Is an Actionable Oncogene Product in Experimental Models. *Gastroenterology,* 151**,** 1192-1205.

MARTÍNEZ, B., BARRIOS, K., VERGARA, C., MERCADO, D., JIMÉNEZ, S., GUSMÃO, L. & CARABALLO, L. 2007. A NOS1 gene polymorphism associated with asthma and specific immunoglobulin E response to mite allergens in a Colombian population. *Int Arch Allergy Immunol,* 144**,** 105-13.

MCPHERSON, M. J. & MØLLER, S. G. 2006. *Pcr,* New York, N.Y. ; London, Garland.

MENG, S., LUO, M., SUN, H., YU, X., SHEN, M., ZHANG, Q., ZHOU, R., JU, X., TAO, W., LIU, D., DENG, H. & LU, Z. 2010. Identification and characterization of Bmi-1-responding element within the human p16 promoter. *J Biol Chem,* 285**,** 33219-29.

MIHIC-PROBST, D., KUSTER, A., KILGUS, S., BODE-LESNIEWSKA, B., INGOLD-HEPPNER, B., LEUNG, C., STORZ, M., SEIFERT, B., MARINO, S., SCHRAML, P., DUMMER, R. & MOCH, H. 2007. Consistent expression of the stem cell renewal factor BMI-1 in primary and metastatic melanoma. *Int J Cancer,* 121**,** 1764-70.

MILYAVSKY, M., SHATS, I., EREZ, N., TANG, X., SENDEROVICH, S., MEERSON, A., TABACH, Y., GOLDFINGER, N., GINSBERG, D., HARRIS, C. C. & ROTTER, V. 2003. Prolonged culture of telomerase-immortalized human fibroblasts leads to a premalignant phenotype. *Cancer Res,* 63**,** 7147-57.

MOLOFSKY, A. V., PARDAL, R., IWASHITA, T., PARK, I. K., CLARKE, M. F. & MORRISON, S. J. 2003. Bmi-1 dependence distinguishes neural stem cell self-renewal from progenitor proliferation. *Nature,* 425**,** 962-7.

MOTIWALA, T., KUTAY, H., GHOSHAL, K., BAI, S., SEIMIYA, H., TSURUO, T., SUSTER, S., MORRISON, C. & JACOB, S. T. 2004. Protein tyrosine phosphatase receptor-type O (PTPRO) exhibits characteristics of a candidate tumor suppressor in human lung cancer. *Proc Natl Acad Sci U S A,* 101**,** 13844-9.

MULLICK, A., XU, Y., WARREN, R., KOUTROUMANIS, M., GUILBAULT, C., BROUSSAU, S., MALENFANT, F., BOURGET, L., LAMOUREUX, L., LO, R., CARON, A. W., PILOTTE, A. & MASSIE, B. 2006. The cumate gene-switch: a system for regulated expression in mammalian cells. *BMC Biotechnol,* 6**,** 43.

MUNYE, M. M., SHOEMARK, A., HIRST, R. A., DELHOVE, J. M., SHARP, T. V., MCKAY, T. R., O'CALLAGHAN, C., BAINES, D. L., HOWE, S. J. & HART, S. L. 2017. BMI-1 extends proliferative potential of human bronchial epithelial cells while

retaining their mucociliary differentiation capacity. *Am J Physiol Lung Cell Mol Physiol,* 312**,** L258-L267.

MUTZ, K. O., HEILKENBRINKER, A., LÖNNE, M., WALTER, J. G. & STAHL, F. 2013. Transcriptome analysis using next-generation sequencing. *Curr Opin Biotechnol,* 24**,** 22-30.

NAWIJN, M. C., HACKETT, T. L., POSTMA, D. S., VAN OOSTERHOUT, A. J. & HEIJINK, I. H. 2011. E-cadherin: gatekeeper of airway mucosa and allergic sensitization. *Trends Immunol,* 32**,** 248-55.

NOONAN, M. J., CHERVINSKY, P., BRANDON, M., ZHANG, J., KUNDU, S., MCBURNEY, J. & REISS, T. F. 1998. Montelukast, a potent leukotriene receptor antagonist, causes dose-related improvements in chronic asthma. Montelukast Asthma Study Group. *Eur Respir J,* 11**,** 1232-9.

OLIVEROS, J.C. (2007-2015) Venny. An interactive tool for comparing lists with Venn's diagrams. http://bioinfogp.cnb.csic.es/tools/venny/index.html

OMORI, H., OGAKI, S., SAKANO, D., SATO, M., UMEDA, K., TAKEDA, N., NAKAGATA, N. & KUME, S. 2016. Changes in expression of C2cd4c in pancreatic endocrine cells during pancreatic development. *FEBS Lett,* 590**,** 2584-93.

ORDOÑEZ, C., FERRANDO, R., HYDE, D. M., WONG, H. H. & FAHY, J. V. 2000. Epithelial desquamation in asthma: artifact or pathology? *Am J Respir Crit Care Med,* 162**,** 2324-9.

OUELLETTE, M. M., MCDANIEL, L. D., WRIGHT, W. E., SHAY, J. W. & SCHULTZ, R. A. 2000. The establishment of telomerase-immortalized cell lines representing human chromosome instability syndromes. *Hum Mol Genet,* 9**,** 403-11.

OZAKI, H., ISHII, K., HORIUCHI, H., ARAI, H., KAWAMOTO, T., OKAWA, K., IWAMATSU, A. & KITA, T. 1999. Cutting edge: combined treatment of TNF-alpha and IFN-gamma causes redistribution of junctional adhesion molecule in human endothelial cells. *J Immunol,* 163**,** 553-7.

PAGGIARO, P. & BACCI, E. 2011. Montelukast in asthma: a review of its efficacy and place in therapy. *Ther Adv Chronic Dis,* 2**,** 47-58.

PANKOV, R. & YAMADA, K. M. 2002. Fibronectin at a glance. *J Cell Sci,* 115**,** 3861-3.

PAPAGATSIAS, T., ROZIS, G., ATHANASOPOULOS, T., GOTCH, F., DICKSON, G., PATTERSON, S. Activity of different vaccine-associated promoter elements in human dendritic cells. *Immunology Letters*, 115, (2), 117-125.

PARK, I. K., MORRISON, S. J. & CLARKE, M. F. 2004. Bmi1, stem cells, and senescence regulation. *J Clin Invest,* 113**,** 175-9.

PARK, J. A., KIM, J. H., BI, D., MITCHEL, J. A., QAZVINI, N. T., TANTISIRA, K., PARK, C. Y., MCGILL, M., KIM, S. H., GWEON, B., NOTBOHM, J., STEWARD, R., BURGER, S., RANDELL, S. H., KHO, A. T., TAMBE, D. T., HARDIN, C., SHORE,

S. A., ISRAEL, E., WEITZ, D. A., TSCHUMPERLIN, D. J., HENSKE, E. P., WEISS, S. T., MANNING, M. L., BUTLER, J. P., DRAZEN, J. M. & FREDBERG, J. J. 2015. Unjamming and cell shape in the asthmatic airway epithelium. *Nat Mater,* 14**,** 1040-8.

PARK, K. S., KORFHAGEN, T. R., BRUNO, M. D., KITZMILLER, J. A., WAN, H., WERT, S. E., KHURANA HERSHEY, G. K., CHEN, G. & WHITSETT, J. A. 2007. SPDEF regulates goblet cell hyperplasia in the airway epithelium. *J Clin Invest,* 117**,** 978-88.

PEDROTTI, S., BUSÀ, R., COMPAGNUCCI, C. & SETTE, C. 2012. The RNA recognition motif protein RBM11 is a novel tissue-specific splicing regulator. *Nucleic Acids Res,* 40**,** 1021-32.

PEITZMAN, E. R., ZAIDMAN, N. A., MANIAK, P. J. & O'GRADY, S. M. 2015. Agonist binding to β-adrenergic receptors on human airway epithelial cells inhibits migration and wound repair. *Am J Physiol Cell Physiol,* 309**,** C847-55.

PEREZ-VILAR, J. 2007. Mucin granule intraluminal organization. *Am J Respir Cell Mol Biol,* 36**,** 183-90.

PEREZ-VILAR, J., SHEEHAN, J. K. & RANDELL, S. H. 2003. Making More MUCS. *Am J Respir Cell Mol Biol,* 28**,** 267-70.

PEZZULO, A. A., STARNER, T. D., SCHEETZ, T. E., TRAVER, G. L., TILLEY, A. E., HARVEY, B. G., CRYSTAL, R. G., MCCRAY, P. B. & ZABNER, J. 2011. The air-liquid interface and use of primary cell cultures are important to recapitulate the transcriptional profile of in vivo airway epithelia. *Am J Physiol Lung Cell Mol Physiol,* 300**,** L25-31.

PEĆINA-SLAUS, N. 2003. Tumor suppressor gene E-cadherin and its role in normal and malignant cells. *Cancer Cell Int,* 3**,** 17.

POST, S., NAWIJN, M. C., JONKER, M. R., KLIPHUIS, N., VAN DEN BERGE, M., VAN OOSTERHOUT, A. J. & HEIJINK, I. H. 2013. House dust mite-induced calcium signaling instigates epithelial barrier dysfunction and CCL20 production. *Allergy,* 68**,** 1117-25.

PRIORI, S. G., PANDIT, S. V., RIVOLTA, I., BERENFELD, O., RONCHETTI, E., DHAMOON, A., NAPOLITANO, C., ANUMONWO, J., DI BARLETTA, M. R., GUDAPAKKAM, S., BOSI, G., STRAMBA-BADIALE, M. & JALIFE, J. 2005. A novel form of short QT syndrome (SQT3) is caused by a mutation in the KCNJ2 gene. *Circ Res,* 96**,** 800-7.

PROMEGA. 2010. *Wizard® Plus SV Minipreps DNA Purification System* [Online]. [Accessed 2nd April 2017].

PROMEGA. 2017a. *JM109 and HB101 competent cells.* [Online]. Available: http://www.promega.co.uk/products/cloning-and-dna-markers/cloning-tools-and-competent-cells/bacterial-strains-and-competent-cells/pro-

5_alpha_-jm109-and-hb101-competent-cells/?activeTab=0 [Accessed 2nd February 2017].

PROMEGA. 2017b. *pGEM®-T Vector Systems* [Online]. Available: http://www.promega.co.uk/products/pcr/pcr-cloning/pgem_t-vector-systems/?activeTab=2 [Accessed 2nd February 2017].

PRYTHERCH, Z. & BERUBE, K. 2013. An in vitro NHBE model of the human bronchial epithelium. *In:* HAYCOCK, J., AHLUWALIA, A. & WILKINSON, J. M. (eds.) *Cellular In Vitro Testing: Methods and Protocols.* Boca Raton, Florida: CRC Press.

QIAGEN. 2017. *QIAquick Gel Extraction Kit* [Online]. Available: http://www.qiagen.com/us/shop/sample-technologies/dna/dna-clean-up/qiaquick-gel-extraction-kit/#productdetails [Accessed 3rd February 2017].

R CORE TEAM (2013). R: A language and environment for statistical computing. R Foundation for Statistical Computing, Vienna, Austria. URL http://www.R-project.org/.

RAMIREZ, R. D., SHERIDAN, S., GIRARD, L., SATO, M., KIM, Y., POLLACK, J., PEYTON, M., ZOU, Y., KURIE, J. M., DIMAIO, J. M., MILCHGRUB, S., SMITH, A. L., SOUZA, R. F., GILBEY, L., ZHANG, X., GANDIA, K., VAUGHAN, M. B., WRIGHT, W. E., GAZDAR, A. F., SHAY, J. W. & MINNA, J. D. 2004. Immortalization of human bronchial epithelial cells in the absence of viral oncoproteins. *Cancer Res,* 64**,** 9027-34.

RANDELL, S. H., BOUCHER, R. C. & GROUP, U. O. N. C. V. L. 2006. Effective mucus clearance is essential for respiratory health. *Am J Respir Cell Mol Biol,* 35**,** 20-8.

RANDOLPH, A. G., LANGE, C., SILVERMAN, E. K., LAZARUS, R., SILVERMAN, E. S., RABY, B., BROWN, A., OZONOFF, A., RICHTER, B. & WEISS, S. T. 2004. The IL12B gene is associated with asthma. *Am J Hum Genet,* 75**,** 709-15.

RENNARD, S. I. 1996. Repair mechanisms in asthma. *J Allergy Clin Immunol,* 98**,** S278-86.

REQUENA, T., CABRERA, S., MARTÍN-SIERRA, C., PRICE, S. D., LYSAKOWSKI, A. & LOPEZ-ESCAMEZ, J. A. 2015. Identification of two novel mutations in FAM136A and DTNA genes in autosomal-dominant familial Meniere's disease. *Hum Mol Genet,* 24**,** 1119-26.

RICHTER, C., THIEME, S., BANDOŁA, J., LAUGSCH, M., ANASTASSIADIS, K. & BRENNER, S. 2013. Generation of inducible immortalized dendritic cells with proper immune function in vitro and in vivo. *PLoS One,* 8**,** e62621.

RITTER, M., MENNERICH, D., WEITH, A. & SEITHER, P. 2005. Characterization of Toll-like receptors in primary lung epithelial cells: strong impact of the TLR3

ligand poly(I:C) on the regulation of Toll-like receptors, adaptor proteins and inflammatory response. *J Inflamm (Lond),* 2**,** 16.

ROGERS, D. F. 1994. Airway goblet cells: responsive and adaptable front-line defenders. *Eur Respir J,* 7**,** 1690-706.

ROGERS, D. F. 2002. Airway goblet cell hyperplasia in asthma: hypersecretory and anti-inflammatory? *Clin Exp Allergy,* 32**,** 1124-7.

ROSE, M. C. & VOYNOW, J. A. 2006. Respiratory tract mucin genes and mucin glycoproteins in health and disease. *Physiol Rev,* 86**,** 245-78.

SAHIN, E. & DEPINHO, R. A. 2010. Linking functional decline of telomeres, mitochondria and stem cells during ageing. *Nature,* 464**,** 520-8.

SANGER, F., NICKLEN, S. & COULSON, A. R. 1977. DNA sequencing with chain-terminating inhibitors. *Proc Natl Acad Sci U S A,* 74**,** 5463-7.

SARETZKI, G., SITTE, N., MERKEL, U., WURM, R. E. & VON ZGLINICKI, T. 1999. Telomere shortening triggers a p53-dependent cell cycle arrest via accumulation of G-rich single stranded DNA fragments. *Oncogene,* 18**,** 5148-58.

SASAKI, M., IKEDA, H., SATO, Y. & NAKANUMA, Y. 2006. Decreased expression of Bmi1 is closely associated with cellular senescence in small bile ducts in primary biliary cirrhosis. *Am J Pathol,* 169**,** 831-45.

SAUER, B. 2006. Cre-Lox-Inducible Gene Targeting. *ENCYCLOPEDIA OF LIFE SCIENCES* [Online]. Available: http://onlinelibrary.wiley.com/doi/10.1038/npg.els.0005979/pdf.

SCHMIDT-SUPPRIAN, M. & RAJEWSKY, K. 2007. Vagaries of conditional gene targeting. *Nat Immunol,* 8**,** 665-8.

SCRIPTURE-ADAMS, D. D., DAMLE, S. S., LI, L., ELIHU, K. J., QIN, S., ARIAS, A. M., BUTLER, R. R., CHAMPHEKAR, A., ZHANG, J. A. & ROTHENBERG, E. V. 2014. GATA-3 dose-dependent checkpoints in early T cell commitment. *J Immunol,* 193**,** 3470-91.

SERRANO, M. 1997. The tumor suppressor protein p16INK4a. *Exp Cell Res,* 237**,** 7-13.

SHAN, J., HUANG, J., LIAO, J., ROBERT, R. & HANRAHAN, J. W. 2011. Anion secretion by a model epithelium: more lessons from Calu-3. *Acta Physiol (Oxf),* 202**,** 523-31.

SHEBANI, E., SHAHANA, S., JANSON, C., ROOMANS, G. M. & GROUP, B. 2005. Attachment of columnar airway epithelial cells in asthma. *Tissue Cell,* 37**,** 145-52.

SHIN, K., FOGG, V. C. & MARGOLIS, B. 2006. Tight junctions and cell polarity. *Annu Rev Cell Dev Biol,* 22**,** 207-35.

SINGH, D., MCCANN, K. L. & IMANI, F. 2007. MAPK and heat shock protein 27 activation are associated with respiratory syncytial virus induction of human bronchial epithelial monolayer disruption. *Am J Physiol Lung Cell Mol Physiol,* 293**,** L436-45.

SLATER, M., TORR, E., HARRISON, T., FORRESTER, D., KNOX, A., SHAW, D. & SAYERS, I. 2016. The differential effects of azithromycin on the airway epithelium in vitro and in vivo. *Physiol Rep,* 4.

SMITH, D. R. 1996. Agarose gel electrophoresis. *Methods Mol Biol,* 58**,** 17-21.

SMITH, J. L., LEE, L. C., READ, A., LI, Q., YU, B., LEE, C. S. & LUO, J. 2016a. One-step immortalization of primary human airway epithelial cells capable of oncogenic transformation. *Cell Biosci,* 6**,** 57.

SMITH, P., NICHOLSON, L. J., SYED, N., PAYNE, A., HILLER, L., GARRONE, O., OCCELLI, M., GASCO, M. & CROOK, T. 2007. Epigenetic inactivation implies independent functions for insulin-like growth factor binding protein (IGFBP)-related protein 1 and the related IGFBPL1 in inhibiting breast cancer phenotypes. *Clin Cancer Res,* 13**,** 4061-8.

SNAPGENE SOFTWARE (from GSL Biotech; available at snapgene.com)

SOCIETY), E. E. R. 2017. *Adult asthma* [Online]. Available: http://www.erswhitebook.org/chapters/adult-asthma/ [Accessed 4th June 2017].

SÖHL, G. & WILLECKE, K. 2004. Gap junctions and the connexin protein family. *Cardiovasc Res,* 62**,** 228-32.

SONESON, C. & DELORENZI, M. 2013. A comparison of methods for differential expression analysis of RNA-seq data. *BMC Bioinformatics,* 14**,** 91.

SONG, L. B., ZENG, M. S., LIAO, W. T., ZHANG, L., MO, H. Y., LIU, W. L., SHAO, J. Y., WU, Q. L., LI, M. Z., XIA, Y. F., FU, L. W., HUANG, W. L., DIMRI, G. P., BAND, V. & ZENG, Y. X. 2006. Bmi-1 is a novel molecular marker of nasopharyngeal carcinoma progression and immortalizes primary human nasopharyngeal epithelial cells. *Cancer Res,* 66**,** 6225-32.

SRINIVASAN, B., KOLLI, A. R., ESCH, M. B., ABACI, H. E., SHULER, M. L. & HICKMAN, J. J. 2015. TEER measurement techniques for in vitro barrier model systems. *J Lab Autom,* 20**,** 107-26.

STEM CELL. 2016. *Air-Liquid Interface Culture for Respiratory Research* [Online]. Available: https://www.stemcell.com/air-liquid-interface-culture-respiratory-research-lp.html [Accessed 19th May 2017].

STEVENS, P. T., KICIC, A., SUTANTO, E. N., KNIGHT, D. A. & STICK, S. M. 2008. Dysregulated repair in asthmatic paediatric airway epithelial cells: the role of plasminogen activator inhibitor-1. *Clin Exp Allergy,* 38**,** 1901-10.

STEWART, C. E., TORR, E. E., MOHD JAMILI, N. H., BOSQUILLON, C. & SAYERS, I. 2012. Evaluation of differentiated human bronchial epithelial cell culture systems for asthma research. *J Allergy (Cairo),* 2012**,** 943982.

STOTT, F. J., BATES, S., JAMES, M. C., MCCONNELL, B. B., STARBORG, M., BROOKES, S., PALMERO, I., RYAN, K., HARA, E., VOUSDEN, K. H. & PETERS, G. 1998. The alternative product from the human CDKN2A locus, p14(ARF), participates in a regulatory feedback loop with p53 and MDM2. *EMBO J,* 17**,** 5001-14.

SUZUKI, Y. & SUZUKI, Y. 2011. Gene regulatable lentiviral vector system. *In:* XU, K. (ed.) *Viral Gene Therapy.* InTech.

SWINDLE, E. J., COLLINS, J. E. & DAVIES, D. E. 2009. Breakdown in epithelial barrier function in patients with asthma: identification of novel therapeutic approaches. *J Allergy Clin Immunol,* 124**,** 23-34; quiz 35-6.

SYSTEM BIOSCIENCES. 2012. *pCDH cDNA Cloning and Expression Lentivectors* [Online]. Available: http://www.systembio.com/downloads/Manual_pCDH_Vector_v5.pdf [Accessed 5th April 2017].

SYSTEM BIOSCIENCES. 2017. *The Cumate Switch Inducible System* [Online]. Available: http://www.systembio.com/lentiviral-technology/cumate-switch-vectors/overview [Accessed 17th May 2017].

SYSTEM BIOSCIENCES. n.d. *SparQ Cumate Switch User Manual* [Online]. Available: http://www.systembio.com/downloads/Manual_Cumate_system.pdf [Accessed 28th March 2017].

TAKAI, Y. & NAKANISHI, H. 2003. Nectin and afadin: novel organizers of intercellular junctions. *J Cell Sci,* 116**,** 17-27.

TALIAFERRO-SMITH, L., NAGALINGAM, A., ZHONG, D., ZHOU, W., SAXENA, N. K. & SHARMA, D. 2009. LKB1 is required for adiponectin-mediated modulation of AMPK-S6K axis and inhibition of migration and invasion of breast cancer cells. *Oncogene,* 28**,** 2621-33.

TAN, N. S. & WAHLI, W. 2014. The emerging role of Nrf2 in dermatotoxicology. *EMBO Mol Med,* 6**,** 431-3.

THANAWALA, V. J., FORKUO, G. S., AL-SAWALHA, N., AZZEGAGH, Z., NGUYEN, L. P., ERIKSEN, J. L., TUVIM, M. J., LOWDER, T. W., DICKEY, B. F., KNOLL, B. J., WALKER, J. K. & BOND, R. A. 2013. β2-Adrenoceptor agonists are required for development of the asthma phenotype in a murine model. *Am J Respir Cell Mol Biol,* 48**,** 220-9.

THERMOFISHER SCIENTIFIC. n.d.-a. *Delivery solutions for immune cells* [Online]. Available: https://www.thermofisher.com/uk/en/home/life-science/cell-culture/cell-culture-learning-center/cell-culture-resource-library/cell-culture-transfection-application-notes/delivery-solutions-immune-cells.html [Accessed 20th May 2017].

THERMOFISHER SCIENTIFIC. n.d.-b. *One Shot® MAX Efficiency® DH5α™-T1 R Competent Cells* [Online]. Available: http://www.thermofisher.com/order/catalog/product/12297016 [Accessed 29th March 2017].

THERMOFISHER SCIENTIFIC. n.d.-c. *Platinum® Taq DNA Polymerase High Fidelity* [Online]. Available: http://www.thermofisher.com/order/catalog/product/11304011 [Accessed 26th March 2017].

THERMOFISHER SCIENTIFIC. n.d.-d. Overview of Western Blotting [Online]. Available: https://www.thermofisher.com/uk/en/home/life-science/protein-biology/protein-biology-learning-center/protein-biology-resource-library/pierce-protein-methods/overview-western-blotting.html [Accessed 24th Dec 2017].

TORR, E., HEATH, M., MEE, M., SHAW, D., SHARP, T. V. & SAYERS, I. 2016. Expression of polycomb protein BMI-1 maintains the plasticity of basal bronchial epithelial cells. *Physiol Rep,* 4.

TRAPNELL, C. 2016. *Cufflinks* [Online]. Available: http://cole-trapnell-lab.github.io/cufflinks/cuffdiff/ [Accessed 30th May 2017].

TRAPNELL, C., HENDRICKSON, D. G., SAUVAGEAU, M., GOFF, L., RINN, J. L. & PACHTER, L. 2013. Differential analysis of gene regulation at transcript resolution with RNA-seq. *Nat Biotechnol,* 31**,** 46-53.

TRAPNELL, C., ROBERTS, A., GOFF, L., PERTEA, G., KIM, D., KELLEY, D. R., PIMENTEL, H., SALZBERG, S. L., RINN, J. L. & PACHTER, L. 2012. Differential gene and transcript expression analysis of RNA-seq experiments with TopHat and Cufflinks. *Nat Protoc,* 7**,** 562-78.

TRAPNELL, C., WILLIAMS, B. A., PERTEA, G., MORTAZAVI, A., KWAN, G., VAN BAREN, M. J., SALZBERG, S. L., WOLD, B. J. & PACHTER, L. 2010. Transcript assembly and quantification by RNA-Seq reveals unannotated transcripts and isoform switching during cell differentiation. *Nat Biotechnol,* 28**,** 511-5.

TSE, R., MARROQUIN, B. A., DORSCHEID, D. R. & WHITE, S. R. 2003. Beta-adrenergic agonists inhibit corticosteroid-induced apoptosis of airway epithelial cells. *Am J Physiol Lung Cell Mol Physiol,* 285**,** L393-404.

TWINE, N. A., JANITZ, K., WILKINS, M. R. & JANITZ, M. 2011. Whole transcriptome sequencing reveals gene expression and splicing differences in brain regions affected by Alzheimer's disease. *PLoS One,* 6**,** e16266.

UNIPROT. 2017. *UniProtKB - P35226 (BMI1_HUMAN)* [Online]. Available: http://www.uniprot.org/uniprot/P35226 [Accessed 31st January 2017].

VERMEER, P. D., HARSON, R., EINWALTER, L. A., MONINGER, T. & ZABNER, J. 2003. Interleukin-9 induces goblet cell hyperplasia during repair of human airway epithelia. *Am J Respir Cell Mol Biol,* 28**,** 286-95.

WADSWORTH, S. J., NIJMEH, H. S. & HALL, I. P. 2006. Glucocorticoids increase repair potential in a novel in vitro human airway epithelial wounding model. *J Clin Immunol,* 26**,** 376-87.

WALFORD, H. H. & DOHERTY, T. A. 2013. STAT6 and lung inflammation. *JAKSTAT,* 2**,** e25301.

WALL, I., TOLEDO, G. S. & JAT, P. S. 2016. Recent advances in conditional cell immortalization technology. *Cell and Gene Therapy Insights* [Online], 2. Available: http://discovery.ucl.ac.uk/1522367/1/Wall.pdf.

WAN, H., WINTON, H. L., SOELLER, C., STEWART, G. A., THOMPSON, P. J., GRUENERT, D. C., CANNELL, M. B., GARROD, D. R. & ROBINSON, C. 2000. Tight junction properties of the immortalized human bronchial epithelial cell lines Calu-3 and 16HBE14o-. *Eur Respir J,* 15**,** 1058-68.

WAN, Y. I., SHRINE, N. R., SOLER ARTIGAS, M., WAIN, L. V., BLAKEY, J. D., MOFFATT, M. F., BUSH, A., CHUNG, K. F., COOKSON, W. O., STRACHAN, D. P., HEANEY, L., AL-MOMANI, B. A., MANSUR, A. H., MANNEY, S., THOMSON, N. C., CHAUDHURI, R., BRIGHTLING, C. E., BAFADHEL, M., SINGAPURI, A., NIVEN, R., SIMPSON, A., HOLLOWAY, J. W., HOWARTH, P. H., HUI, J., MUSK, A. W., JAMES, A. L., BROWN, M. A., BALTIC, S., FERREIRA, M. A., THOMPSON, P. J., TOBIN, M. D., SAYERS, I., HALL, I. P. & CONSORTIUM, A. A. G. 2012. Genome-wide association study to identify genetic determinants of severe asthma. *Thorax,* 67**,** 762-8.

WANG, P., QIN, J., QIN, Y., ZHU, Y., WANG, L. Y., LI, M. J., ZHANG, M. Q. & WANG, J. 2015. ChIP-Array 2: integrating multiple omics data to construct gene regulatory networks. *Nucleic Acids Res,* 43**,** W264-9.

WANG, W., GRIMMER, J. F., VAN DE WATER, T. R. & LUFKIN, T. 2004. Hmx2 and Hmx3 homeobox genes direct development of the murine inner ear and hypothalamus and can be functionally replaced by Drosophila Hmx. *Dev Cell,* 7**,** 439-53.

WANG, W. M., GE, G., LIM, N. H., NAGASE, H. & GREENSPAN, D. S. 2006. TIMP-3 inhibits the procollagen N-proteinase ADAMTS-2. *Biochem J,* 398**,** 515-9.

WANG, Z., GERSTEIN, M. & SNYDER, M. 2009. RNA-Seq: a revolutionary tool for transcriptomics. *Nat Rev Genet,* 10**,** 57-63.

WEISS, S. T. 2012. New approaches to personalized medicine for asthma: where are we? *J Allergy Clin Immunol,* 129**,** 327-34.

WHITE, J. H., CHIANO, M., WIGGLESWORTH, M., GESKE, R., RILEY, J., WHITE, N., HALL, S., ZHU, G., MAURIO, F., SAVAGE, T., ANDERSON, W., CORDY, J., DUCCESCHI, M., VESTBO, J., PILLAI, S. G. & INVESTIGATORS, G. 2008. Identification of a novel asthma susceptibility gene on chromosome 1qter and its functional evaluation. *Hum Mol Genet,* 17**,** 1890-903.

WORLD HEALTH ORGANISATION. 2017. *Asthma* [Online]. Available: http://www.who.int/respiratory/asthma/en/ [Accessed 17th May 2017].

WOODS, N. B., MUESSIG, A., SCHMIDT, M., FLYGARE, J., OLSSON, K., SALMON, P., TRONO, D., VON KALLE, C. & KARLSSON, S. 2003. Lentiviral vector transduction of NOD/SCID repopulating cells results in multiple vector integrations per transduced cell: risk of insertional mutagenesis. *Blood,* 101**,** 1284-9.

WU, R., SATO, G. H. & WHITCUTT, M. J. 1986. Developing differentiated epithelial cell cultures: airway epithelial cells. *Fundam Appl Toxicol,* 6**,** 580-90.

XIAO, C. & LUONG, J. H. 2003. On-line monitoring of cell growth and cytotoxicity using electric cell-substrate impedance sensing (ECIS). *Biotechnol Prog,* 19**,** 1000-5.

XIAO, C., PUDDICOMBE, S. M., FIELD, S., HAYWOOD, J., BROUGHTON-HEAD, V., PUXEDDU, I., HAITCHI, H. M., VERNON-WILSON, E., SAMMUT, D., BEDKE, N., CREMIN, C., SONES, J., DJUKANOVIĆ, R., HOWARTH, P. H., COLLINS, J. E., HOLGATE, S. T., MONK, P. & DAVIES, D. E. 2011. Defective epithelial barrier function in asthma. *J Allergy Clin Immunol,* 128**,** 549-56.e1-12.

XIAO, H., RIZZO, A. N., SIEGLER, J. & CHEN, W. 2013. The importance of bronchial epithelial junction integrity in asthma. *Journal of Allergy and Therapy,* [Online], S11.

XU, C. R., LEE, S., HO, C., BOMMI, P., HUANG, S. A., CHEUNG, S. T., DIMRI, G. P. & CHEN, X. 2009. Bmi1 functions as an oncogene independent of Ink4A/Arf repression in hepatic carcinogenesis. *Mol Cancer Res,* 7**,** 1937-45.

XU, S. M., BRILL, E., LLEWELLYN, D. J., FURBANK, R. T. & RUAN, Y. L. 2012. Overexpression of a potato sucrose synthase gene in cotton accelerates leaf expansion, reduces seed abortion, and enhances fiber production. *Mol Plant,* 5**,** 430-41.

XUE, M. Z., BONNY, O., MORGENTHALER, S., BOCHUD, M., MOOSER, V., THILLY, W. G., SCHILD, L. & LEONG-MORGENTHALER, P. M. 2002. Use of constant denaturant capillary electrophoresis of pooled blood samples to identify single-nucleotide polymorphisms in the genes (Scnn1a and Scnn1b) encoding the alpha and beta subunits of the epithelial sodium channel. *Clin Chem,* 48**,** 718-28.

YAMAUCHI, K., PIAO, H.M., NAKADATE, T., SHIKANAI, T., NAKAMURA, Y., NIISATO, M., ITO, H., MOURI, T., KOBAYASHI, H., MAESAWA, C., SAWAI, T., OHTSU, H., INOUE, H. 2008. Progress in Allergy Signal Research on Mast Cells: The

Role of Histamine in Goblet Cell Hyperplasia in Allergic Airway Inflammation – a Study Using the Hdc Knockout Mouse, *Journal of Pharmacological Sciences*, 106, (3), 354-60.

YANG, L., ARIAS, L. R., LANE, T. S., YANCEY, M. D. & MAMOUNI, J. 2011. Real-time electrical impedance-based measurement to distinguish oral cancer cells and non-cancer oral epithelial cells. *Anal Bioanal Chem,* 399**,** 1823-33.

YIP, Y. L., PANG, P. S., DENG, W., TSANG, C. M., ZENG, M., HAU, P. M., MAN, C., JIN, Y., YUEN, A. P. & TSAO, S. W. 2013. Efficient immortalization of primary nasopharyngeal epithelial cells for EBV infection study. *PLoS One,* 8**,** e78395.

YUAN, J., TANG, Z., YANG, S. & LI, K. 2013. CRABP2 promotes myoblast differentiation and is modulated by the transcription factors MyoD and Sp1 in C2C12 cells. *PLoS One,* 8**,** e55479.

YUKAWA, T., READ, R. C., KROEGEL, C., RUTMAN, A., CHUNG, K. F., WILSON, R., COLE, P. J. & BARNES, P. J. 1990. The effects of activated eosinophils and neutrophils on guinea pig airway epithelium in vitro. *Am J Respir Cell Mol Biol,* 2**,** 341-53.

ZEEBERG, B. R., RISS, J., KANE, D. W., BUSSEY, K. J., UCHIO, E., LINEHAN, W. M., BARRETT, J. C. & WEINSTEIN, J. N. 2004. Mistaken identifiers: gene name errors can be introduced inadvertently when using Excel in bioinformatics. *BMC Bioinformatics,* 5**,** 80.

ZHANG, Z. H., JHAVERI, D. J., MARSHALL, V. M., BAUER, D. C., EDSON, J., NARAYANAN, R. K., ROBINSON, G. J., LUNDBERG, A. E., BARTLETT, P. F., WRAY, N. R. & ZHAO, Q. Y. 2014. A comparative study of techniques for differential expression analysis on RNA-Seq data. *PLoS One,* 9**,** e103207.

ZHANG, L., GAO, J., LI, L., LI, Z., DU, Y. & GONG, Y. 2011. The neuronal pentraxin II gene (NPTX2) inhibit proliferation and invasion of pancreatic cancer cells in vitro. *Mol Biol Rep,* 38**,** 4903-11.

ZHENG, X., WANG, Y., LIU, B., LIU, C., LIU, D., ZHU, J., YANG, C., YAN, J., LIAO, X., MENG, X. & YANG, H. 2014. Bmi-1-shRNA inhibits the proliferation of lung adenocarcinoma cells by blocking the G1/S phase through decreasing cyclin D1 and increasing p21/p27 levels. *Nucleic Acid Ther,* 24**,** 210-6.

ZHOU, C., QIN, Y., XIE, Z., ZHANG, J., YANG, M., LI, S. & CHEN, R. 2015. NPTX1 is a novel epigenetic regulation gene and associated with prognosis in lung cancer. *Biochem Biophys Res Commun,* 458**,** 381-6.

# 7.Appendix

## Gel electrophoresis

A 1% agarose gel was made up for gel electrophoresis by the addition of agarose to 20ml/L TAE buffer (using 50x stock consisting of 242g/l UltraPure Tris and 100ml/L 0.5M EDTA, pH 8). This was heated in the microwave until dissolved. Once the solution had cooled sufficiently, ethidium bromide 10mg/ml was added (2.5µl/50ml) and it was poured into the gel cassette to set, using a comb to create wells. DNA samples were prepared by the addition of 6x Orange G dye (Thermo Fisher Scientific).

## SDS PAGE Gel

Components required for Western Blotting:

**TBST** (20mM Tris-HCl, pH7.5; 150mM NaCl; 0.1% Tween 20)

**Tris-glycine/SDS running buffer** (250mM Tris base; 1.92M glycine)

**Transfer Buffer** (25mM Tris base; 192mM glycine, 20% v/v methanol)

**10% APS** 0.5g ammonium persulphate in 5ml of water

| Component | Volume |
|---|---|
| Distilled water | 3.1ml |
| 30% (w/v) acrylamide (Sigma, A3699) | 4.2ml |
| 10% SDS (Sigma, L5750) | 100µl |
| 1.5M Tris-HCl (pH 8.8) | 2.5ml |
| 10% APS | 100µl |
| TEMED | 4µl |

**Table S1. Components and volumes required for resolving gel in Western Blotting**

| Component | Volume |
|---|---|
| Distilled water | 3.4ml |
| 30% (w/v) acrylamide | 830µl |
| 10% SDS | 50µl |
| 1M Tris-HCl (pH 6.8) | 630 µl |
| 10% APS | 50µl |
| TEMED | 5µl |

**Table S2. Components and volumes required for stacking gel in Western Blotting**

1. Components for the resolving gel were mixed and poured into 0.75mm gel cassette and left to set. Once set, the stacking gel was mixed and poured on top of the resolving gel. A comb was inserted and the gel left to set. The gel was placed in 1x Tris-glycine/SDS running buffer and samples were added to the wells.
2. Samples were run at 100V through the stacking gel and then 200V through the resolving gel.

## Bacterial culture

Bacteria was grown on agar plates. 16g/L of LB Agar (Fisher, BPE1425-500) in 400ml water was autoclaved. Before pouring into plates, the agar was heated and ampicillin added to a final concentration of 100μM.

Bacteria was grown in LB Broth (Fisher, BPE1426-500). 12.5g of LB Broth powder was added to 500ml of water and autoclaved. Ampicillin was added to a final concentration of 100μM.

## Genes identified as up-regulated in transcriptomic analyses

| | | | | | |
|---|---|---|---|---|---|
| ABCC8 | CHD5 | GABRE | LBH | NTNG2 | RYR1 |
| ACAN | CHST15 | GAL | LGI2 | NTRK1 | SARDH |
| ACE | COL15A1 | GAP43 | LINGO1 | NTSR1 | SCARA3 |
| ADAMTS10 | COL22A1 | GLIPR2 | LINGO3 | NXN | SCN4B |
| ADAMTS2 | CRABP2 | GPRC5C | LMX1B | PAGE1 | SEPT3 |
| AKR1C2 | CRLF1 | GRID1 | MAOB | PARM1 | SHANK1 |
| ALX4 | CRMP1 | GRTP1 | MAST1 | PCK1 | SLC14A1 |
| ARHGEF16 | CXCL1 | HAPLN4 | MEGF11 | PCSK6 | SNCB |
| ATP2B2 | CYP2S1 | HES4 | MEGF6 | PDZD4 | SORCS2 |
| BCL2A1 | DKK1 | HHIP | MERTK | PIEZO2 | SOX8 |
| BMI1 | DMKN | HMX3 | MLC1 | PNMT | SYT7 |
| BMP7 | EBF4 | HTRA3 | MLXIPL | PPAPDC1A | TCF15 |
| C2CD4C | EEF1A2 | IGF2 | NECAB2 | PPP2R2C | TLE2 |
| CA12 | EFEMP1 | IGFBP7 | NETO1 | PRRX2 | TMEM130 |
| CACNA1C | ELFN2 | IGFBPL1 | NEURL1B | PTH1R | TMEM150C |
| CACNA1H | EMID1 | IL2RB | NFASC | PTPN7 | TNS1 |
| CACNG7 | EMILIN3 | IL8 | NKD2 | PTPRU | TP53I11 |
| CCDC88C | EPAS1 | ITGA11 | NOTUM | PXDN | TSPAN18 |
| CDH11 | FAM19A3 | JAG2 | NOVA2 | RASD2 | UNC13A |
| CDH15 | FAM20A | KCNH2 | NPTX1 | RASGRP2 | VIT |
| CDH23 | FAM57B | KCNK6 | NPTX2 | RBP7 | WNK2 |
| CDH3 | FIBCD1 | KCNN1 | NRXN2 | RCAN2 | WNT5B |
| CDHR1 | FN1 | KRT6B | NTF4 | RCN3 | WSCD1 |
| CEACAM1 | FOXF1 | LAMC3 | NTN1 | RTN4RL1 | ZIC5 |

**Table S3. List of 144 genes which were significantly up-regulated in samples from A375 cells engineered to over-express Bmi1, as identified by CuffDiff, Rank Prod and Ferretti *et al.* (2016).**